



UIT

THE ARCTIC  
UNIVERSITY  
OF NORWAY

Institute of Geosciences, UiT, The Arctic University of Norway

# Interaction of submarine tailings with natural sediments in three northern Norwegian coastal areas:

*Sedimentological, mineralogical and geochemical constraints*

**Nikolai Figenschau**

*Master's thesis in geosciences      May 2018*



# Acknowledgement

I would like to thank NYKOS for giving me the opportunity to be part of a very exciting project. To the research partners that have been involved in my master thesis: Thanks to the Geological Survey of Norway (NGU), Environmental Waste Management (EWMA), Akvaplan-niva and Sibelco Nordic AS for gathering and sharing material and data with me. Thanks to NYKOS for funding meet-ups with my supervisors in Trondheim, as well as funding the lab-work.

A special thanks to my co-supervisors, Nicole Baeten (NGU) for introducing me to lab-work in both Trondheim and Tromsø (with great patience), Juho Junttila (IG, UiT) for lab supervision and Aivo Lepland (NGU) for advising me through a maze of geochemical struggles. Also, a huge thanks to the girls in the lab: Karina Monsen, Trine Dahl and Ingvild Hald.

Last but not least, my formal main supervisor – Matthias Forwick. Your feedback has been so valuable, if not priceless. Despite being the busiest man on earth, you have always been there if I needed your help, and for that I am very grateful!

Finally, I would like to thank my family, friends and girlfriend for mental and financial (mostly my family) support, and for offering your spare time to correct my lousy understanding of plural and singular verb rules (that goes for you too Matthias).



## **Abstract**

Submarine tailings placements (STPs) is an alternative practice of handling mine waste, which involves deposition of tailings into submarine environments. However, the environmental impacts of STPs remain poorly understood.

This thesis is a contribution to improve the understanding of how submarine tailings placements interact with natural sediments. It is based on multi-proxy analyses of 10 sediment cores from three northern Norwegian coastal areas with submarine tailings histories: the fjords Bøkfjorden and Ranfjorden, as well as the sound Stjernesundet. The tailings in Bøkfjorden and Ranfjorden are associated with extraction of iron ore, whereas Stjernesundet is associated with extraction of nepheline syenite.

The applied proxies included physical properties (e.g. magnetic susceptibility), geochemical properties (qualitative and quantitative element geochemistry), bulk mineral assemblages and lithological analyses. Three depositional environments are distinguished: a natural depositional environment (endmember 1), tailings depositional environment (endmember 2) and transitional depositional environment (mix of endmember 1 & 2). Endmember 1 is defined by alternating grain size, low magnetic susceptibility and stable geochemistry. Endmember 2 is defined by fine-grained sediments, high magnetic susceptibility and elevated levels of tailings associated elements. Transitions are defined by gradual increase (tailings-dominance) or decrease (natural dominance) in grain size, magnetic susceptibility and tailings associated elements.

The relation and composition of the identified depositional environments reflect either gradual or abrupt changes in sediment supply, sedimentary and depositional processes. Ranfjorden and Bøkfjorden show a large lateral extent of tailings (> 15 km) due to a high sediment input of fine-grained tailings, bed load transportation and associated submarine meandering channel systems. Stjernesundet shows a limited lateral extent of tailings (< 2 km) due to a low sediment input of relatively coarse-grained tailings. The analyzed material from Ranfjorden and Stjernesundet reflects a gradual evolving dominance of tailings, whereas the material from Bøkfjorden reflect an abrupt evolving dominance of tailings.

# Table of Contents

1	Introduction .....	1
1.1	Objectives.....	1
1.2	Background .....	2
1.2.1	Mining activity and waste .....	2
1.2.2	The principle of submarine tailings placement: .....	6
1.3	Previous investigations and history of tailings deposition .....	7
1.3.1	Ranfjorden .....	7
1.3.2	Bøkfjorden.....	9
1.3.3	Stjernesundet .....	12
2	Study area .....	15
1.1	Ranfjorden.....	15
2.1.1	Physiographic setting: .....	15
1.1.1	Geological setting.....	17
1.1.2	Sediment sources.....	19
1.1.3	Hydrology.....	20
1.2	Bøkfjorden.....	20
2.1.2	Physiographic setting .....	20
1.2.1	Geological setting.....	22
1.2.2	Hydrology.....	23
1.3	Stjernesundet.....	25
1.3.1	Physiographic setting and climate:.....	25
1.3.2	Geological setting.....	26
1.3.3	Hydrology.....	27
3	Material and methods .....	28
3.1	Sediment collection .....	28
3.1.1	Ranfjorden .....	28
3.1.2	Bøkfjorden.....	29
3.1.3	Stjernesundet .....	31
3.2	Laboratory work – sediment cores: .....	33
3.2.1	X-radiography .....	33
3.2.2	Physical properties .....	33
3.2.3	Opening of cores .....	35
3.2.4	Spectrophotometry .....	35
3.2.5	Visual description.....	35

3.2.6	Grainsize distribution analysis .....	35
3.2.7	X-Ray Fluorescence Core Scanner (XRF core scanner) .....	36
3.2.8	X-Ray Fluorescence Spectrometer (XRF spectrometer) .....	39
3.2.9	X-ray Diffraction (XRD) .....	40
4	Sediment Cores .....	41
4.1	Ranfjorden .....	41
4.1.1	Core P1502-001 .....	41
4.1.2	Core P1502-013 .....	45
4.1.3	Core P1502-015 .....	48
4.1.4	Core P1502-004 .....	51
4.2	Bøkfjorden .....	54
4.2.1	P1505-011 .....	54
4.2.2	IG16-1811GC .....	56
4.2.3	IG16-1798GC .....	59
4.3	Stjernesundet .....	62
4.3.1	Core P1707-005 .....	62
4.3.2	Interpretation .....	62
4.3.3	Core P1707-018 .....	64
4.3.4	Core P1707-010 .....	67
5	Discussion .....	69
5.1	Sedimentary processes in Ranfjorden, Bøkfjorden and Stjernesundet .....	69
5.1.1	Ranfjorden .....	69
5.1.2	Bøkfjorden .....	76
5.1.3	Stjernesundet .....	82
5.1.4	Comparisons between the fjords: similarities and differences .....	85
6	Conclusion .....	89
	Works cited .....	91

## List of Tables

Table 1: Positions, water depths and core lengths of the four sediment cores. ....	28
Table 2: Positions, water depths and core lengths of the four sediment cores. ....	29
Table 3 Positions, water depths and core lengths of the four sediment cores. ....	31

## List of Figures

Figure 1 Annual world production of minerals by continents from 1984-2015 (without construction minerals, in million metric tons). Data from Reichl et al. (2017) .....	2
---	---

Figure 2 show the different steps in an ore processing plant (from Government of Canada) .....	3
Figure 3 Representation of the different marine tailings placements-methods. A) coastal tailings placement; B) Submarine Tailings Placement and C) Deep-Sea Tailing Placement. (From Ramirez-Lodra et al, 2015) .....	4
Figure 4 Overview of active STP-location In the world. From Friends of the Earth Norway (2015) evt. Løkeland (2015). .....	5
Figure 5 Overview map of inner Ranfjorden. Two points (G & F) indicate the tailings output source of coarse-grained tailings (G) and fine-grained tailings (F). .....	9
Figure 6 Overview map of Bøkfjorden, showing the adjacent mine (red) and the tailings output source location (blue). .....	12
Figure 7 Overview of the studyarea, Stjernesundet. Marked in red is the mountain Nabbern (Location of the local mine). Marked in orange is Lillebukta (deposition site for tailings). .....	14
Figure 8 A show an overview map of Europe, showing the region where the studysites are located. B show Northern Norway, the bathymetry of the coastal areas and the three study sites Ranfjorden (south), Stjernesundet (north-west) and Bøkfjorden (north-east). Dark blue represents deep water, and red represent shallow water. ....	15
Figure 9 Overview map of Ranfjorden, showing the full extent of the fjord (marked in red). .....	16
Figure 10 A bathymetric map of inner Ranfjorden, showing the presence of two sub-marine canyons stretching from the coarse-grained (G) and fine-grained (F) tailings output location down to the meandering channel system along the fjord bed. Depths ranging from shallow (red) to deep (blue). ..	17
Figure 11 Geological map with overview of the regional bedrock from Svartisen in the north, to the innerpart of Ranfjorden in the south. Derived from Geological Survey of Norway's (NGU) database. ....	18
Figure 12 Map of ice flow direction in the Rana region during last glacial period. From Blake & Olsen (1999). .....	19
Figure 13 Overview map of Bøkfjorden, showing the full extent of the fjord (marked in yellow). .....	21
Figure 14 A bathymetric map of inner Bøkfjorden, showing the presence of sub-marine channels. Showing the tailings output source (blue circle) and depths ranging from shallow (red) to deep (blue). .....	22
Figure 15 Geological map with overview of the regional bedrock from Varangerfjorden in the north, to Kirkenes in the south. (Derived from Geological Survey of Norway's (NGU) database .....	23
Figure 16 Map of ice flow direction in the Sout-Varanger region during since last glacial maximum. From Marthinussen (1974). .....	23
Figure 17 A show horizontal and vertical changes in turbidity throughout Bøkfjorden, whereas blue is high and white is low turbidity. From Berge et al., 2011 .....	24
Figure 18 Overview map of the studysite Stjernesundet.....	26
Figure 19 Geological map with overview of the regional bedrock with Stjernøya situated in the north and the mainland peninsula in the south. Derived from Geological Survey of Norway's (NGU) database. ....	27
Figure 20 Bathymetry dataset of inner Ranfjorden with core locations.....	29
Figure 21 Bathymetry dataset of inner Bøkfjorden with core locations.....	30
Figure 22 Overview map of Stjernesundet with core locations .....	32
Figure 23 Conseptual 3D-model of a GEOTEK MSCL-XCT x-ray imaging system. (From Research laboratory in Paleomagnetism and Marine geology).....	33
Figure 24 Conseptual model of a GEOTEK MSCL-S, displaying the most important components (From GEOTEK manual, 2000).....	34

Figure 25 Example showing XRF core scanner setup and potential contacts of landing triangle and sediment surface.....	36
Figure 26 Principle of Bohr’s atomic model and the generation of secondary radiation .....	37
Figure 27 Line-scan image, X-radiograph, visual description, as well as grain-size distribution, physical properties and element geochemistry of core P1502-001.....	43
Figure 28 Line-scan image, X-radiograph, visual description, as well as grain-size distribution, physical properties and element geochemistry of core P1502-013 .....	46
Figure 29 Line-scan image, X-radiograph, visual description, as well as grain-size distribution, physical properties and element geochemistry of core P1502-015 .....	49
Figure 30 Line-scan image, X-radiograph, visual description, as well as grain-size distribution, physical properties and element geochemistry of core P1502-004.....	52
Figure 31 Line-scan image, X-radiograph, visual description, as well as grain-size distribution, physical properties and element geochemistry of core P1505-011 .....	55
Figure 32 Line-scan image, X-radiograph, visual description, as well as grain-size distribution, physical properties and element geochemistry of core IG16-1811GC.....	58
Figure 33 Line-scan image, X-radiograph, visual description, as well as grain-size distribution, physical properties and element geochemistry of core IG16-1798GC.....	61
Figure 34 Line-scan image, X-radiograph, visual description, as well as grain-size distribution, physical properties and element geochemistry of core P1707-005.....	63
Figure 35 Line-scan image, X-radiograph, visual description, as well as grain-size distribution, physical properties and element geochemistry of core P1707-005.....	66
Figure 36 Line-scan image, X-radiograph, visual description, as well as grain-size distribution, physical properties and element geochemistry of core P1707-010.....	68
Figure 37 Comparison between vertical sediment profiles of tailings from core P1502-013 from Ranfjorden (above) and core 76-7 from Rupert Inlet, British Columbia (below). Due to low resolution of quantitative XRF, the most proper correlation in of the tailings in Bøkfjorden is magnetic susceptibility with respect to mean particle size. ....	72
Figure 38 Vertical Pb and Zn profile from chapter 4.3.1 and Skei & Paus (1978), the dashed lines mark the start and end of the transition zones.....	74
Figure 39 Summary of the sedimentary processes occurring in Ranfjorden.....	75
Figure 40 Comparison between vertical sediment profiles of tailings from core IG16-1811GC from Bøkfjorden (above) and core 76-7 from Rupert Inlet, British Columbia (below). Due to low resolution of quantitative XRF, the most proper correlation in of the tailings in Bøkfjorden is magnetic susceptibility with respect to mean particle size. Red arrows mark observed trends.....	79
Figure 41 Comparison between vertical sediment profiles of tailings from core IG16-1798GC from Bøkfjorden (above) and core 76-6 from Rupert Inlet, British Columbia (below). Due to low resolution of quantitative XRF, the most proper correlation in of the tailings in Bøkfjorden is magnetic susceptibility with respect to mean particle size. Red arrows mark observed trends.....	80
Figure 42 Summary of sedimentary processes in Bøkfjorden.....	82



# 1 Introduction

## 1.1 Objectives

This thesis is one out of three theses that was conducted at UiT, The Arctic University of Norway, as part of the NYKOS project (New knowledge on sea disposal) during the period June 2017 – May 2018. The NYKOS project is a collaboration between SINTEF (project lead), The Norwegian University of Science and Technology (NTNU), The Norwegian Institute for Water Research (NIVA), UiT, The Arctic University of Norway (UiT), Geological Survey of Norway (NGU) and the mining companies Nussir ASA, Sibelco Nordic, Rana Gruber, Omya Hustadmarmor, Nordic Mining and Titania. The purpose of the project is to increase the knowledge of the environmental effects of submarine deposition of fine-grained tailings from the mineral industry, and enable the development of new sound environmental criteria and monitoring technologies that prepare for a sustainable mineral industry in Norway.

In order to cover as much data as possible, the master project has been divided into three theses, whereas this thesis focuses on the interplay between tailings and natural sediments and the sedimentological, mineralogical, and geochemical constraints. The overall goal of the project is to improve the understanding of how submarine tailings placements (STPs) interact with natural sediments. The goal shall be achieved by:

- Multi-proxy analyses of sediment cores from Ranafjorden, Bøkfjorden and Stjernesundet, northern Norway, containing contact zones between natural sedimentation and STPs, with the purpose of
  - Investigating the physical and geochemical mixing of STPs with natural deposits.

A detailed examination of contact zones between disposed tailings and underlying sediments is expected to allow the assessment of physical mixing and geochemical disturbances caused by disposal. Given that disposed sediments can cover and isolate contaminated sediments in areas with long industrial track record (such as Mo i Rana), the contact zones in sediment cores can also be used for evaluating the sealing effects of tailings.

## 1.2 Background

### 1.2.1 Mining activity and waste

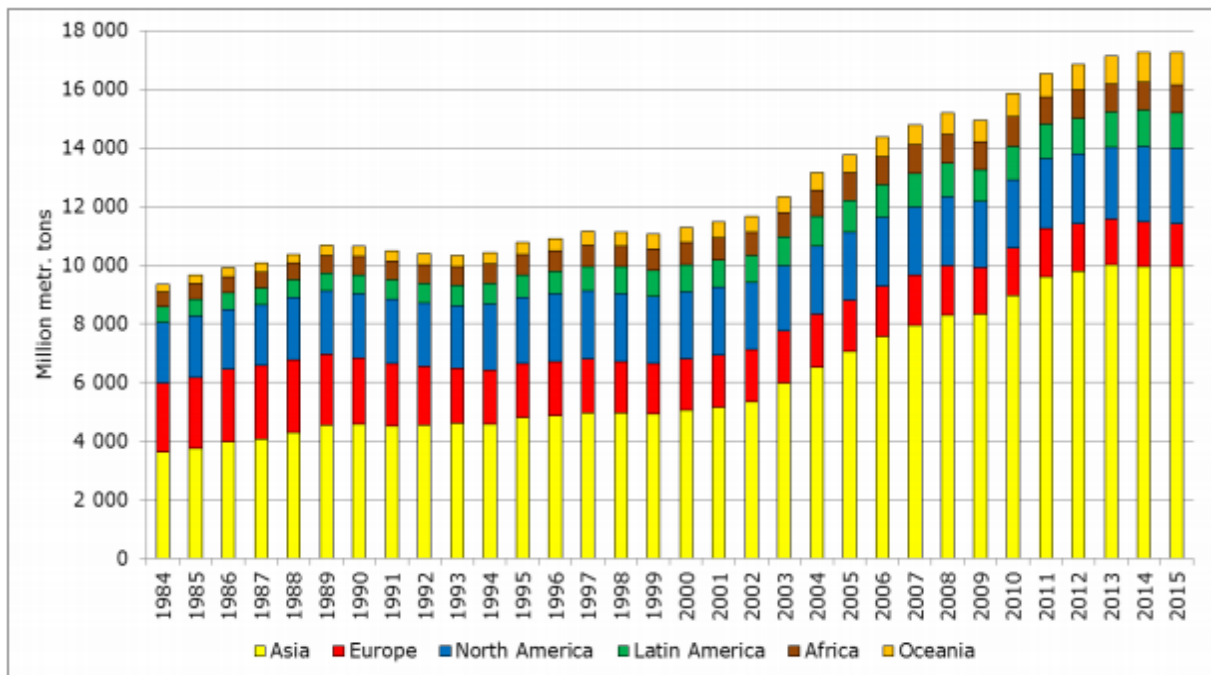


Figure 1 Annual world production of minerals by continents from 1984-2015 (without construction minerals, in million metric tons). Data from Reichl et al. (2017)

Through economic and technological growth (new green-energy technology), the world's need for new materials and metals is continuously increasing (Vogt 2013, Ramirez-Llodra et al., 2015; Arrobas et al., 2017). With an increasing demand for metals, one would expect an increased mining activity, which data from Reichl et al. (2017) supports (figure 1).

Furthermore, increased mining activity results in more extracted metals and its host rocks. Associated with extraction of hard rock are mine tailings. Tailings are the residual material after the targeted metal (iron, copper etc.) has been separated from the ore through both chemical and physical processes in the mining process plant. Figure 2 show the process of ore to tailings, which goes through numerous processes:

1. Dry crushing - coarse size reduction.
2. Grinding - fine size reduction with added chemicals (cyanide, lime, sulphur dioxide etc.).
3. Separation – physical or chemical separation of ore from gangue rock (floatation, magnetic, gravitational and chemical separation)
4. Separated ore is sent to further processing, whereas the residual (tailings) are sent to a tailings management facility.

(Vogt, 2013)

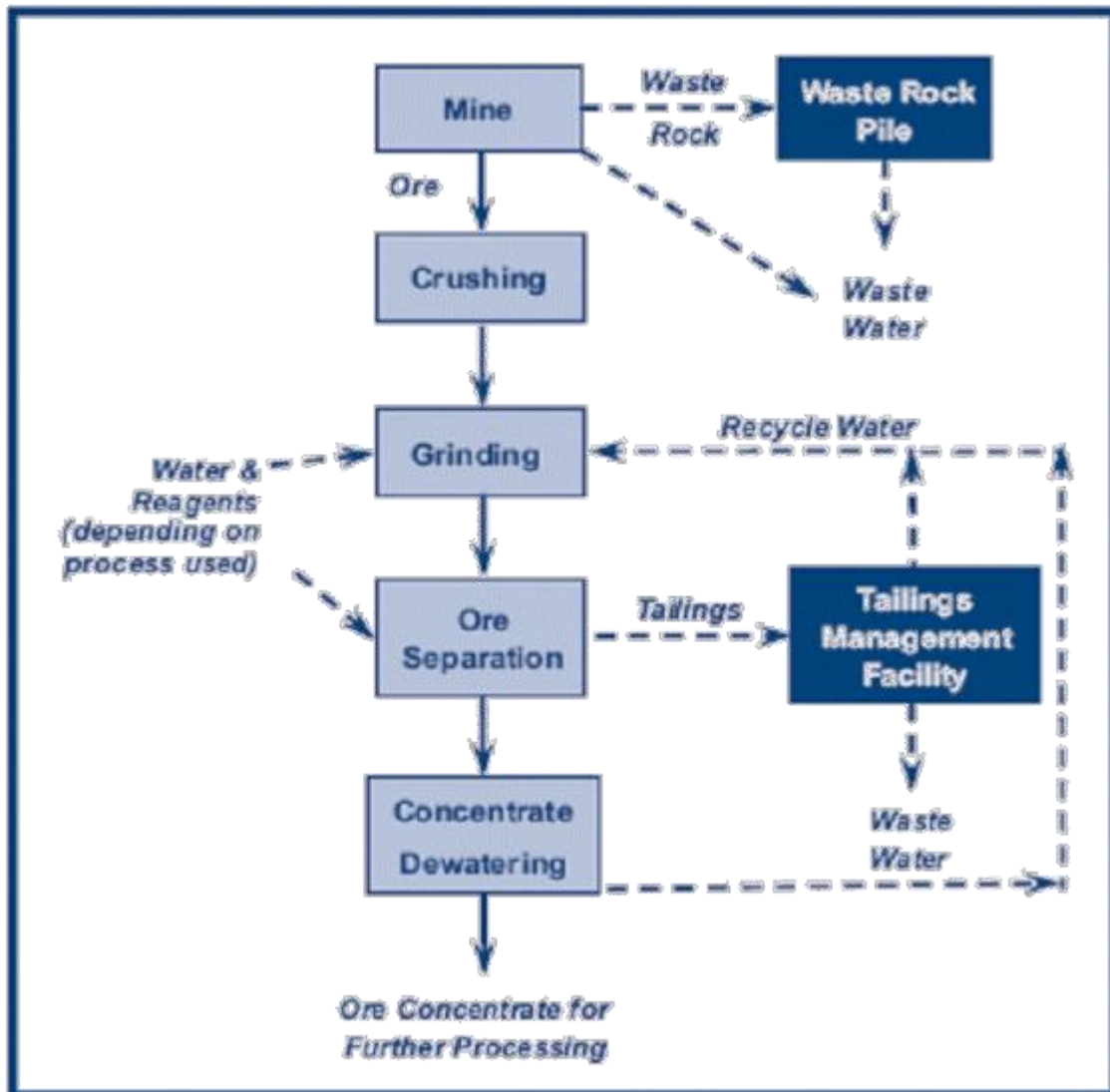


Figure 2 show the different steps in an ore processing plant (from Government of Canada)

Tailings are characterized as a fine-grained slurry mud, and depending on ore-type and processing technique, they can contain very high proportions of the ore and processing-chemicals (Ramirez-Llodra et al., 2015). The composition of tailings varies with ore-type and processing methods, but is typically known for containing heavy metals, processing chemicals from the separation processes and sulphide bearing minerals (Vogt, 2013).

Today, the majority of the active mines worldwide use conventional land-based dams for managing the tailings produced by adjacent mines. The main reason for using conventional dams is the economic benefits from reduced processing-operations of extracted rock. On the other hand, this method requires large areas of land, in addition to a long-term waste management strategy from the mines (Cornwall, 2013). Many environmental challenges are

associated with mine tailings, and according to Vogt (2013) the main challenge is conducting an environmentally safe mine. Ramirez-Llodra et al. (2015) supports Vogt by stating that poor waste management of dams may cause severe destruction and pollution of large land areas, through acidification (acidic rock leakage) or heavy metal pollution (congestion and bioavailability) into rivers, lakes or ground water. Furthermore, the effects from water pollution may impact the surrounding ecosystem for several hundreds or thousands of years (Vogt, 2013; Ramirez-Llodra et al., 2015). A study by Martin & Davies (2010), estimated to about 2-5 major, and 35 minor annually dam failures, globally, which have and still is causing harm to the local environment (Ramirez-Llodra et al., 2015).

An alternative to on-land dams is a practice called “Submarine Tailings Placements” (STP). It is argued that STPs are a more secure way of disposing mine waste, as the sea bottom is considered to be more stable, less likely to oxidize (acidification), less likely to release heavy metals (bioavailable) and economically more feasible. (Ramirez-Llodra et al., 2015). The STP-practice is divided into three separate methods; Coastal Tailings Placement (CTP), Deep Sea Tailings Placement (DSTP) Submarine Tailings Placement (STP). CTP is disposal of tailings through a pipe into the beach zone (fig. 3A), while STP is defined as placements of tailings through a pipe into a relatively shallow water depth (<100 m) (fig. 3B). DSTP is the method concerning placement of tailings through a pipe at greater water depths (>100 m) (fig. 3C) (Ramirez-Llodra et al., 2015). In theory, by using STP and DSTP one should be able to avoid dispersion and mixing of tailings in the upper layers of the ocean (photic zone). Based on the waterbody’s properties, at a

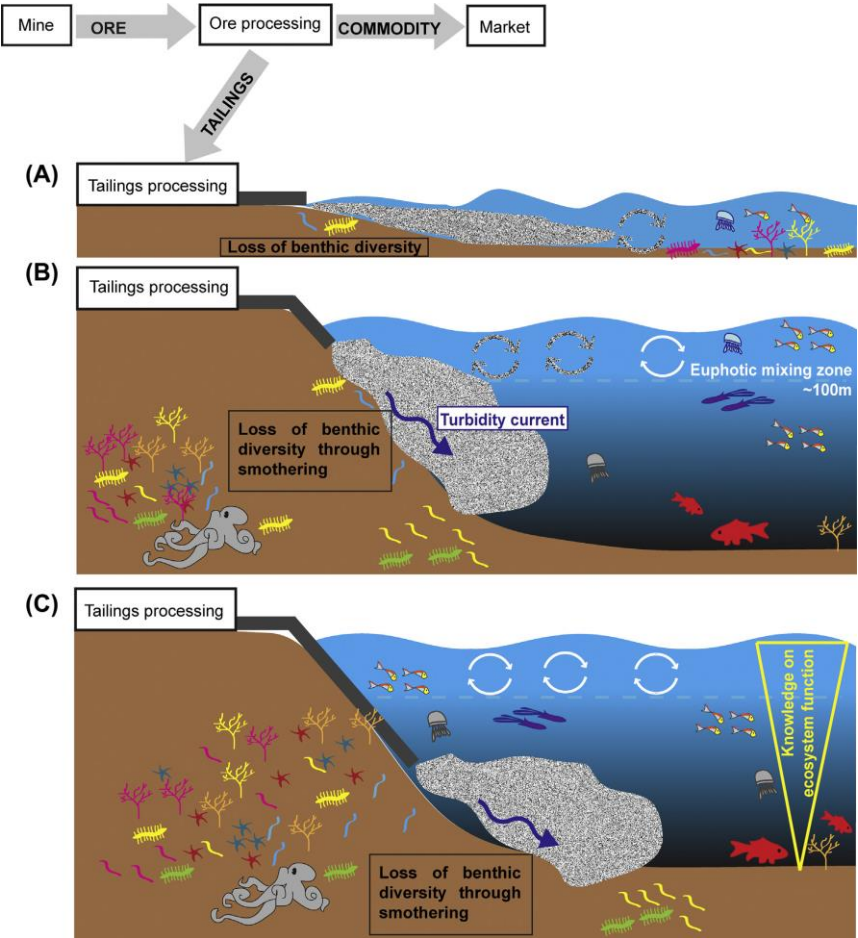


Figure 3 Representation of the different marine tailings placements-methods. A) coastal tailings placement; B) Submarine Tailings Placement and C) Deep-Sea Tailings Placement. (From Ramirez-Llodra et al, 2015)

certain depth the overlaying water is denser than the muddy mix of tailings due to a distinct pycnocline (density boundary, a combination of mainly halo- and thermocline), which ultimately suppresses the particles to mix into suspension, and further transportation (Cornwall, 2013). Again, this is the theoretical concept of the two methods, and there are still many uncertainties about effects on biota, oceanography and the reestablishment of ecosystem, amongst other issues (Ramirez-Llodra et al., 2015). Due to the uncertainties regarding tailings and environmental effects, STP is not a very common practice. In fact, about 0.6% of the 2500 large-scale mines use STP (Vogt, 2013; Ramirez-Llodra et al., 2015). Ramirez-Llodra and others (2015) conclude with Norway as the main contributor (7 active, 11 inactive, and two up for approval, anno 2015), followed by Papua New Guinea (3). Other nations using STP are Greece (1), Indonesia (1), France (1), Chile (1) and Turkey (1). Throughout the history, there has been a decrease in mines using STP due to increased awareness of potential hazards, eventually leading to an increase in national regulations/laws forbidding active STP (figure 4) (Løkeland, 2011)

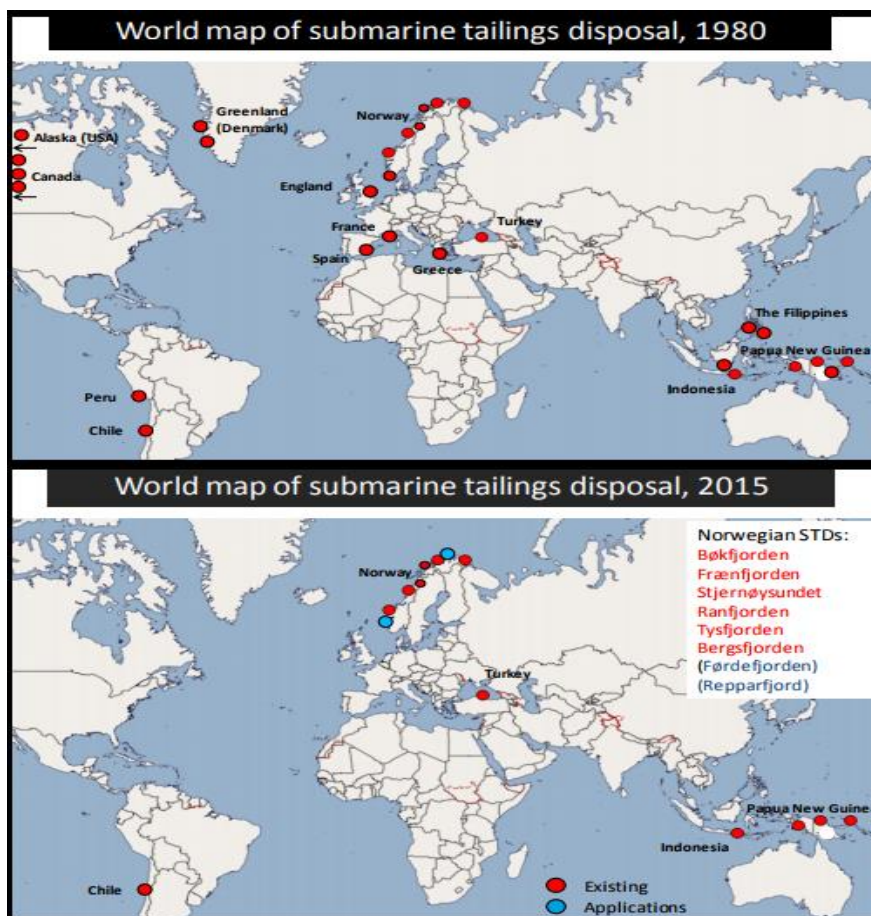


Figure 4 Overview of active STP-location In the world. From Friends of the Earth Norway (2015) evt. Løkeland

### **1.2.2 The principle of submarine tailings placement:**

The placement of tailings are conducted by tailings-discharge through a submarine pipeline. The pipeline stretches to depths > 30 m, allowing the tailings to flow downslope, limiting mixing with the biologically active surface layers of the stratified coastal areas (Vogt, 2013). After release into the marine water, mine tailings flow towards the deepest point in the given tailings recipient, where they are deposited. Rate of discharge and slope inclination are important factors for how the tailings are deposited. If the slope is greater than 12°, the chance of tailings accumulation proximal to the discharge site is minimized, and the tailings flow down slope. If the slope is less than 12° and has a high discharge-rate, tailings may accumulate, resulting in topographic changes that may block the pipeline (Vogt, 2013). Rapid sedimentation and steep slopes may result in episodic slope failures (Tesaker 1978, as cited in Syvistki, 1987; Ramirez-Llodra et al., 2015).

Based on experience from STP-sites throughout history, a so called “best practices” for the given methods have been made. According to Ellis (2008), a suitable STP area should be:

1. Located below the photic zone, meaning a minimum of >50-100 m below water surface.
2. Located at a low-resource area, hence not located near coral reefs, fishing grounds etc.
3. Located at an area with low velocity currents.
4. Tailings should contain chemically inert sediments

By combining all of the statements above, one will minimize formation of suspension plumes from tailings-discharge, lower the risk of oxidizing potential toxic minerals (i.e. oxidization of sulphides may cause harm to surrounding environment (Simón, 2001)), minimize the rate of erosion and large scale dispersion of tailings (Ellis, 2008; Franks et al., 2011).

The best practice is made to avoid environmental challenges, which are many in marine environments. According to Ramirez-Llodra et al. (2015), the main challenges are connected to the conflict of interest between a diverse, highly active and not fully understood marine ecosystem and an excess input of anthropogenic sediments. Tailings are often associated with habitat heterogeneity due to hyper-sedimentation (1), metal and process chemicals toxicity (2), changes in organic content, grainsize, angularity, sediment plumes and turbidity (3) and materials re-suspension, upwelling and slope failure (4).

- (1) Hyper-sedimentation leads to smothering of fjord-bed fauna and natural sediments, changing seafloor topography and characteristics.
  - (2) Metal and process chemical toxicity is due to input of tailings with high toxic metal or chemical concentrations. If given the right conditions, the toxic substance becomes bioavailable, allowing uptake of toxic compounds into animals.
  - (3) Changes in organic content, grainsize and angularity may cause disturbance in both the pelagic and benthic fauna.
  - (4) Up-welling and slope failures may occur episodically, which results in remobilization of sediments and higher lateral dispersion of tailings.
- (Ramirez-Llodra et al., 2015)

### **1.3 Previous investigations and history of tailings deposition**

The three study areas, Bøkfjorden, Ranfjorden and Stjernsundet, have a long relationship with human impact due to pollution from industrial and sewage sources. As a result of this, many environmental assessments have been written in order to define the environmental status of the fjords.

#### **1.3.1 Ranfjorden**

Since the early 1900s, mining companies have extracted iron-, zink-, lead- and copper-ore from the surrounding bedrock, disposed the residual remains in the adjacent fjord, alongside a growing population, the fjord has been influenced by pollution from both industry and sewage (Syvitski et al., 1987).

Today's mining company, Rana Gruber, has since 1965 been at full-scale production. The company mines iron ore from sedimentary rocks. The associated tailings consist mainly of fine-grained quartz, micas and iron, sorted into two fractions: 1) A coarse-grained fraction, with particles up to 800  $\mu\text{m}$  and 2) a fine-grained fraction, where 20 % of the tailings are  $\leq 45 \mu\text{m}$  (Johnsen et al., 2004). Both fine- and coarse-grained tailings have been and are disposed into the fjord through a pipeline. The coarse-grained tailings disposal is situated outside the river-mouth of Ranaelva, whereas the fine-grained tailings disposal is situated 1.5 km south-east of the river-mouth (figure 5) (Helland et al., 1994). The two discharge pipes for the coarse- and fine-grained tailings are situated at 30 and 45 m depth, respectively (Ramirez-Llodra et al., 2015).

The average input of tailings to the fjord has fluctuated throughout history, being about 1.8 million tons from 1980-88, 1.1 million tons from 1989-1994 (~50 % of coarse fraction was

deposited on land due to land use purposes) and 0.9 between 1995-1997 (due to reduction in production) (Johnsen et al., 2004). According to Vogt (2013), in 2013, approximately 2 million tons of tailings was disposed into the fjord. Additionally, the tailings contain the floatation chemical Lilaflo D817M, which has a discharge about 40 kg/year (Ramirez-Llodra et al., 2015). The tailings are mixed with fresh water from the Rana River before discharge; the water flux is about 2200 m<sup>3</sup>/h for the fine fraction and 1100 m<sup>3</sup>/h for the coarse fraction (Golmen & Norli, 2013).

Due to anthropogenic influence from multiple sources, many assessments have been initiated in order to define the environmental impact of human activities. In 1980, the Norwegian Environment Agency initiated a comprehensive study in order to assess the environmental state and address the main sources of pollution. The study concluded that the inner fjord (about 90 km<sup>2</sup>) hosted sediments and water with high concentrations of polycyclic aromatic hydrocarbons (PAHs) and heavy metals (mainly Pb). Not only was toxicity high, but physical smothering of the fjord-bed occurred, which caused negative impact on the local fauna, ultimately decreasing biodiversity (Kirkerud et al., 1986). At the time, organisms in the fjord contained such high PAH-concentrations that eating the organisms was considered hazardous (Kirkerud et al., 1986). The main sources of PAH-pollution was established to derive from the local ironworks and coke plant. Heavy metals were released into the fjord through the discharge of tailings, which at the time, was about 2.1 million tons of tailings, were Pb, Zn and Cd were the main pollution contributors (Kirkerud et al., 1986).

A more recent assessment by the Norwegian Institute for Water Research (NIVA) on behalf of Rana Municipality was committed in 2003 (Walday et al., 2004). This assessment stated that the fjord was considered to be little affected by sewage except some local discharge locations. Furthermore, the report stated that the elevated input of inorganic particles from mine tailings had a larger impact on the environmental quality, as it leads to smothering of hard- and soft-bottom fauna communities in the fjord. In addition, the fjord floor was in general moderately polluted by heavy metals (Cd, Cu, Pb and Zn) and (PAHs).

Despite being moderately polluted, the levels of heavy metal and PAHs pollution is considered a significant decrease in pollutants (since 1986), and the report states that it is most likely due to local environmental measures and closure of polluting industry.



A local project in Ranfjorden, “Fylkesvise tiltaksplaner: Nordland” (regional action plans: Nordland) has shown that current information on discharges of pollutants into Ranfjorden is insufficient. Due to lack of data, a direct correlation between decreasing sediment concentration and decrease in discharges cannot be made. (Olsson et al., 2003 & NIVA 4839-2004, p. 11.). This emphasizes once again the need for more research on the impact of tailings in fjords.

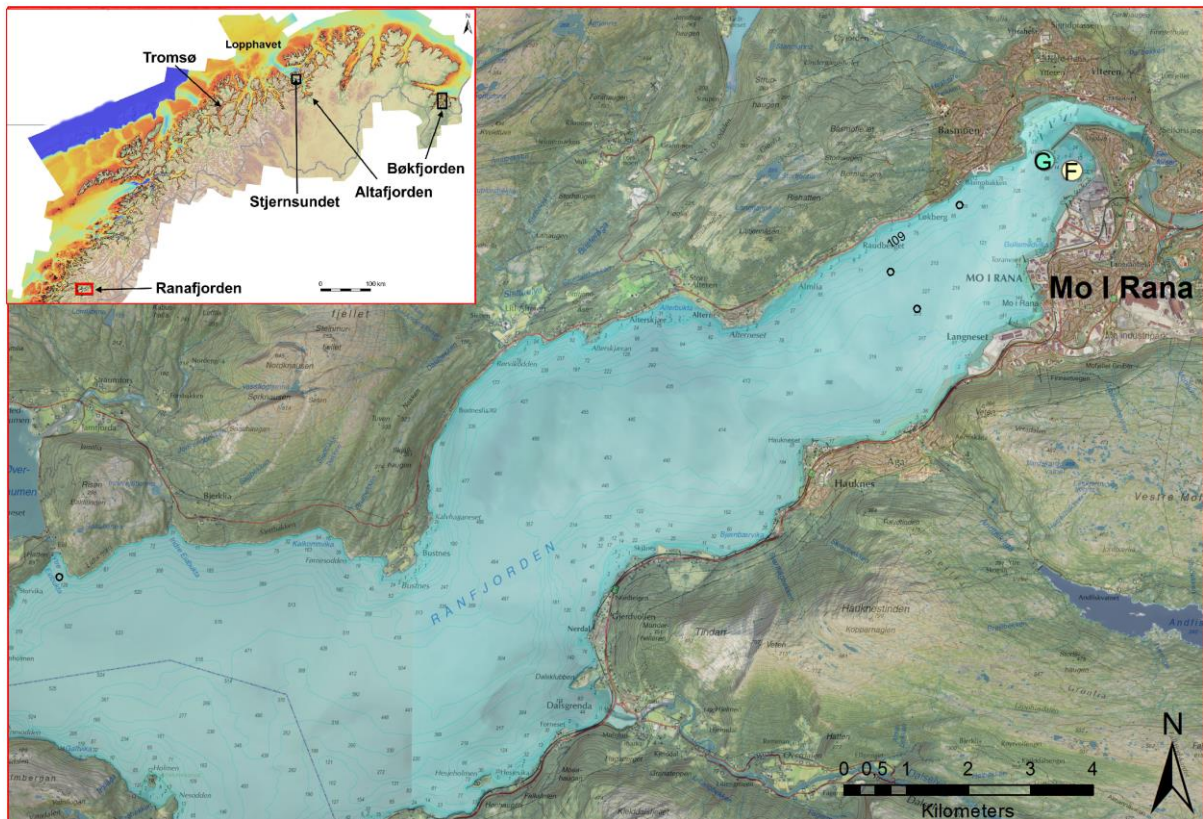


Figure 5 Overview map of inner Ranfjorden. Two points (G & F) indicate the tailings output source of coarse-grained tailings (G) and fine-grained tailings (F).

### 1.3.2 Bøkfjorden

Bøkfjorden has a long history of tailings deposition, and the fjord has hosted gangue rock from the adjacent mining activity, under the direction of the local mining company AS Sydvaranger (later Sydvaranger Gruve AS). The company started extracting iron-ore in 1906, from an open pit mine located in Bjørnevattn (figure 6), situated 8 km south-southwest from Kirkenes city center. The iron-ore in Bjørnevattn is extracted from two zones in an amphibolite. Within the amphibolite, the iron-ore occurs in banded iron-ore formations (BIFs), which are alternating layers (2 – 10 mm thick) of quartz and magnetite, whereas

magnetite is the targeted mineral (Ramberg et al., 2013). The tailings have been disposed by pipeline, after being thickened, mixed with seawater and deaerated (Vogt, 2013). Today (2018) the local mine is inactive.

Bøkfjorden was used as recipient of tailings in 1976. (Simonsen, 2017). Prior to making Bøkfjorden the host of tailings, Langfjorden, a narrow side inlet to Bøkfjorden west of Kirkenes, was used. During 1906 - 1974, an unquantified amount of gangue rock was released into Langfjorden (Simonsen, 2017), which caused changes in the fjord-topography, consequently making the mining company to change deposition-site to Bøkfjorden. From 1976-1997, approximately 56 millions of tons of mine tailings was released through a submarine pipeline (Simonsen, 2017). After a 12-year long halt in operations, the mine reopened in 2009, under the name of Sydvaranger Gruve AS and released approximately 24 million tons of tailings over a 6-year period before closing down, again (Simonsen, 2017). At first, tailings were led through a submarine pipeline to 20m water depth (Skei and Rygg, 1989), gradually moved deeper and further out-fjord, resulting in a pipeline stretching 450m out-fjord from Kirkenes, releasing mine tailings at a depth of 28m (Berge et al., 2012) as shown in figure 6.

Overall, the mining activity has led to a release of 80 million tons of mine tailings into the fjord over a 27 year period, making the annual discharge about 3 million tons (Simonsen, 2017). The tailings consist mostly of extremely fine-grained quartz, amphibole and some magnetite. In addition to gangue rock, seawater and floatation chemicals have been added to the tailings in order to make the mix of particles denser than surrounding water, making the masses sink towards deeper depths (Berge et al., 2012). In connection with the long record of tailings, many assessments have been written on Bøkfjorden. Skei & Rygg (1989) assessed the fjord's environmental status and mapped areas influenced by tailings by investigating bed-sediments, soft-bed fauna and particle distribution in connection with mining waste disposal activities in the fjord. The study concluded that a 26 km<sup>2</sup> area as far as 13 km out-fjord had been, at the time, significantly influenced by tailings (area in-fjord from/south of Reinøy). The area showed a reduction in fauna diversity, mainly caused by physical smothering of the fjord-bed and reduction in organic content in the bed-sediments. Skei & Rygg (1989) defined the environmental state to be in a "moderate state" at the fjord head, and in a "normal state" further out-fjord toward Reinøy. No evidence of influence from tailings was found north of Reinøy. Regarding heavy metal pollutions, the general sediment-concentrations in the fjord were considered to be at background state (class I), except at the station close by the river

mouth of Pasvik river. In this area, the Ni-levels were elevated (30-40 mg/kg), which is considered to be a good state (class II) (Skei & Rygg, 1989).

In 1989, Skei mapped the distribution and sedimentation of tailings in Bøkfjorden, and concluded that most of the sedimentation occurred proximal to the disposal source (Skei, 1990). In 1994, Skei and others followed up on the report from 1989 and 1990, investigating fjord-fauna, -sediments and suspended particles. The report concluded that there was little evidence of improved environmental status, which was classified as the same (moderate biodiversity, and background levels of heavy metals) (Skei et al., 1995). A new report for monitoring the environmental status and rehabilitation-rate of the fjord was conducted in 2007 by Norwegian Institute for Water Research (NIVA) (Skaare et al., 2007). At the time, Sydvaranger Gruve had been inactive for approximately 10 years. Based on a 10-year long halt in output of mine waste into Bøkfjorden, the researchers from NIVA expected a distinguishably different sediment cover on top of previously tailings-influenced fjord-bed (Skaare et al., 2007). The report concluded that the sediment cover in the fjord showed new characteristics. An increase in TOC (Total organic content), crease in biological activity, thus resulting in well-oxygenized sediment top-layer in most areas of the fjord. Soft-bed fauna in close proximity to the pipeline still showed a distinct contrast to the outer-fjord fauna, in terms of lowered biodiversity and species numbers and was considered to be of moderate (class III) to good conditions (class II) by Norwegian environmental standards (Skaare et al., 2007).



Figure 6 Overview map of Bøkfjorden, showing the adjacent mine (red) and the tailings output source location (blue).

### 1.3.3 Stjernesundet

Since 1961, there have been mining activities related to the nepheline-syanite rich bedrock in the mountain Nabbar on Stjernøya in Finnmark. Two mining companies, Elkem Nefelin (from 1. January 1993: North Cape Nefelin AS) and Sibelco Nordic AS have been extracting minerals from 1961-1993 and 1994 to present, respectively (Larsen et al., 2012). In 1977, Elkem Nefelin got a permit to dispose an amount of 200 000 tons of tailings annually (Larsen et al., 1993). In 1994, Sibelco Nordic AS was granted a new disposal-license with increase of emissions to a maximum of 300 000 tons annually (Trannum & Vögelle, 2000; Larsen et al., 2012), and the license is still valid today. The tailings are disposed into Lillebukta, a 1km

wide and 50m deep bay at the foot of Nabbern, on the brink of Stjernøya, leading out into Stjernesundet (figure 7). The tailings have been (and still are) disposed in the bays shoreline (within the tidal zone), and consist of fine-grained, dry-crushed particles with no exposure of processing-solvents or flocculation chemicals (Larsen et al., 2012).

The tailings constitute amphibole, feldspar, nepheline, pyroxene and biotite. About 45% of the tailings particles are <63  $\mu\text{m}$  and 15% <20  $\mu\text{m}$  (Industry, 2014). Heier (1961) showed that the nepheline syenite on Stjernøy is characterized by silica (Si)-deficiency and excess aluminum (Al) (Heier, 1964).

Due to multiple renewals in emission licenses (and increase in production), environmental assessments have been written in order to assess the environmental effects of the tailings disposal into Lillebukta. Environmental studies from 1993, 2000, 2004 and 2012 conducted by NIVA and Akvaplan-niva, have shown significant influence by the disposal of tailings into Lillebukta (Larsen et al., 1993; Trannum and Vögelle, 2000; Larsen et al., 2004; Larsen et al., 2012). The four surveys carried out, stated that an increase in environmental impact of tailings between 1993 and 2000 occurred, followed by a stabilizing trend – no or little changes in environmental effect from 2000 – 2012. Throughout a 40-year history of tailings deposition in Lillebukta, a significant impact on both soft-bed and hard-bed fauna has been observed. In shallow marine waters stretching up to 2 km west and east from Lillebukta, the smothering from tailings is present (due to high sedimentation rates), and have led to visible effects on fauna (Larsen et al., 1993). Tailings have formed a hard, compact and nutrient-poor sediment-bed, which has depleted the soft-bed fauna. Most of the remaining soft-bed species are opportunistic species, which tolerate high sedimentation-rates (Larsen et al., 2012). There is evidence of movement of tailings into the deeper waters of Stjernesundet. Through episodic submarine mass wasting of tailings in Lillebukta, the waste moves to deeper depths, hence resulting in lower TOC-content (Larsen et al., 2012). Despite some input of tailings into Stjernesundet, the sound is considered to be unaffected by tailings (Larsen et al., 1993; Trannum and Vögelle, 2000; Larsen et al., 2004; Larsen et al., 2012).



Figure 7 Overview of the studyarea, Stjernsundet. Marked in red is the mountain Nabbern (Location of the local mine). Marked in orange is Lillebukta (deposition site for tailings).

## 2 Study area

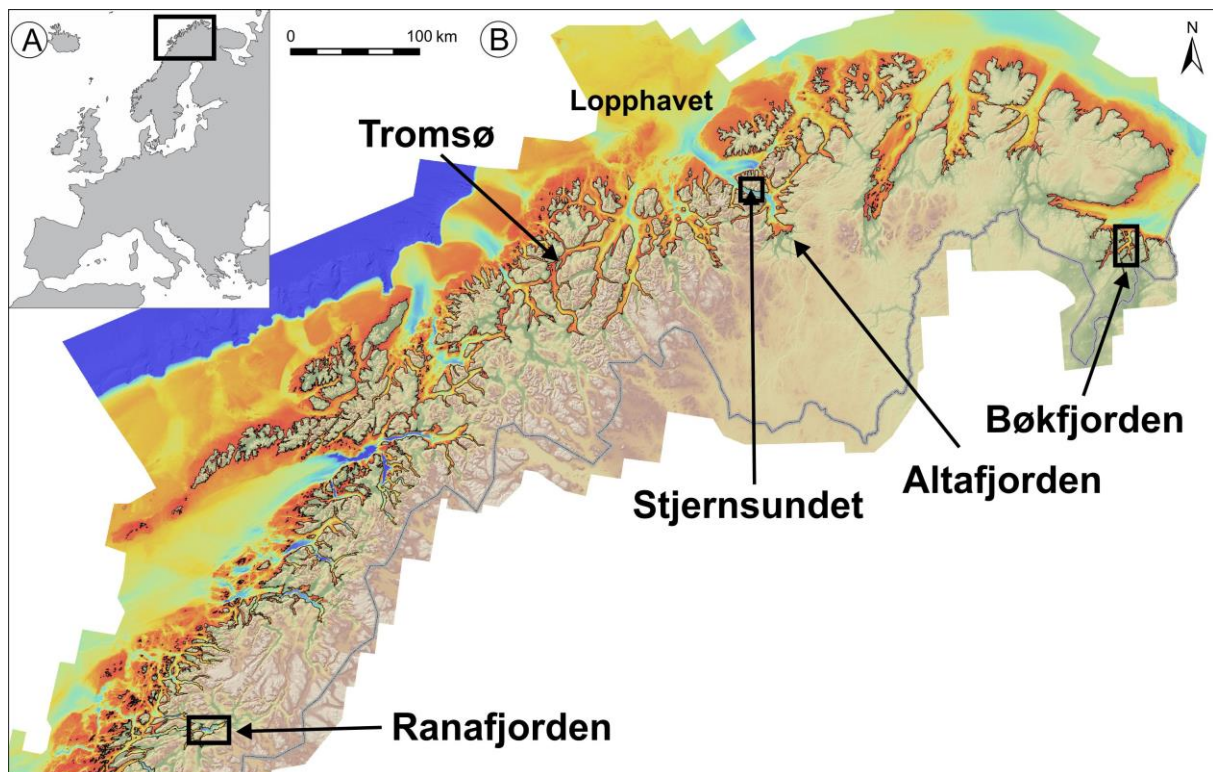


Figure 8 A show an overview map of Europe, showing the region where the studysites are located. B show Northern Norway, the bathymetry of the coastal areas and the three study sites Ranfjorden (south), Stjernesundet (north-west) and Bøkfjorden (north-east). Dark blue represents deep water, and red represent shallow water.

### 1.1 Ranfjorden

#### 2.1.1 Physiographic setting:

Ranfjorden is a 67 km long and 2-4 km wide WSW-ENE oriented temperate fjord situated about  $66^{\circ}10' - 66^{\circ}23' N$  and  $13^{\circ}00' - 14^{\circ}10' E$  in northern Helgeland, Nordland, Northern Norway (figure 8 & 9) (Lyså et al., 2011). The fjord stretches N-E from the Norwegian sea in the south-west, towards the city of Mo i Rana at the fjord head in the north-east. The total area is about  $175 \text{ km}^2$ , separated by four main basins and two submarine thresholds (Lyså et al., 2004; Walday et al., 2004). The deepest and widest basin is the innermost basin, with depths up to 530 m, whereas the outermost basin is narrow and shallow, with depths up to  $\sim 300$  m deep. (Lyså et al., 2004). The fjord is recipient for sediments and water from an about  $4500 \text{ km}^2$  drainage area, including run-off from three glaciers (Svartisen, Høgtuvbreen and Okstindbreen) and multiple rivers. The fjord is situated in a valley – and fjord-dominated landscape (mountain peaks up to 800 meters above sea level (m.a.s. l.) Lyså et al., 2004).

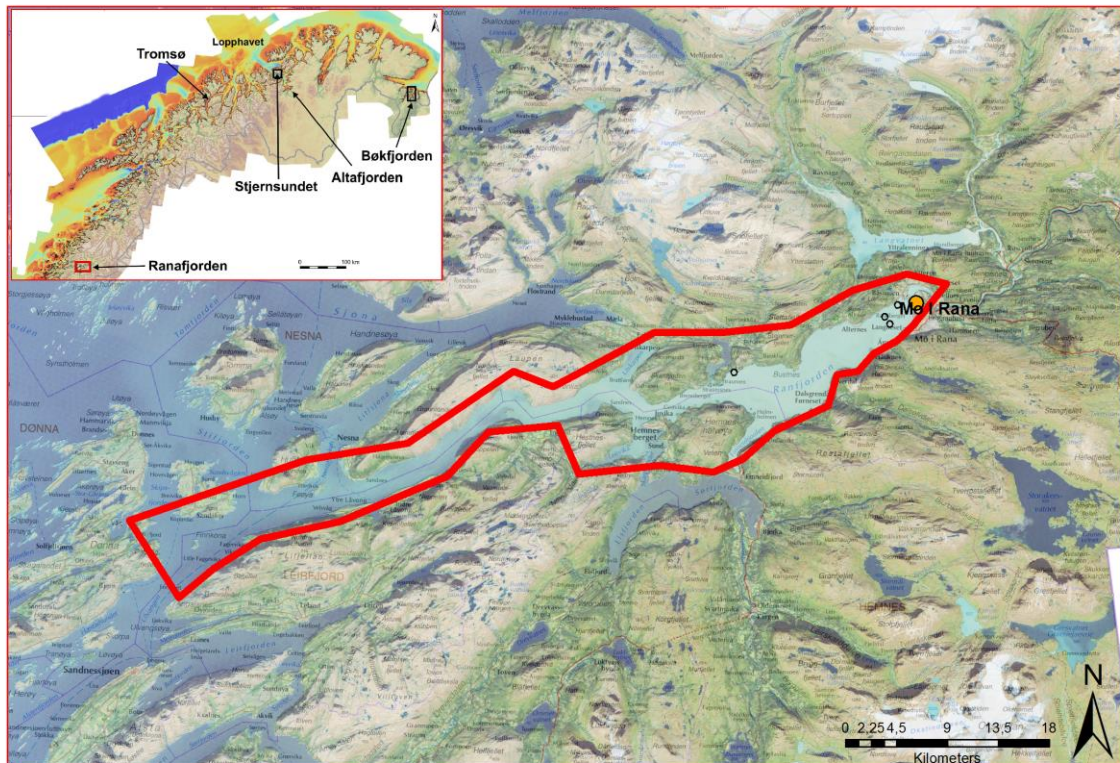


Figure 9 Overview map of Ranfjorden, showing the full extent of the fjord (marked in red).

The area of interest is situated in the innermost basin, and is approximately 26 km long, stretching from Mo I Rana harbor at the fjord head, towards the first threshold located outside Langnes oden (Walday et al., 2004). The main discharge of freshwater comes from two local rivers, Dalselven (mean discharge of  $8 \text{ m}^3/\text{s}$  during 1930 – 1960) and Ranaelva ( $174 \text{ m}^3/\text{s}$ ) (Walday et al., 2004). The river mouth is located north of the local harbor, with relatively shallow depths (10 – 40 m). The fjord bathymetry changes quite drastically about 100 m outside the river mouth and harbor, with a  $6^\circ$  slope inclination reaching up to 200 meter deep. The fjord-bed has a inclination of  $>2^\circ$ , moving from 100 m to  $\sim 500\text{m}$  outside Bustnes, 10 km out-fjord from Mo I Rana harbor. Additionally, the fjord-bed in the innermost part of Ranfjorden features two submarine canyons stretching from a) the river mouth and disposal site of coarse-grained sediments of Ranaelva and b) the tailings disposal source, towards the deep part of inner Ranfjorden (see figure 10). The two canyons merges into a submarine meandering channel system, with one main channel alongside abandoned channels. The channels leads further out-fjord to the deep basin.



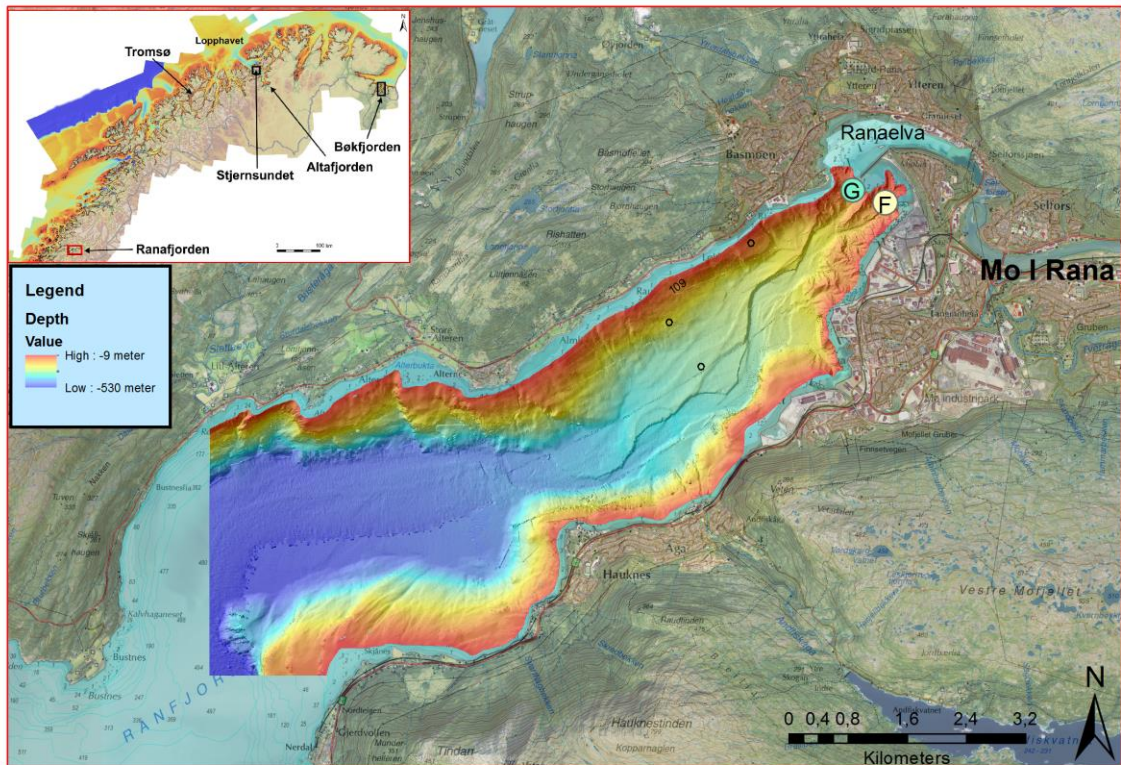


Figure 10 A bathymetric map of inner Ranfjorden, showing the presence of two sub-marine canyons stretching from the coarse-grained (G) and fine-grained (F) tailings output location down to the meandering channel system along the fjord bed. Depths ranging from shallow (red) to deep (blue).

### 1.1.1 Geological setting

The surrounding mountains are constituted by series of thrust faults of Caledonian origin (490-390 million years ago (Ma)), whereas the innermost part of Ranfjorden is part of the lower Rödningsfjäll-complex, a Caledonian-sub group (Ramberg et al., 2013). The complex is dominated by medium grade metamorphosed rocks (mica-rich schists and marble) and sedimentary rocks with high Fe-grade iron ores as the metamorphosed rocks contains large amounts of hematite and magnetite (up to 33 % iron-content) (see figure 11). In addition, sulphide ores occur in the region alongside with amphibolites, granites, tonalities and gabbros. (Ramberg, 2013).

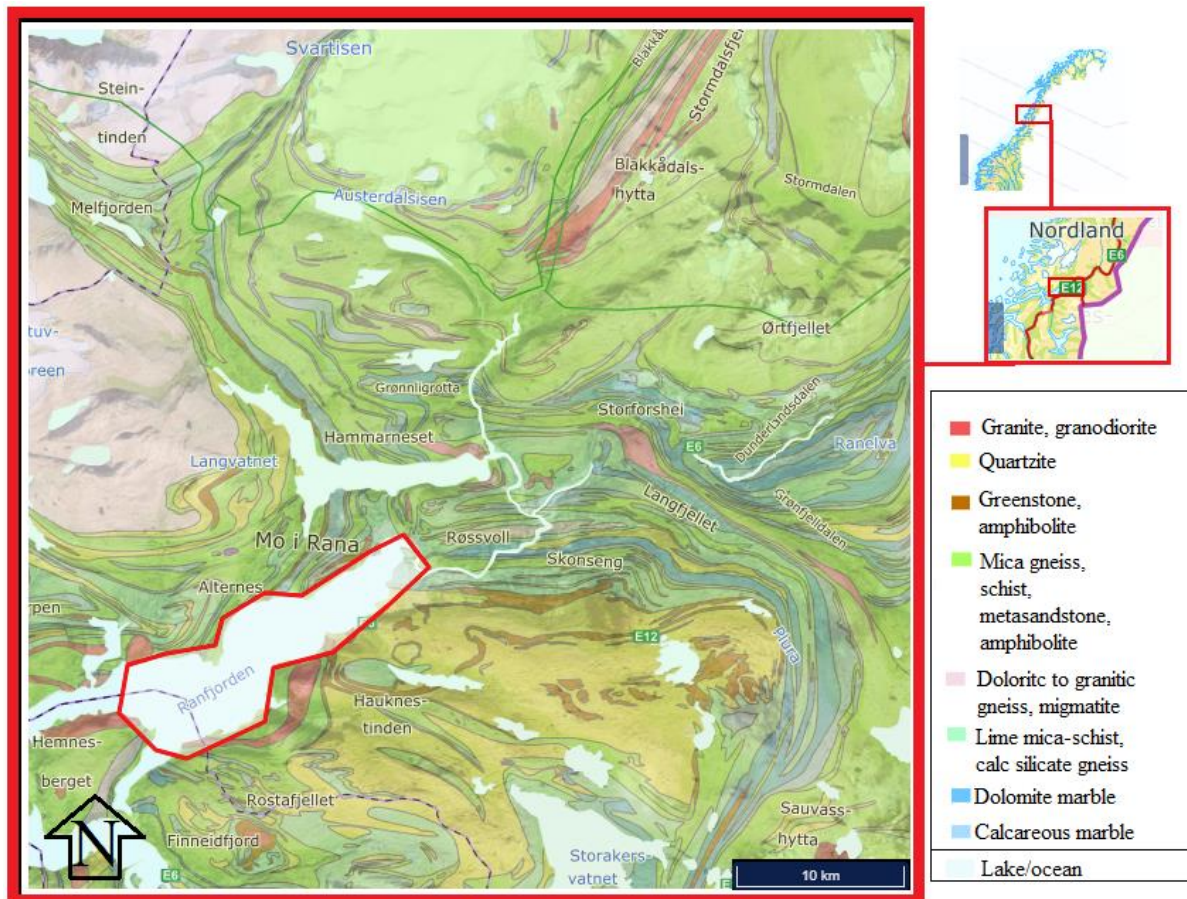


Figure 11 Geological map with overview of the regional bedrock from Svartisen in the north, to the innerpart of Ranfjorden in the south. Derived from Geological Survey of Norway's (NGU) database.

According to Øyehaug (2016), the landscape has since the formation of the orogenic bedrock, been through uplift and erosion in the pre-glacial phase (Devonian – Neogene). Throughout the past 2.6 Ma (Quaternary), multiple glaciation and deglaciations (up to 40 ice sheet covers) have shaped the valley- and fjord-dominated landscape (Øyehaug, 2016). Local scour marks and glacial landforms from last glacial maximum (24-21 ka B.P (thousands of years before present)) indicate that the ice sheet had a westward movement. As the ice-sheet became thinner during the deglaciation, the ice-sheet movement became gradually more topographically controlled, resulting in a southwestern-flowing ice-sheet, hence forming glacial valleys, with outlet into Ranfjorden (figure 12) (Øyehaug, 2016). Around 9.5 ka BP, further melting of the ice-sheet led to a separation between the continental ice-sheet and a satellite glacier, today known as Svartisen was formed (Blake & Olsen, 1999). Blake & Olsen (1999) concluded Ranfjorden and surrounding areas have been ice-free since about 9.31 ka

BP. Post glacial cover, Ranfjorden has been the the main recipient of sediment and water runoff from Svartisen.

Furthermore, the Rana-region is considered the most seismically active area in mainland Norway, and is known for the largest earthquake in Fennoscandia in the recent times (1819) (Hicks et al., 2000). The study conducted by Hicks and others (2000) conclude that the high occurrence earthquakes are most likely a result of post-glacial crustal up-lift.

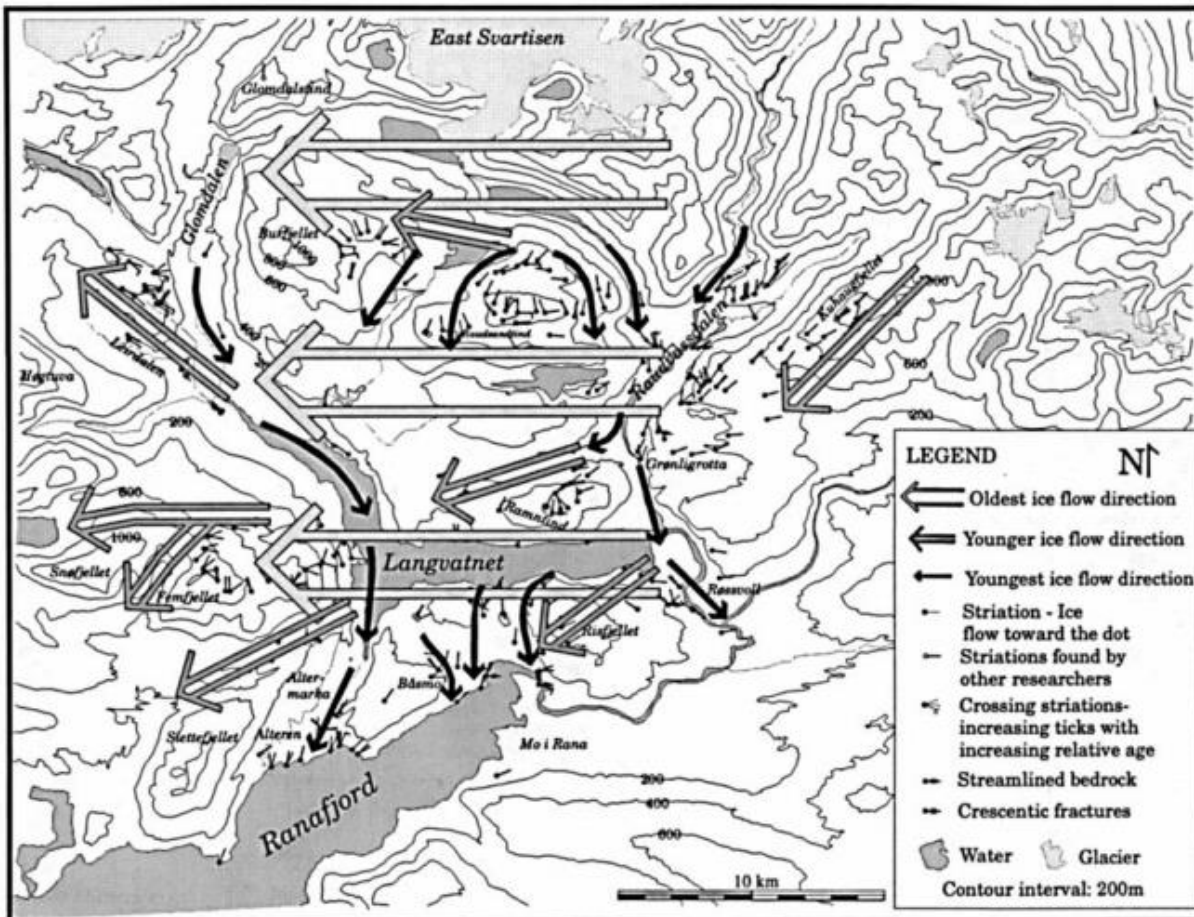


Figure 12 Map of ice flow direction in the Rana region during last glacial period. From Blake & Olsen (1999).

### 1.1.2 Sediment sources

According to Johansen et al. (2004), the main supplier of naturally derived sediments to Ranfjorden is Ranaelva, with an annual input of 35,000 tons of inorganic sediments, which origin from both erosional products and waste from mines situated in the river's catchment area. The coarse-grained riverine sediments are deposited proximal to the river mouth, whereas the fine-grained particles enter suspension and are transported further out-fjord (Due to the regional geology, the river carries elevated levels of metals (Fe, Zn, Pb and Cu) (Kirkerud et al., 1977). Anthropogenic sources have become the main supplier of inorganic sediment, due to input of tailings from a local coking plant, ironworks and the mining

company Rana Gruber. During the 1980's the coking plant and ironworks closed down, making Rana Gruber the main contributor with an annual input of 2,000,000 tons of tailings (Johansen et al., 1994).

### **1.1.3 Hydrology**

According to CTD measurements (conductivity, temperature and density) conducted by Johansen et al. (2004), the stratification of Ranfjorden is separated into two layers. A brackish surface layer which forms as the high freshwater run-off to Ranfjorden from Ranaelva (174 m<sup>3</sup>/s) mixes with the saline fjord-water. Seasonal changes in river runoff changes the thickness of the surface layer (high runoff (spring/summer) = thick, low runoff (winter) = thin). Below the brackish layer, a homogenous saline water mass is situated. The water masses are considered very stable (Johansen et al., 2004).

Transmission measurements were also conducted by Johansen et al. (2004), which showed that the water masses in the inner part of Ranfjorden carried suspended particles with concentrations from 5 to 20 mg/l at certain depths (20 – 30 m and 40 – 50 m). Current measurements conducted in the same study showed that the shallow (15 m depth), innermost parts of Ranfjorden, proximal to the tailings disposal sites had a north or north-east direction, where the currents upwelled to about 1-2 m, which is a strong indication of estuarine circulation (compensation current from river-generated out-flow). Along the submarine meandering channel the main current direction was outward, although frequent shifts in direction indicated tidal influence. The current shifted from moving in- and out-fjord (north-east and south-west) (Johansen et al., 2004).

## **1.2 Bøkfjorden**

### **2.1.2 Physiographic setting**

Bøkfjorden is a 23 km long, 2-3 km wide N-S oriented fjord, situated about 69.7429°N 30.0521° in Sør-Varanger, East-Finnmark, Northern Norway (figure 13) (Simonsen, 2017). The fjord stretches from the main fjord Varangerfjorden and island Kjelmøya at the fjord mouth in the north, towards the city of Kirkenes at the fjord-head. The surrounding landscape is characterized by flat, undulating mountains (up to 200 m high), varying between steep and gradually sloping mountainsides, descending into the fjord.

Moving from Kirkenes and further out-fjord, the fjord gradually becomes deeper, ranging from 10 - 290 m. The shallowest areas are located at the fjord head east and south of

Kirkenes, whereas the deeper part is situated west of Reinøy and further out-fjord. At Kirkenes, Bøkfjorden is separated into two, whereas Langfjorden branches off towards SW, and Bøkfjorden continues towards Elvenes, south-east of Kirkenes (Simonsen, 2017). Further out-fjord, Bøkfjorden meets Reinøy, and the side-fjord inlet of Korsfjorden. At the fjord mouth, situated between Kjelsmøya and the mainland peninsula, a 100 m deep sill separates Bøkfjorden and the main fjord Varangerfjorden.

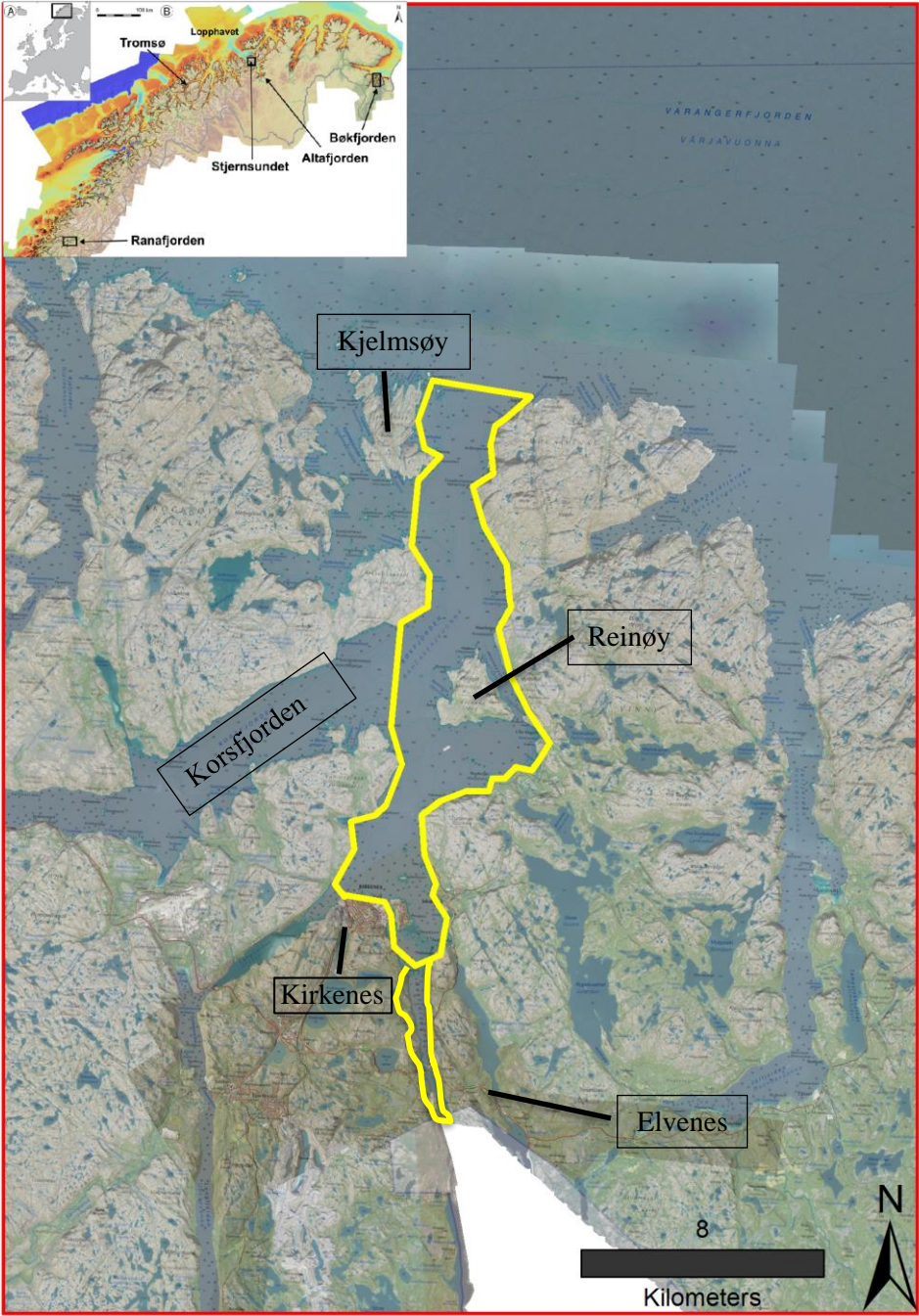


Figure 13 Overview map of Bøkfjorden, showing the full extent of the fjord (marked in yellow).

The innermost parts of Bøkfjorden feature sub-marine channels (figure 14). The channels occur around the tailings output location, about 100 m north of Kirkenes harbor. Over a 1.5 km distance, multiple channels merge into one large and wider channel, forming a submarine canyon at the deep basin slope, situated west of Reinøy. The shallow inner part of Bøkfjorden has a slope inclination of 1.2°, whereas the submarine canyon has a 5° slope inclination.

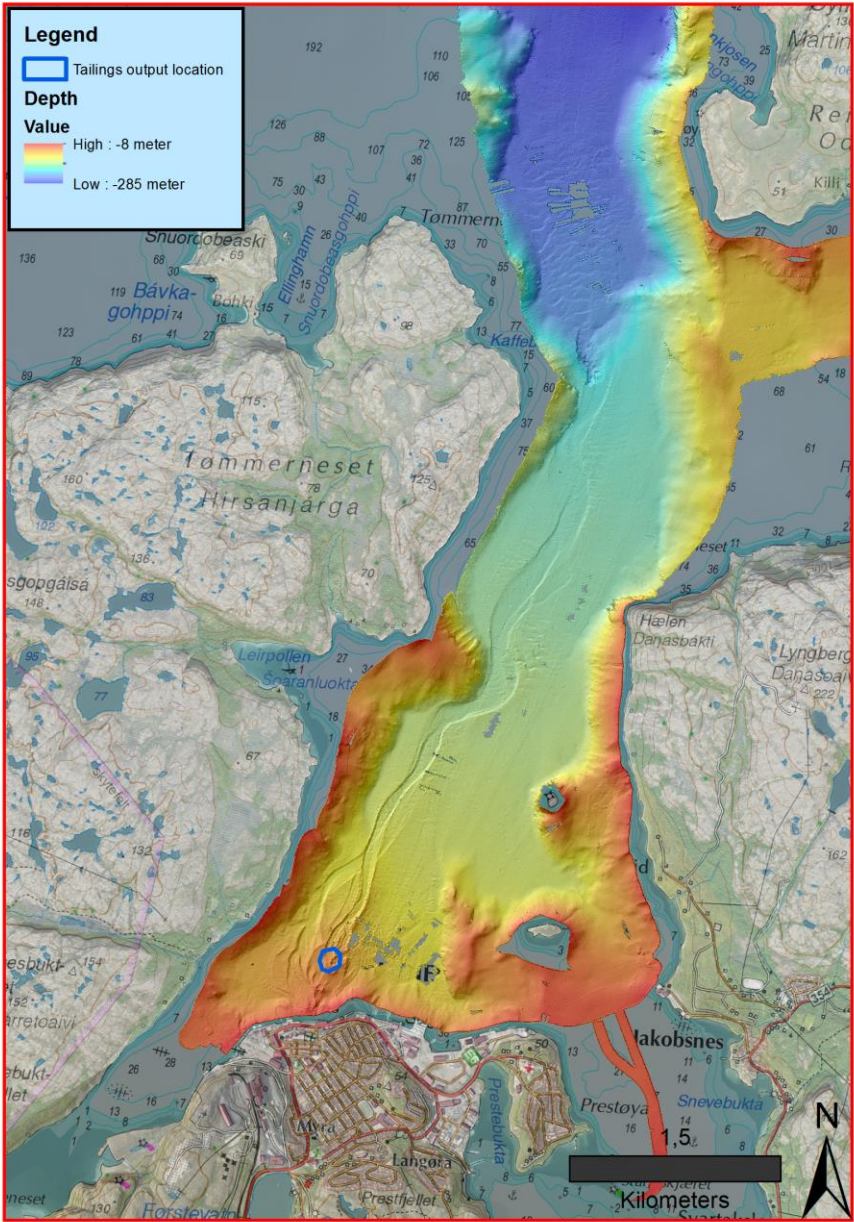


Figure 14 A bathymetric map of inner Bøkfjorden, showing the presence of sub-marine channels. Showing the tailings output source (blue circle) and depths ranging from shallow (red) to deep (blue).

**1.2.1 Geological setting**

Based on the geological map from NGU, the surrounding bedrock consist mainly of gneiss, migmatite, schist, metasandstone and amphibolite (figure 15). The rocks are part of the

Sørvaranger-Kola-complex, which is of Precambrian origin (>1600 Ma). The Archean bedrock have undergone multiple orogenesis-, rifting- and seafloor-spreading-events, making the rocks heavily deformed (Ramberg et al., 2013).

Glacial processes have formed today's landscape. Reconstruction of ice movement since LGM conducted by Marthinussen (1974), show that the region was fully covered by ice at LGM. Despite being fully covered by ice, the landscape has been exposed to sub-glacial erosion, whereas observed striations indicate an NNE-NE moving ice-flow (see figure 15) (Marthinussen, 1974). Sub-glacial erosion have been heavily influenced by local and regional topography, hence leading to directional changes in the ice-flow. Bøkfjorden seems to be a result of a) converging ice-streams (Korsfjorden and Bøkfjorden) and b) topographically controlled ice-movement, leading to a relatively deep fjord-basin, with a N-S-direction (Marthinussen, 1974).

### 1.2.2 Hydrology

According to the study conducted by Berge and others (2012), Bøkfjorden is a stratified fjord, divided into two distinct layers based on density (salinity):

- 1) Surface layer,
  - a. 3 m thick brackish water, heavily influenced by freshwater from rivers
  - b. Present throughout Bøkfjorden

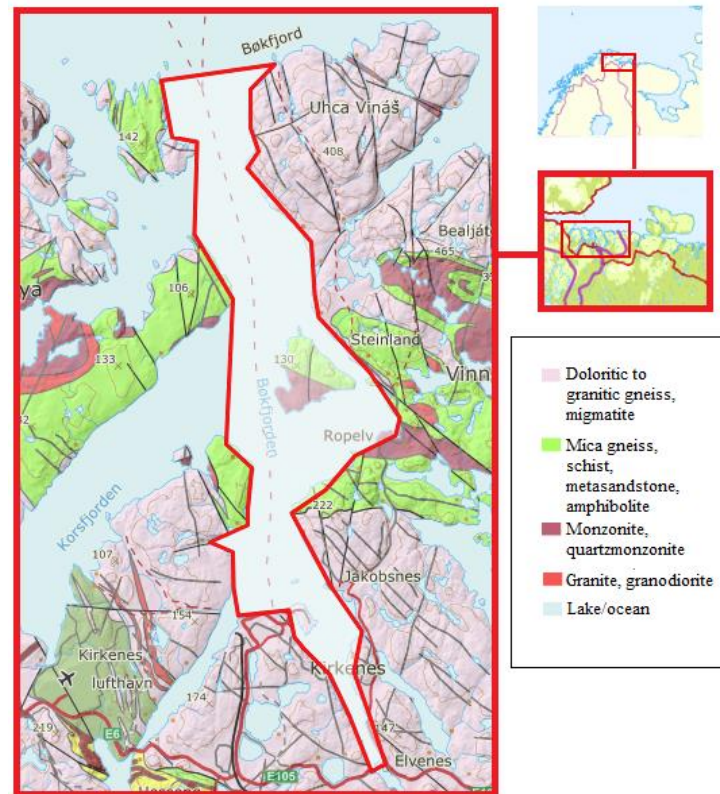


Figure 15 Geological map with overview of the regional bedrock from Varangerfjorden in the north, to Kirkenes in the south. (Derived from Geological Survey of Norway's (NGU) database)

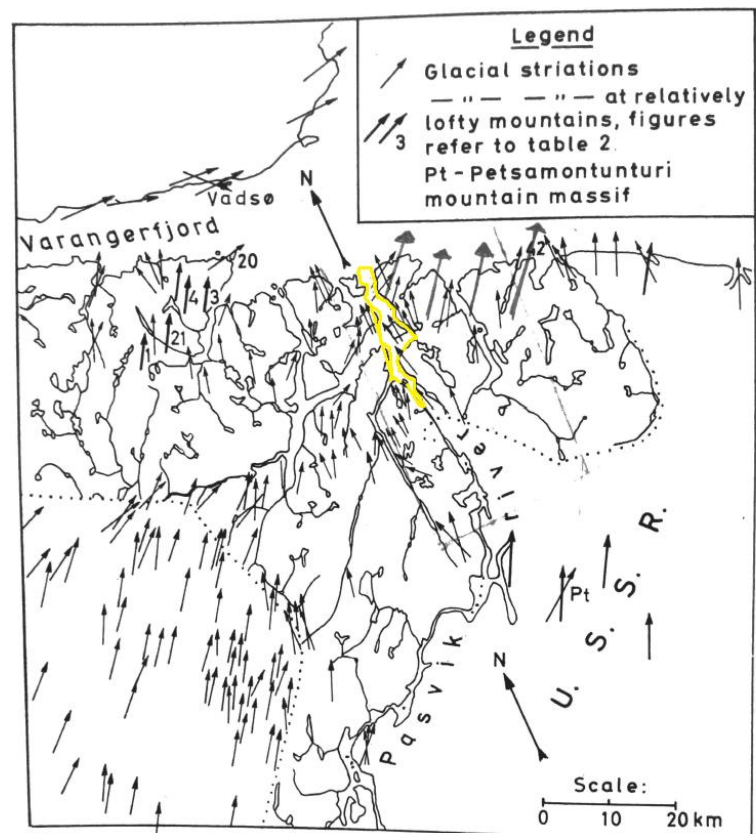
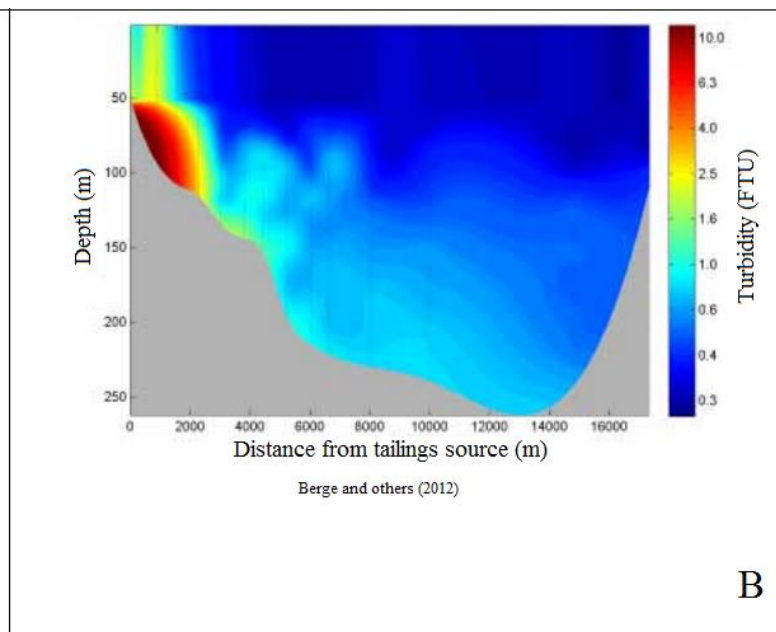
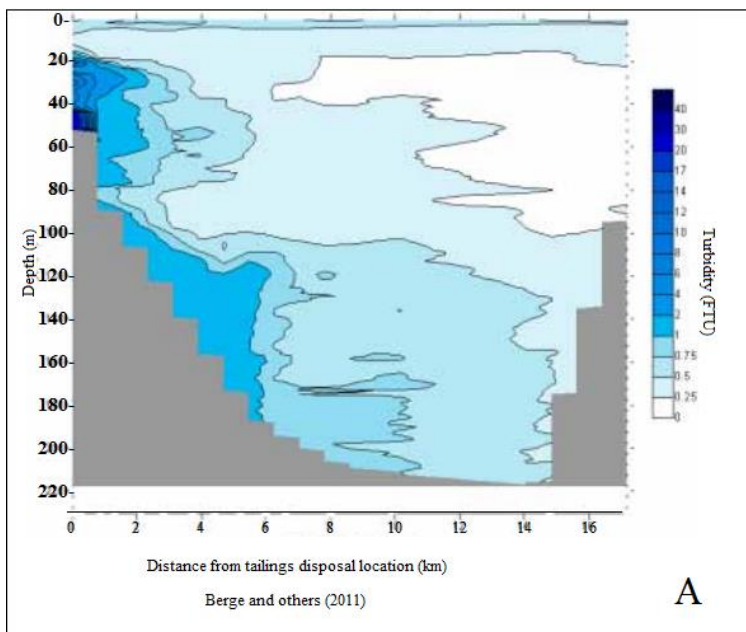


Figure 16 Map of ice flow direction in the Sout-Varanger region during since last glacial maximum. From Marthinussen (1974).

## 2) Saline deep/intermediate layer

- a. Thickness varies – between brackish layer and fjord-bed.
- b. Relative homogenous salinity – 34-35 PSU (Practical Salinity Unit (1 PSU = 1 g/kg))

The main supplier of freshwater and sediments into Bøkfjorden is the river Pasvikelva, which supplies the fjord with a mean input of  $180 \text{ m}^3/\text{s}$ , hence creating the less saline surface-layer. As of temperature changes in the fjord, no distinct thermohalines are present, only a gradual decrease in temperature from surface to bottom is seen ( $10 - 4 \text{ }^\circ\text{C}$ ). Ultimately, salinity is the deciding factor for density and stratification of the fjord (Berge et al., 2012). As of water exchange between Bøkfjorden and Varangerfjorden, it is concluded that the sill east of Kjelmsøy limits the rate of exchange, keeping the water below 100 m inside Bøkfjorden. The study by Berge and others (2011) used turbidity to visualize the transportation of particles, which indirectly show the stratification of the fjord (see figure 16). Turbidity is measured in FTU (Formazin Turbidity Units), which measures the translucency of water. The higher FTU, the more particles are present in the water (1 FTU is  $\sim 1 \text{ mg/L}$ ). In figure 17, one can clearly see the  $\sim 3 \text{ m}$  thick surface layer transporting sediments out-fjord ( $\sim 0.5 \text{ FTU}$ ). Furthermore, a high-turbidity area occurs along the fjord-bed, stretching about 6 km out-fjord. This is the transportation of fine-grained tailings from the pipeline outside Kirkenes harbor, which is contained within Bøkfjorden, inside the sill (Berge et al., 2012).





## 1.3 Stjærnsundet

### 1.3.1 Physiographic setting and climate:

Stjærnsundet is a 24 km long, 4 km wide sound with a NW-WE orientation, situated 70.2381° N 22.6240° E, between Stjærnøya and Øksfjord, 36 km NW of Alta, in Alta municipality, Finnmark, Northern Norway (figure 18). The sound stretches from LoppHAVet in the west to Altafjorden in the east. The sound is mostly 400 – 500 m deep, divided by a 250 m deep sill located south of the mountain Stobuktfjellet, west of the mountain Nabbaren. The sill is of glacial origin, characterized as a marginal moraine with an active cold-water coral reef situated on top (Plassen, Bøe & Lepland, 2009).

Apart from the sill, little changes in bathymetry occurs to the east, making Stjærnsundet the deepest basin east on the eastside of the sill, while Stjærnsundet merges with Øksfjord on the west side, gradually becoming deeper towards LoppHAVet (figure 18). The surrounding landscape is characterized by high mountains (700 – 900 m. a. s. l.) with steep mountain sides, descending into the sound. The climate is part of an arctic climate, meaning the winters are long, dark and wet, with frequent storms during both winter and autumn. The summers are relatively short and sunny (midnight sun) (Heier, 1961). The mean temperature is -8.4 °C during winter and 8.6 °C during summer (Norwegian Meteorological Institute).

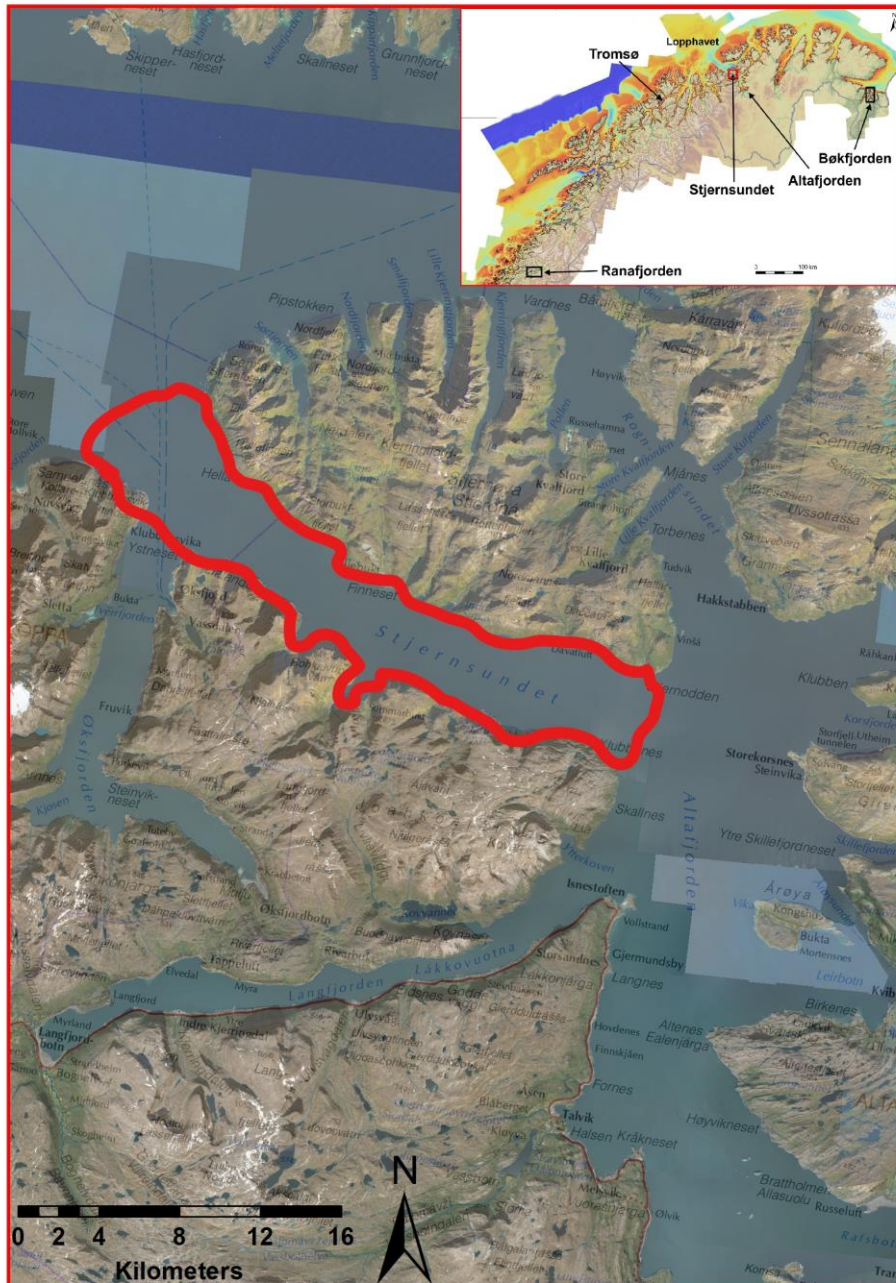


Figure 18 Overview map of the study site Stjernsundet.

### 1.3.2 Geological setting

The surrounding mountains consist mainly of mafic and ultramafic rocks, part of the Seiland-complex of Caledonian origin, whereas rocks found on Stjernøya indicate that rocks of non-orogenic origin are present, such as carbonatites and nepheline syenite (Heier, 1961). Based on the geological map from NGU, the most abundant rock is gabbro, with nepheline syenite,

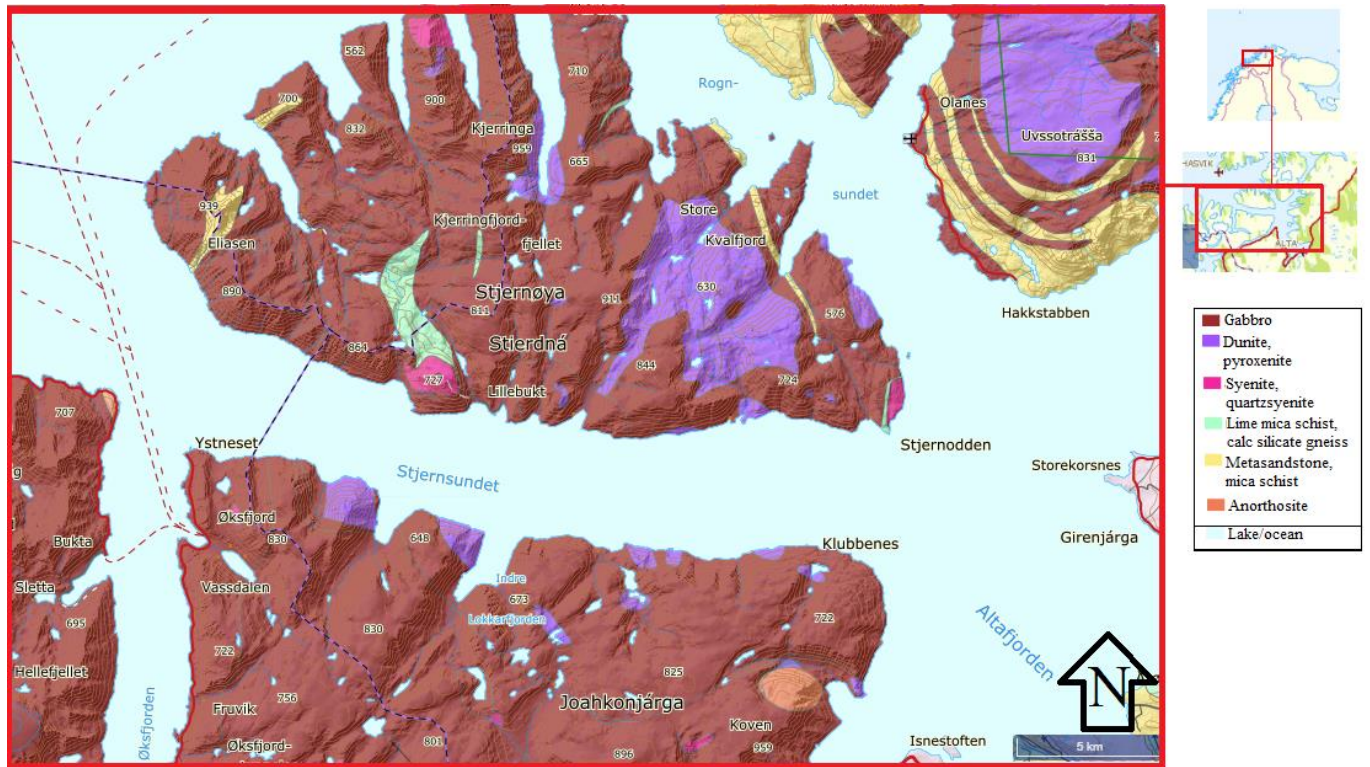


Figure 19 Geological map with overview of the regional bedrock with Stjernøya situated in the north and the mainland peninsula in the south. Derived from Geological Survey of Norway's (NGU) database.

dunite and pyroxenite occurring in smaller amounts. Findings of marginal moraines outside the trough of Stjernerundet, indicate that an ice stream has drained through the area, hence shaping of the surrounding landscape since LGM (Vorren & Kristiansen, 1986). After the retreat of the Scandinavian ice sheet, the sound has hosted a cold-water coral reef on top of the morainic sill situated mid-sound (Joseph et al., 2012).

### 1.3.3 Hydrology

According to Freiwald et al. (1997), the water exchange within the fjord is driven by the estuarine circulation, due to freshwater input in Altafjorden. CTD measurements conducted by Larsen et al. (1993) confirms this observations as a 5 – 10 m thick brackish surface layer is defined, becoming thickest at midfjord. Transmission measurements conducted in the same study show that suspension of particles occurs mainly in the upper 10 m of the water column. Elevated particle concentrations was observed at two stations located in the shallow parts of Lillebukta (30 – 70 m), 300 m from the tailings discharge site.

Lillebukta is heavy influenced by tidal and wind currents, which observations of west- and east-drifting suspension plumes by Larsen et al. (1993) indicate.

### 3 Material and methods

#### 3.1 Sediment collection

A total of 61 sediment core-samples were retrieved from all three locations. Coring was performed by the Geological Survey of Norway (NGU) within the frame of the NYKOS project, as well as the Department of Geosciences within the project Environmental Waste Management (EWMA) led by UiT The Arctic University of Norway. 10 sediment cores provide the basis for this study. This includes 4 Niemistö cores from Ranfjorden, 3 Niemistö cores from Stjernesundet and 1 Niemistö core and 2 gravity cores from Bøkfjorden.

##### 3.1.1 Ranfjorden

Four cores provide the basis for the investigations in Ranfjorden. These are P1502-001, P1502-004, P1502-013 and P1502-015 (table 1, for location see figure 20). Core P1502-001 is considered to be “reference” core archiving exclusively natural sedimentation.

*Table 1: Positions, water depths and core lengths of the four sediment cores.*

Core ID	Latitude *	Longitude *	Water depth	Core length	Coring tool
P1502001	66.26865	13.778	100 m	36 cm	Niemistö corer
P1502004	66.32445	14.099	65 m	38 cm	Niemistö corer
P1502013	66.30942	14.084	282 m	35 cm	Niemistö corer
P1502015	66.31469	14.074	180 m	24 cm	Niemistö corer
* Decimal degrees					

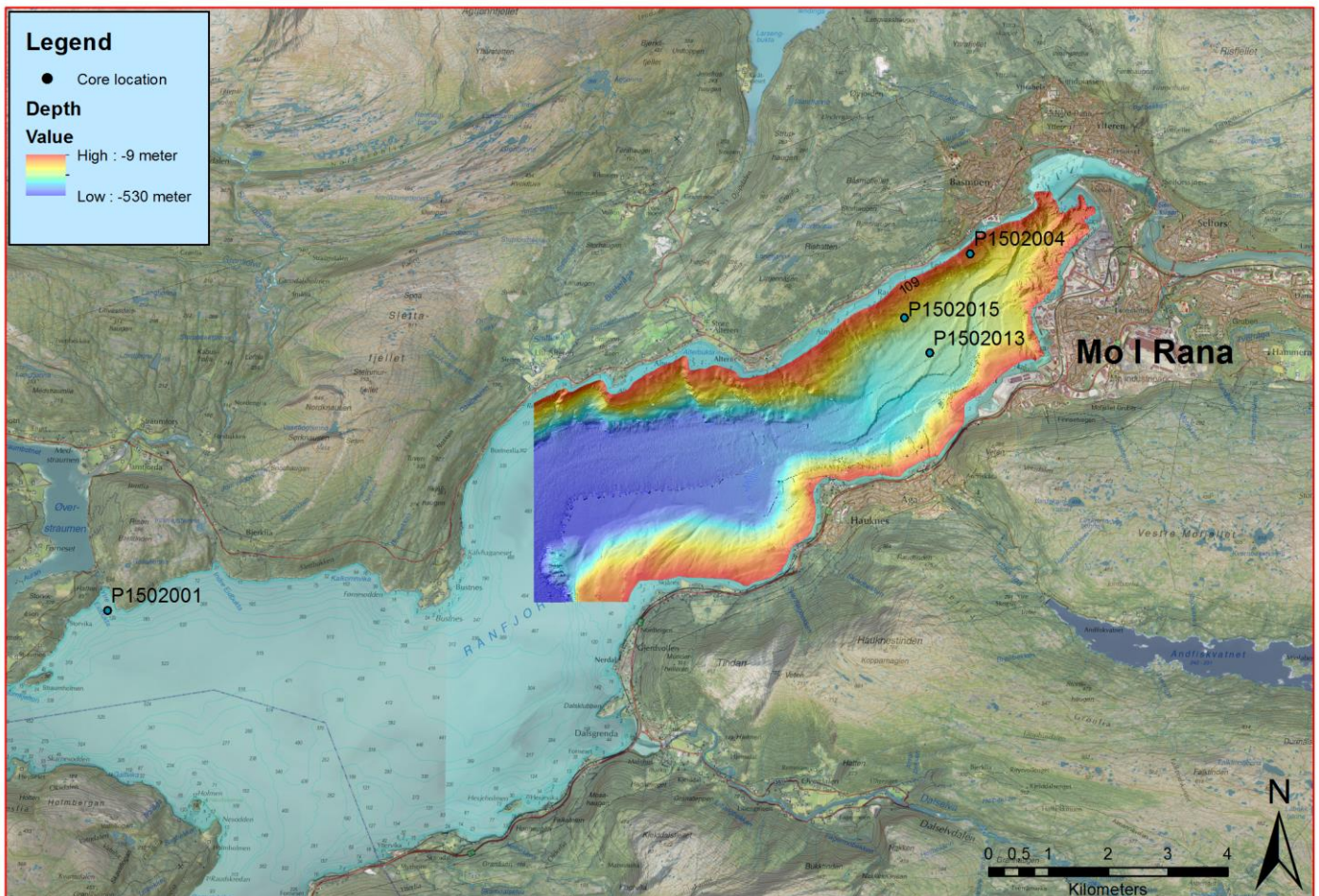


Figure 20 Bathymetry dataset of inner Ranfjorden with core locations.

### 3.1.2 Bøkfjorden

Three cores provide the basis for the investigations in Bøkfjorden. These are P1505-011, IG16-1798GC and IG16-1811GC (table 2, for location see figure 21). Core P1505-011 is considered to be “reference” core archiving exclusively natural sedimentation.

Table 2: Positions, water depths and core lengths of the four sediment cores.

Core ID	Latitude *	Longitude *	Water depth	Core length	Coring tool
P1505-011	69.730	30.119	243 m	31 cm	Niemistö corer
IG16-1798GC	69.743	30.073	105 m	150 cm	Gravity corer
IG16-1811GC	69.809	30.113	285 m	75 cm	Gravity corer
* Decimal degrees					

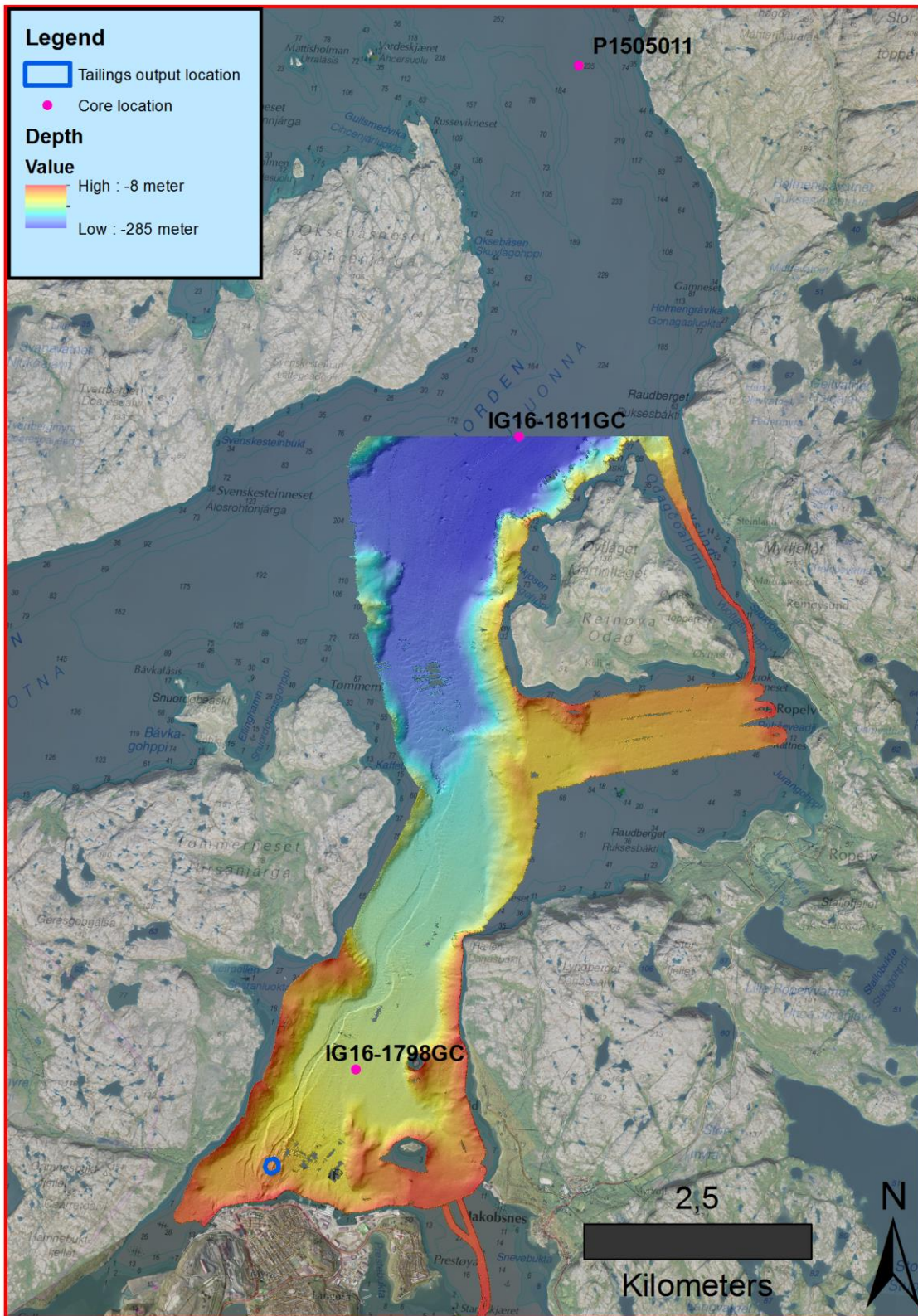


Figure 21 Bathymetry dataset of inner Bøkfjorden with core locations.

### 3.1.3 Stjernesundet

Three cores provide the basis for the investigations in Bøkfjorden. These are P1707-005, P1707-010 and P1707-018 (table 2, for location see figure 21). Core P1707-005 is considered to be “reference” core archiving exclusively natural sedimentation.

*Table 3 Positions, water depths and core lengths of the four sediment cores.*

Core ID	Latitude *	Longitude *	Water depth	Core length	Coring tool
P1707-005	70.230	22.720	480 m	28 cm	Niemistö corer
P1707-010	70.260	22.621	50 m	22 cm	Niemistö corer
P1707-018	70.242	22.605	460 m	31 cm	Niemistö corer
* Decimal degrees					



Figure 22 Overview map of Stjernerundet with core locations



### 3.2 Laboratory work – sediment cores:

The Niemestö cores from Ranfjorden and Bøkfjorden were opened and partly analysed at the laboratories of NGU in Trondheim in 2015/2016. The Niemestö cores from Stjernesundet were opened and analysed at NGU in 2017. Additional analyses of the Niemestö cores, as well as all analyses of the gravity cores, were performed in 2017 and 2018 at the laboratory of the Department of Geosciences (IG) at UiT The Arctic University of Norway.

The laboratory analyses at the NGU laboratory included Multi Sensor Core Logger (MSCL), X-ray fluorescence (XRF), X-ray imaging (XRI), X-ray diffraction (XRD) and fallcone shear test. The methods applied at the laboratory at UiT are explained below.

#### 3.2.1 X-radiography

X-radiographs were acquired with a GEOTEK MSCL-XCT x-ray imaging machine on unopened cores from Bøkfjorden. The apparatus is for x-ray imaging exclusively and for preservation purposes, the x-ray imaging was performed on unopened cores. The GEOTEK MSCL-XCT apparatus at the IG laboratory is not able to rotate, hence unable to identify three-dimensional structures. X-radiographs reflect density, which can be used to identify internal structures, clasts and dating material (shell fragments e.g.).

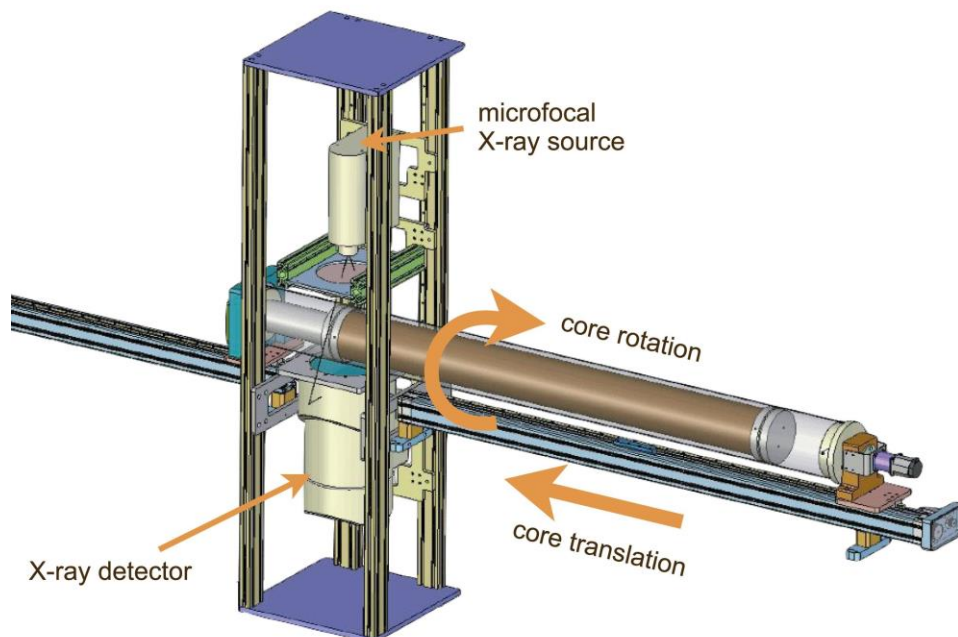


Figure 23 Conceptual 3D-model of a GEOTEK MSCL-XCT x-ray imaging system. (From Research laboratory in Paleomagnetism and Marine geology)

#### 3.2.2 Physical properties

Prior to opening of the cores, logging physical properties were conducted by use of a GEOTEK Standard Multi Sensor Core Logger apparatus (MSCL-S) (figure 24). Parameters

such as gamma-ray attenuation (wet-bulk density), p-wave velocity, p-wave amplitude, core thickness, magnetic susceptibility, temperature and colour changes. A core is logged by being placed onto the MSCL track, and pushed through the different sensors by a core pusher, which scan the core as it passes (from right hand side towards left (figure 24)) (Geotek manual, 2016).

In this project, the instrument was used for measuring magnetic susceptibility (Mag Sus) and color spectrophotometry, which was conducted by using a point and loop sensor.

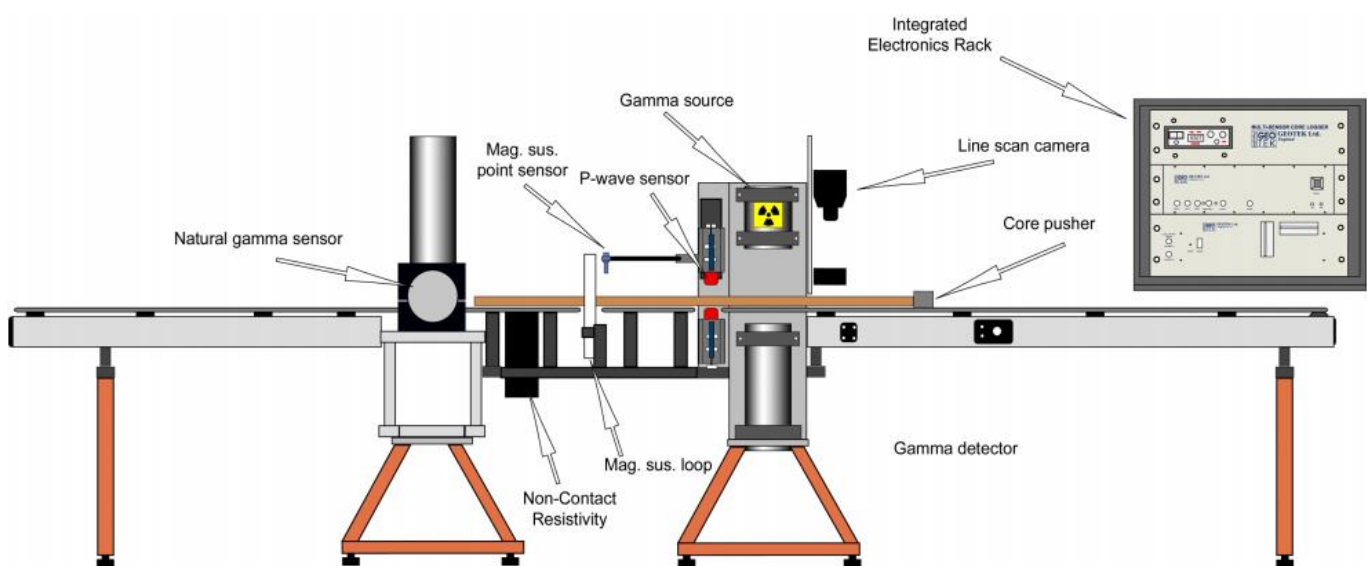


Figure 24 Conceptual model of a GEOTEK MSCL-S, displaying the most important components (From GEOTEK manual, 2000)

### 3.2.2.1 Magnetic Susceptibility

As a point or loop sensor moves over the core surface, any increase or decrease in magnetic susceptibility reflects an increase or decrease in magnetic material that constitute the sediment at any given area. Therefore, magnetic susceptibility reflects changes in sediment composition without physically disturbing the sediments. For instance one can indirectly define relative changes in non-magnetic (quartz) and magnetic (magnetite) material (Nowaczyk, 2002).

The MSCL-S instrument is equipped with both a loop (Bartington loop sensor MS2C) and point sensor (Bartington point sensor MS2E) that measure the magnetic susceptibility. Only point sensor measurements was conducted on the two given cores. The loop sensor is used for unopened sediment cores. The point sensor on the surface of sediment split cores, providing a high resolution, but less sensitive data (GEOTEK manual, 2016).

### **3.2.3 Opening of cores**

Exclusively the gravity cores were opened at the laboratory at IG in August 2017, lengthwise with a circular saw. The saw is equipped with two circular, vibrating blades on each side of a movable core liner frame cutting the core liner from two sides. A steel wire was pulled through the opened liner, prior to separation of the sediment with an osmotic knife. One half was marked as working half and the other half as archive. Both cores were wrapped in plastic and stored under cool conditions (4°C) until further analysis.

### **3.2.4 Spectrophotometry**

The MSCL-S instrument is equipped with a Konica Minolta CM-700d spectrophotometer. This apparatus allows the user to efficiently measure changes in core-surface-color without destruction by acquiring color-information from the surface reflected light (400 – 700 nm wavelengths) (CM-700d manual, 2018). Changes in color indicate changes in sediment-composition, which may be used for defining areas of interest of the core.

Prior to color imaging, the core surface was cleaned and smoothed by use of plastic cards. The treatment of the sediment surface after opening and storage of cores is important for maximizing the image resolution as small surface irregularities can distort the reflected signals.

### **3.2.5 Visual description**

After spectrophotometry, systematic description of the working half of the sediment cores were conducted. Physical properties were identified and described based on visual observations of the sediment surface. Variations in grainsize such as grainsize, colour (defined by Munsell Sediment Color Chart (MSCC)), bioturbation, structures, clasts and fragments are logged. Lithological logs were made for representing the visual changes. This analysis was conducted on all of the given cores.

### **3.2.6 Grainsize distribution analysis**

A total of 307 sediment samples were extracted from 7 sediment cores. 37 samples from core P1502-001, 46 samples from P1502-004, 39 samples from P1502-013, 34 samples from P1502-015, 33 samples from P1505-011, 72 samples from IG16-1798GC and 46 samples from IG16-1811GC.

Sampling, preparation and grainsize distribution measurements was conducted by Ander E. Haugen and Anette Klev Ladstein. For full explanation of the grainsize distribution analysis method, read the associated theses of Haugen (unpublished) and Ladstein (2018).

### 3.2.7 X-Ray Fluorescence Core Scanner (XRF core scanner)

The archive half of the cores were prepared for X-ray fluorescence scanning (XRF). XRF core scanning is based on the principle of emission of fluorescent X-rays from matter, which rapidly determines the chemical composition of marine bottom sediments without disturbing the sediment (non-destructive). By releasing electrons from a cathode inside a X-ray source-tube, the electrons are guided towards an anode made of rhodium. The rhodium-anode emits rhodium X-rays from electron collision. The emitted X-rays hit the sediment surface, which through collision between the emitted electron and electrons within the surface sediment atoms results in a secondary radiation through electron excitation (figure 25). The secondary radiation or fluorescence enters a detector that registers incoming energy signals (figure 26). Every element has characteristic secondary radiation wavelengths, making identification of the chemical composition of the sediment possible. (Forwick, 2013; Avaatech, 2018).

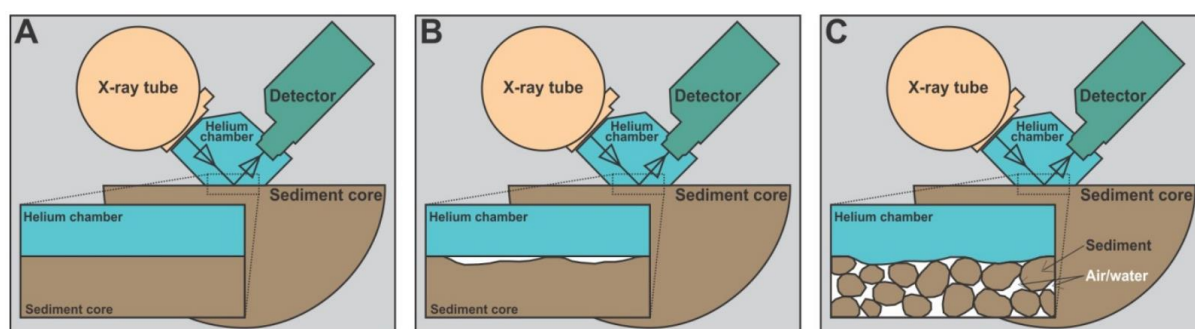


Figure 25 Example showing XRF core scanner setup and potential contacts of landing triangle and sediment surface.

The generation of secondary radiation occur when emitted X-rays collide with electrons surrounding the positively charged nucleus. When collision occurs, electrons may be ejected from their orbits, which result in a vacancy within one of the electron shells of the atom (figure 26). The vacancy is filled by an electron from a higher shell, which due to electrostatic forces release excess energy (less energy needed to stay within lower shells). The excess energy is the fluorescence of an element.

XRF core scanning was performed with an Avaatech XRF core scanner at IG. The instrument can retrieve qualitative measurements of the elements from a 0.1 – 10.0 mm (in down core direction) and 2-15 mm (in horizontal core direction) irradiated area (magnesium (Mg) to

uranium (U)) in solid, liquid or powder materials (Avaatech, 2018). For more reliable results on the lighter elements (aluminum (Al), silica (Si) and magnesium (Mg) e.g.), the equipped helium chamber should ideally be in continuous contact with the sediment surface to avoid friction of the primary and secondary radiation with air (Forwick, 2013; Avaatech, 2018).

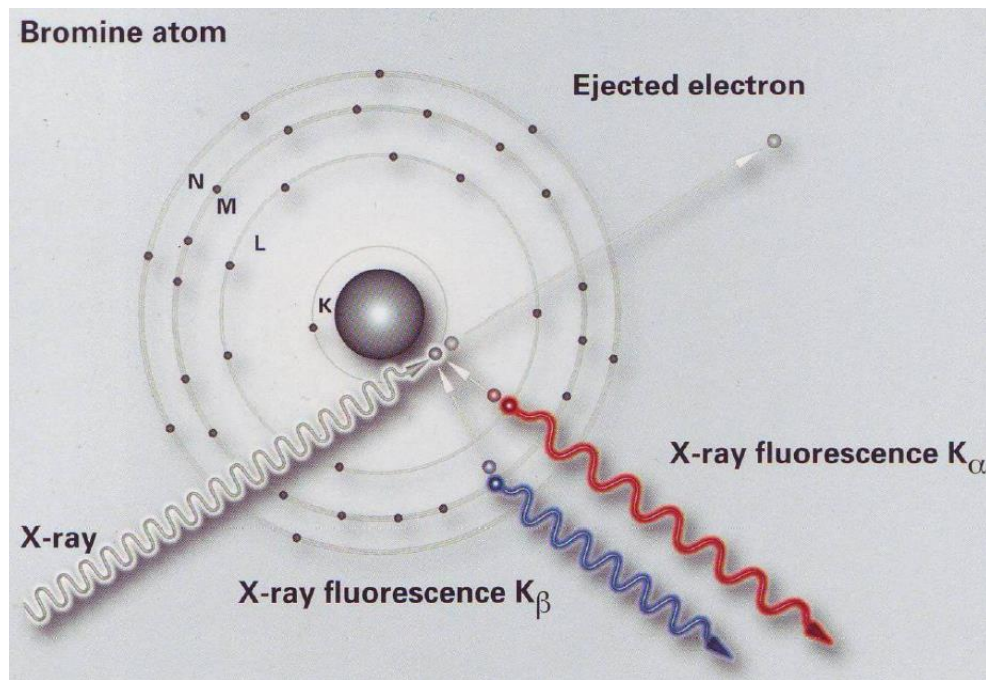


Figure 26 Principle of Bohr's atomic model and the generation of secondary radiation

Prior to scanning, the sediment cores were adjusted to room temperature, followed by smoothening and covering of the core surfaces with a 4 $\mu$ m thin foil to reduce contamination. According to Tjallingii et al. (2007) and Weltje & Tjallingii (2008), presence of water between the plastic sheeting and core surface may reduce the signal of the lightest elements, and should be avoided if possible. In addition to avoiding a wet surface, the sediment surface should ideally be smooth and compact to avoid the presence of air and, thus, friction of the primary and secondary radiation with air. If the core surface is irregular, cavities may form pockets of air or water, increasing friction, thus reducing the signal from the lighter elements. Another important factor for achieving reliable XRF-data, according to Weltje & Tjallingii (2008), is the use element-ratios instead of single element “counts”. By using element-ratios (Fe/Sum for instance, which is used in this data-set) one reduces the impact of matrix effects.

Matrix effects are irregularities in the matrix of the material that reduces or enhances the different XRF-signals, resulting in “polluted” data (Weltje & Tjallingii, 2008).

During scanning, all sediment cores from Trondheim (P150X-XXX) were scanned with 5 mm down core slit size, 30 sec measuring time with these settings:

- 10 kV, 1000  $\mu$ A, no filter, to measure light elements from Mg to Co
- 30 kV, 2000  $\mu$ A, Pd-thick filter, to measure medium-heavy elements from Ni to “ca.” Mo
- 50 kV, 2000  $\mu$ A, Cu-filter, to measure heavy elements from “ca.” Mo to U.

The three cores from IG (IG16-XXXXG) were scanned with mainly 10 mm intervals (5 mm at areas of special interest (transition zones from natural sedimentation to tailings deposition e. g.)). The following settings were applied, 10 sec measuring time on 10 and 30 kV, increasing it to 20 sec for 50 kV measurement. Other settings used:

- 10 kV, 1000  $\mu$ A, 10 sec, no filter, to measure light elements from Mg to Co
- 30kV, 2000 $\mu$ A, 10 sec, Pd-Thick filter, to measure medium-heavy elements from Ni to “ca.” Mo
- 50kV, 2000 $\mu$ A, 20 sec, Cu-filter, to measure heavy elements from “ca.” Mo to U.

Each core was scanned on each of the three settings as mentioned above. The smaller counts the detector registers, the less reliable are the data. The most relevant elements for this study are found within the 10 kV-results (Fe, Al, Si, Ti, K and Mn), alongside with 30 kV elements (Zn and Pb) and are considered important elements for distinguishing mine tailings from natural sediments (Fe, Zn and Pb are associated to mining in Ranfjorden e.g. (Skei & Paus, 1979). Data provided from a XRF core scanner is semi-quantitative, i.e. it shows reliable records of changes in element-content through a sediment core, which is used for interpreting sediment characteristics, source, processes and stratigraphy (Richter et al., 2006). As previously mentioned, element-content is shown in ratios, showing an element based on number of counts of another element. In this study, the total sum of the most abundant element assemblages are used as the “reference” element in order to determine relative changes in element composition and limit potential matrix effects (Forwick, 2013) . Elements that are important to map throughout the sediment record are based on a) elements connected to mining activity (Fe, Si & Ca), b) elements considered as toxic (Pb and Zn) c) elements characteristic for clay and sand (K and Si, respectively). After scanning the data has to be

processed, as the data is presented as “total counts of energy pulses” of the respective element during the measuring time. Each abundant element is added to a “total sum”, which is used as the reference. Each element-count is then divided by the total counts of each interval.

In Trondheim, XRF measurements were conducted in a GEOTEK MSCL-S apparatus.

### **3.2.8 X-Ray Fluorescence Spectrometer (XRF spectrometer)**

Quantitative element-geochemical measurements were performed with a Bruker S8 Tiger XRF Spectrometer at IG. XRF spectrometry is an analytical method that provides quantitative data in minerals, ores, rocks and sediments amongst others, which is important for the study as it says something about the chemical concentrations within the sediment core, giving valuable data for desirable or non-desirable elements (Sitko & Zawisza, 2012).

Unlike the XRF core scanner, the XRF spectrometer method is a destructive process due to the preparation of the material required for measurements.

#### **3.2.8.1 Sampling and sample preparations**

Sixty XRF spectrometer measurements were performed on samples from four cores; IG16-1798GC (15 samples), IG16-1811GC (8 samples), P1502-013 (15 samples) and P1502-015 (22 samples), respectively. The selection of samples was based on gradual transitions from natural deposition to deposition influenced by mine tailings.

A minimum dry-weight of 09.5400 g sediment was needed for reliable data (0.5400g for major elements, 9.0g for trace elements). Therefore a minimum of 15 g bulk sediment was extracted from the wet core, with 1 cm intervals, to ensure high resolution and sufficient available material after drying. To measure major elements (>0.5%) and trace elements (<0.5%), one needs to apply different preparation methods for pressed pellets and fused beads, respectively.

Pressed pellets:

9 g of dried sediments from each sample were grinded to rock powder for 5 minutes in a Retsch Mortar Grinder with 9 “POLYSIUS POLAB Mahlhilfe wax tablets (for increased cohesion). The rock powder mix was then inserted to a metal cylinder inside a fluXana – VANEON hydraulic piston apparatus. After pressing, the samples were marked with a marker pen and placed in a plastic container until trace element analysis.

Fused beads:

0.5400 g of dried sediments from each sample were grinded to rock powder for 90 seconds in a Retsch Mortar Grinder. The rock powder was transferred to a glass container with 1.6200 g of flux (Li-tetraborate) and mixed (by shaking) for 15-20 seconds. By adding flux to the rock powder, the melting point is lowered to 875 °C. After mixing, the samples were transferred to the Pt-crucible, and placed into the moulds inside the xrFuse 2 fusion machine, where the samples were heated to maximum 1250°C. After heating, the melted samples cooled to glass beads, which were marked and stored until major element analysis. Between fusions of samples, the crucibles were put into a solution of water and citric acid in order to remove potential contamination of residual cooled melt from previously fused beds.

### **3.2.8.2 Scanning**

For trace elements analysis (< 0.5 %), GEO-QUANT T was used as the trace element standard, which is developed by Bruker AXS for geological research, and the out-put data is presented as element-concentrations (PPM) (Bruker AXS)

For major elements (> ca. 0.5%), Major felsic – mafic was used as the major element standard which is developed by Erling Ravna at IG. The out-put data is presented as oxide-concentrations (%)

### **3.2.9 X-ray Diffraction (XRD)**

XRD measurements were performed on the cores P1502-015 and P1505-011. The XRD-analysis is a method for identifying minerals by diffraction, which is how a substance interfere with waves moving through it. X-ray diffraction patterns reveal the state of a substance, as the diffraction pattern is determined by the exact atomic arrangement in a material. By X-rays through a mineral one can identify the mineral by the diffraction pattern (Suryanarayana & Norton, 1998).

Mineralogical analyses were carried out by XRD on unoriented preparations scanned by a Bruker D8 Advance diffractometer (Cu K $\alpha$  radiation in 3-75° 2 $\theta$  range) at the Geological Survey of Norway, Trondheim. Mineral identification was carried out with automatic and/or manual peak search and match function in Bruker's Diffraction EVA V3.1 software. Mineral quantification was performed using Rietveld modeling with software TOPAS 5.



## 4 Sediment Cores

14 sediment cores have been analyzed. 10 of 14 cores (4xRanfjorden, 3xBøkfjorden and 3xStjærnsundet) was focused on. The core lithology results are based on the various methods mentioned in chapter 3.

By compiling results from visual descriptions, line-scan images, x-ray images, grain-size and chemical data, the given cores were divided into sequences with similarities.

### 4.1 Ranfjorden

See figure 20 for core sample location overview.

#### 4.1.1 Core P1502-001

Core P1502-001 is located in outer Ranfjorden (Fig. 20). It is 36 cm long and divided into three units, P1502-001A, P1502-001B and P1502-001C (see figure 27).

##### 4.1.1.1 Unit P1502-001A (36-25 cm)

Unit A is predominantly massive, and a greyish color (5Y 4/1 by Munsell Sediment Color Chart (MSCC)) is prominent from 36-28 cm, with a gradual yellowing towards the unit boundary at 25 cm (gradual boundary). Some black laminae features are observed at 32.5 - 30 cm, whereas the X-ray image (XRI) show no internal structures. From 30-25 cm, internal structures are observed. The unit consist mainly of medium silt (mean particle size  $\approx 10 \mu\text{m}$ ), with small changes in grain size throughout the unit. The magnetic susceptibility is relatively low and constant at about  $30 \cdot 10^{-5} \text{SI (m}^3/\text{kg)}$ .

In opposition to grain size and magnetic susceptibility, the XRF-data show distinct variations in Fe-, Si-, Ca-, Pb- and Zn-ratios. Throughout the unit, Fe, Pb and Zn reflect a see-saw pattern, while Si slightly towards the top of unit A. Ca on the other hand, is somewhat constant throughout the unit except the peak observed at 32.5 cm. Furthermore, Ca and Si show an inverse relation to Fe-, i.e. an increase in Fe- correlates with decreases in Si- and Ca-ratios. On the other hand, Pb- and Zn-ratios typically increase in phase with the Fe-ratio.

##### 4.1.1.2 Unit P1502-001B (25-5 cm)

Unit B is a yellowish-gray (5Y 4/2 MSCC), massive unit, with a more chaotic internal structure than unit A. Based on the XRI, a sequence with elevated presence of shell fragments and clasts is observed between 17.5-10 cm. A gradual increase in grainsize occurs (mean particle size, which increases from medium silt ( $\sim 10 \mu\text{m}$ ) to coarse silt ( $\sim 17 \mu\text{m}$ )), which correlates with an increased input of sand. Towards the top, a gradual boundary is

identified as the sand-content increases slightly. The magnetic susceptibility levels are generally very low throughout the unit, with slight decrease in the interval 25-15 cm. Furthermore, two peaks in magnetic susceptibility are observed at 22 cm and 8 cm, respectively.

The XRF data show a change in element-relationship throughout the unit. The Ca-ratio gradually decreases from bottom towards the top of the unit. Si and Fe, on the other hand continue the inverse relationship as shown in unit A. From 25-16 cm, the Si-ratio increase and Fe-ratio decrease. Between 16-11 cm, a distinct decrease in Si and increase in Fe occurs, whereas the elevated Fe-ratio correlates with the presence of clasts shown in the XRI. A new drop in Fe is observed from 11-9 cm, alongside an increased Si-ratio. Moreover, the upper 4 cm show a stabilization of both Si- and Fe-ratio, with only small fluctuations. Finally, the Pb- and Zn-ratios generally increase in phase with the Fe-ratio, except the upper 4 cm of unit B.

#### **4.1.1.3 Unit P1502-001C (5-0 cm)**

In unit C, the gradual boundary to the underlying unit is marked by a gradual transition towards the same prominent grey color as found in unit A. From 5 cm – 3 cm, the color changes from yellow-grayish (5Y 4/2 MSCC) towards a more grayish (5Y 4/1 MSCC) color. Within the same interval, laminating features are observed on the XRI. From 3 – 1 cm, the

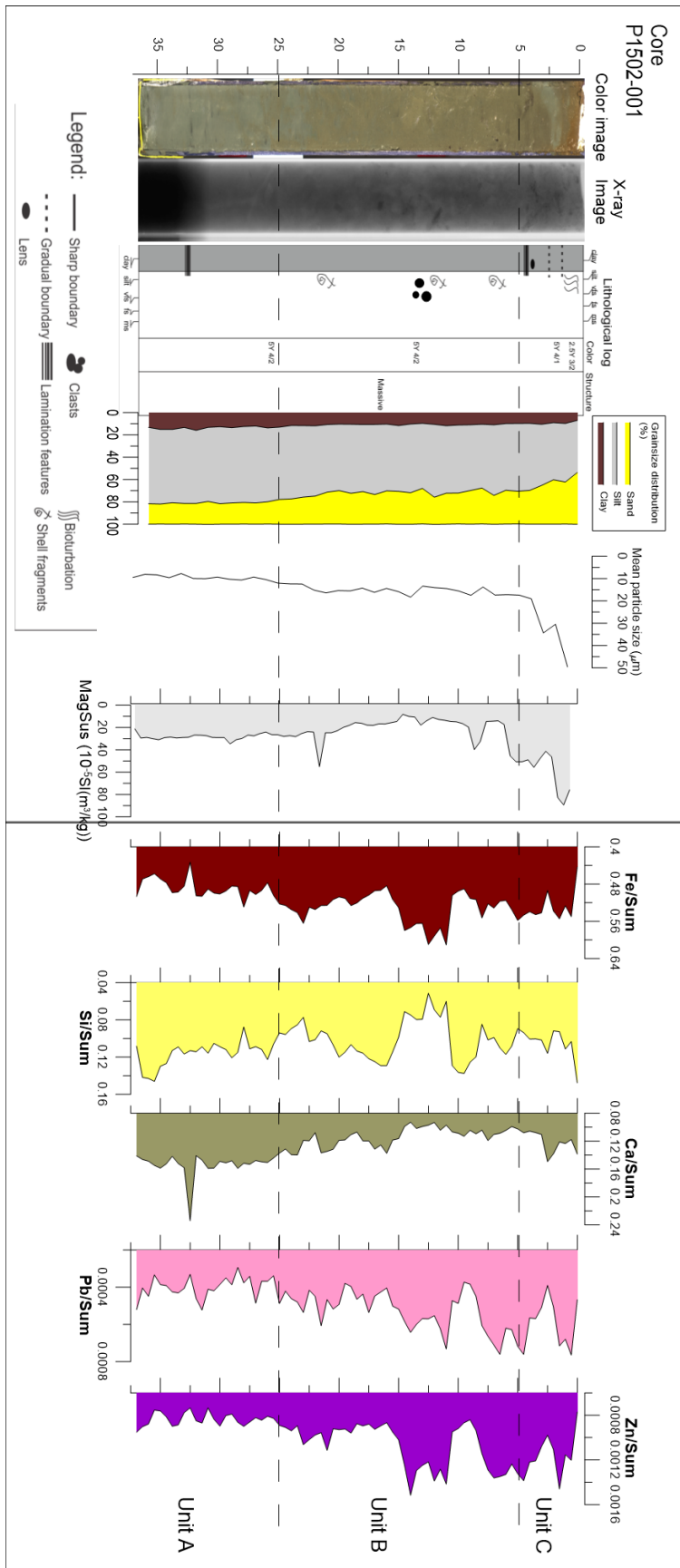


Figure 27 Line-scan image, X-radiograph, visual description, as well as grain-size distribution, physical properties and element geochemistry of core P1502-001.

gray color is prominent, without any structures. A new, gradual change in color is observed (2 – 0 cm), as the sediment is becoming more brown-reddish (2.5Y 3/2 MSCC) towards the top of the unit. Additionally, bioturbation marks are observed in the upper cm of the unit. The sand content increases gradually throughout the unit, resulting in a coarsening of the mean grain size, ranging from coarse silt (17  $\mu\text{m}$ ) to very coarse silt (50  $\mu\text{m}$ ).

Further, the magnetic susceptibility increases from  $\sim 50$  to  $\sim 90 \cdot 10^{-5}\text{SI}$  between 5 – 1 cm, ultimately peaking the upper cm of the unit ( $\sim 80 \cdot 10^{-5}\text{SI}$ ). Within the same interval, the XRF data show the same relations as described in the two previous units. The Fe- and Si-ratios somewhat continue in the relatively stable pattern as in the upper cm of unit B, while Ca has a slight increase towards the top of unit C. Pb and Zn stabilizes at relatively high ratios, without an increase in Fe-ratio. Within the interval 4 – 2.5 cm, the Fe-, Pb- and Zn-ratios drop, while the Si- and Ca-ratios peak. The upper cm of the unit show correlation between a peak in magnetic susceptibility, Pb- and Zn-ratio.

#### **4.1.1.4 Interpretation:**

The gradual color change and increased grainsize which occurs up-core, is due to an increased input of sand, which the grainsize distribution graph shows in figure 27. Furthermore, the grainsize seems to correlate with the geochemistry, which shows a more dominant Fe-ratio in certain sequences with respect to the Si-ratio. For instance, the Fe-peak is located within the clast-interval (14 – 10 cm) in unit B, which significantly decreases the Si-ratio. On the other hand, the increase of Si and decrease of Fe from 25 – 16 cm in unit B correlates with a  $\sim 10\%$  increase in sand, implying a possible input of quartz.

The core most likely reflects a natural sedimentation, as an alternation of a dominating input of more silica- and iron-bearing minerals occurs. Based on the XRF data, which show that an increase in Si-ratio has a negative impact on the Fe-, Pb- and Zn-ratio, one can deduce that the sediment source is of quartz exclusively (mainly  $\text{SiO}_2$ ), while the Fe-bearing minerals is more likely to derive from magmatic sources, as the Fe-ratio coincides with the Pb- and Zn-ratio. The geological map of the area (figure 11) shows that the surrounding bedrock of the core location consist of mainly mica gneiss, schist, metasandstone, amphibolite, granite and granodiorite. The only possible “pure” silica-source is metasandstone. The other rock-groups add less silica, hence more iron and trace metals. Finally, the upper 1 cm show a change in physical properties. A reddening of the sediment alongside with a peak in magnetic susceptibility, which correlates with an increased Pb- and Zn-ratio, but not the Fe-ratio. This

change in susceptibility might imply a new type of iron-input, iron oxide, which becomes red when oxidized. Also, the increase in Pb- and Zn, may occur as a result of the mentioned industrial pollution that Ranfjorden has been exposed to throughout history (see chapter 1.3.1)

#### **4.1.2 Core P1502-013**

P1502-013 is 38cm long, making it the longest retrieved core from Ranfjorden (figure 20). The sediment core is divided into three units, P1502-013A, P1502-013B and P1502-013C (figure 28).

##### **4.1.2.1 Unit P1502-0013A (38-28cm)**

Unit A is massive, has no structures and a dark red color (10YR 3/2 MSCC), with a gradual darkening toward the gradual boundary to the overlaying unit B. Despite having no structures, the mean grain size varies between 20 and 28  $\mu\text{m}$  (coarse silt). The magnetic susceptibility also reflects a homogenous unit, as there are little changes.

Both qualitative and quantitative measurements of the element geochemistry were performed. The results reveal a generally good correlation of the data sets. In general, the Fe-, Ca- and Si-ratio show the same inverse relationship as in core P1502-001, and Zn and Pb seems to have a direct relationship to the Si-ratio. Furthermore, element-ratios show little changes, supported by the quantitative measurements. The unit mostly consist of  $\text{SiO}_2$  (52-49%) and a significant amount of the  $\text{Fe}_2\text{O}_3$  (~15%). The most significant changes occurs in Pb and Zn-content, which decreases.

##### **4.1.2.2 Unit P1502-013B (28 – 18 cm)**

Unit B contains several lamina features, which are alterations of red and slightly darker colored lamina (10YR 3/1 and 10YR 3/2 MSCC). Within the unit, two distinct areas with laminations are observed, at 26-22cm and 21-18cm. Throughout the laminated sequences, changes in mean particle size occurs, ranging from 18-35 $\mu\text{m}$  (coarse to very coarse silt). From 23 – 18 cm, towards the boundary to the overlaying unit, the mean particle size decreases. The boundary between unit B and C is defined with as an abrupt boundary. Furthermore, magnetic susceptibility fluctuates throughout the unit between 400 and 900  $10^{-5}\text{SI}$ , with three distinct peaks (at 27, 24 and 20 cm) and two dips (25 and 22 cm).

Unit B contains several lamina features, which are alterations of red and slightly darker colored lamina (10YR 3/1 and 10YR 3/2 MSCC). Within the unit, two distinct areas with

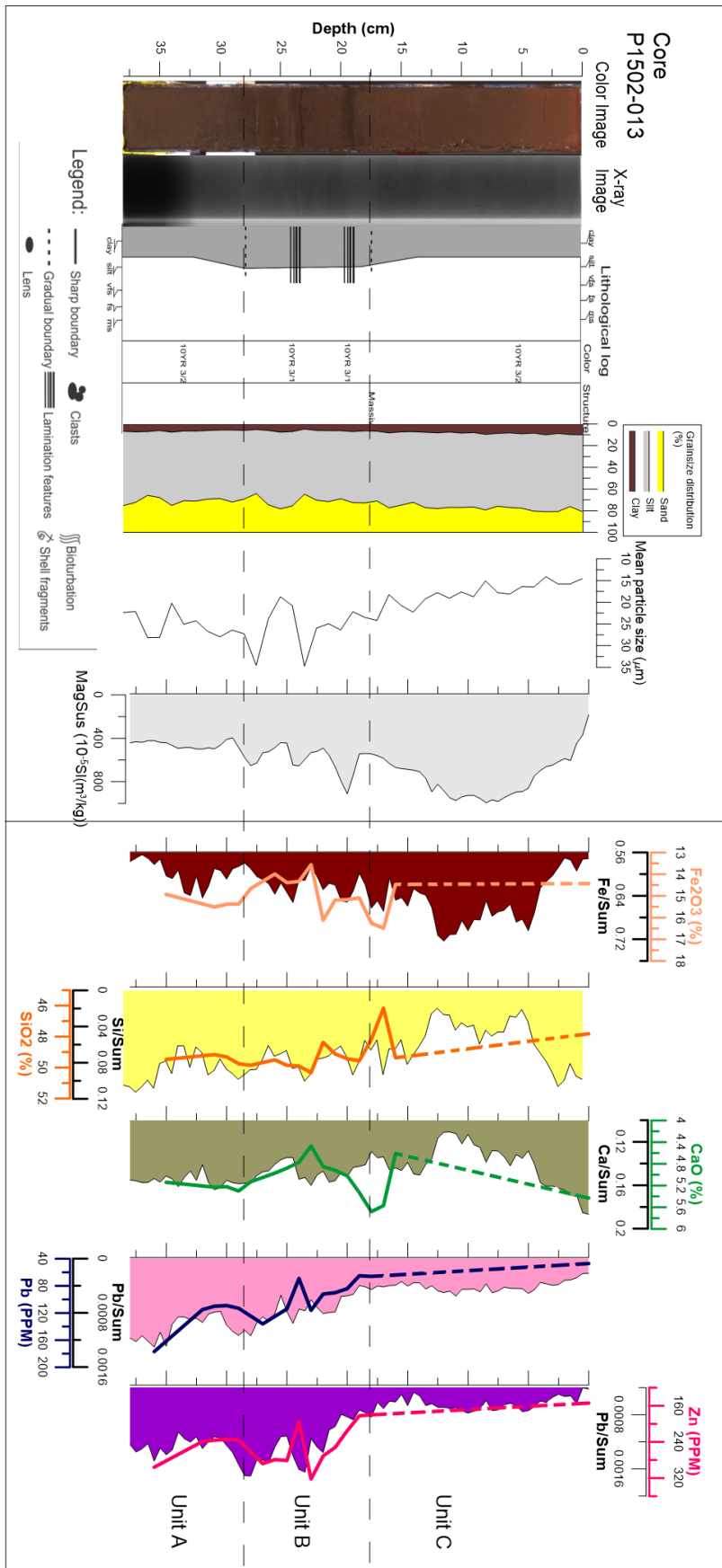


Figure 28 Line-scan image, X-radiograph, visual description, as well as grain-size distribution, physical properties and element geochemistry of core P1502-013

laminations are observed, at 26-22 cm and 21-18 cm. Throughout the laminated sequences, changes in mean particle size occurs, ranging from 18-35 $\mu$ m (coarse to very coarse silt). From 23 – 18 cm, towards the boundary to the overlaying unit, the mean particle size decreases. The boundary between unit B and C is defined with as an abrupt boundary. Furthermore, magnetic susceptibility fluctuates throughout the unit between 400 and 900  $10^{-5}$ SI , with three distinct peaks (at 27, 24 and 20 cm) and two dips (25 and 22 cm).

In unit B, the element-ratios show mostly the same trends as in unit A. Si, Ca, Pb and Zn show a decrease the first 4 cm of the unit, whereas only Fe increase. From 24 cm and towards the top of unit B, the element-ratios fluctuate. However, Ca, Pb and Zn decrease overall slightly from the base to the top of the unit. Quantitative XRF mostly correlates with the element-ratios, except an opposite correlation of CaO and Ca/Sum at 23 cm. As of for Fe/Sum, Si/Sum, Pb/Sum and Zn/Sum, the quantitative data show a good correlation (Quantitative Pb and Zn has a slight up-core offset relative to the element/Sum-ratio).

#### **4.1.2.3 Unit P1502-0013C (18-0cm)**

Unit C is similar to unit A, with a massive, structure-less red-colored appearance. The grainsize is gradually decreasing, from ~25 to ~15  $\mu$ m up-core (coarse to medium silt). As the grainsize decreases, the color-nuance of red changes, becoming brighter towards the top. Alongside the decrease in grainsize, the magnetic susceptibility increases (between 18 – 5 cm) to a value of 1000  $10^{-5}$ SI . The upper 7.5 cm of the unit gradually become less susceptible, with a ~800  $10^{-5}$ SI decrease.

Three quantitative XRF-data samples are represented in unit C (two samples from the lower two cm, and one reference sample the upper cm of the unit). Only element-ratio is represented as a continuous record throughout the unit. The element ratio shows an increase (14 – 5 cm) and a decrease (5 – 0 cm) in Fe, which correlates with changes in magnetic susceptibility. Si and Ca have inverse relations to the Fe, while Pb and Zn are continuously low throughout the unit, with a slight increase correlating the increase in iron (14 – 5 cm).

#### **4.1.2.4 Interpretation**

Core P1502-013 has an elevated magnetic susceptibility relative to core P1502-001. A high magnetic susceptibility and the distinct red color may indicate at Fe-oxide-bearing sediment. Based on the quantitative XRF, the core contains between 13.5 and 16.5 % Fe<sub>2</sub>O<sub>3</sub>, which is expected to be slightly higher in the Fe/Sum-peak between 14 and 5 cm, in unit C.

Furthermore, the iron-content seems to correlate well with the input of fine-grained particles (25 cm for instance), which has a negative effect on all the other element-ratios.

Due to the interplay between Fe/Sum, Fe<sub>2</sub>O<sub>3</sub>-content and grainsize, the iron-content must derive from Rana Gruber's tailings output source, just outside Rana harbor (see figure 5) which are very crushed, fine-grained residue from ore-processing. As mentioned in chapter 1.3.1, the tailings consist mostly of fine-grained hematite, which results in a red, fine-grained and magnetic susceptible sediment.

Throughout units A and B, the direct relation between coarser grainsize, Si, Ca, Pb and Zn indicates that all these elements are connected to another sediment-input, which does not derive from the output of iron-bearing tailings. The sediment-input may come from the Rana-river, which due to industrial pollution adds more Zn and Pb to the sediment. Further up-core, the heavy metals significantly decrease, and remain relatively low throughout unit C, in correlation with increased Fe-ratio.

### **4.1.3 Core P1502-015**

P1502-015 is located in inner Ranfjorden and 35cm long (figure 20). The core is divided into three units, P1502-015A, P1502-015B and P1502-015C (figure 29).

#### **4.1.3.1 Unit P1502-0015A (35-17.5cm)**

Unit A is massive, with a yellow-gray color (2.5Y 4/1 MSCC). The only observed structure is a six cm thick irregular lens consisting of red-colored flakes (33-27cm). The red flakes dissolve into smaller pieces when smeared between fingers. Throughout the unit, the mean particle size is stable around 19 μm. At the top of the unit, a gradual boundary is defined by the peak in mean particle size, followed with a drop (~21μm and ~13μm, respectively). Unit A has a low magnetic susceptibility, with a slight increase towards the top.

Element-ratios show a direct relation between Fe, Pb and Zn, which has an inverse relation to Si and Ca. After a significant change in Si and Fe the lower 2 cm, all element-ratios somewhat stabilizes throughout the unit, with only small changes forming a see-saw pattern. Towards the upper unit boundary, the Fe-, Pb- and Zn-ratio increases and the Si- and Ca-ratio decreases. Quantitative XRF supports the element-ratios (except the Pb-content), which in correlation to XRD-data show that as Fe, Pb and Zn increases, an input of hematite occurs. In general, unit A consist mostly of quartz (~22 %), illite/muscovite (~17%) and biotite (~15%).



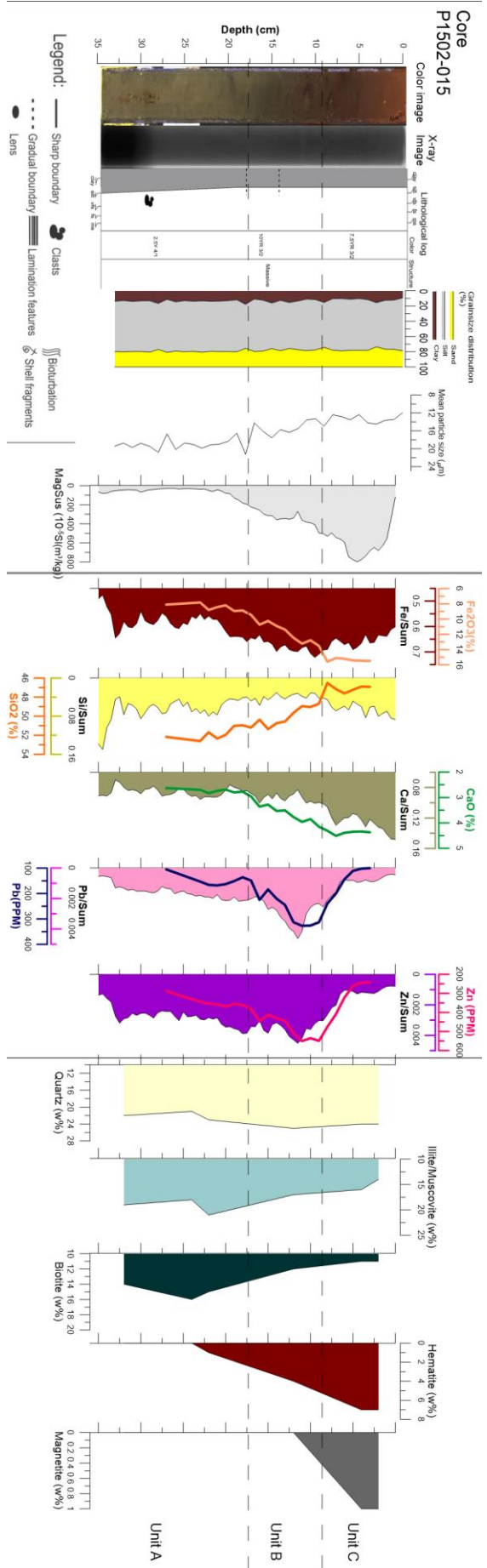


Figure 29 Line-scan image, X-radiograph, visual description, as well as grain-size distribution, physical properties and element geochemistry of core P1502-015

#### **4.1.3.2 Unit P1502-015B (17.5-9cm)**

The following unit is defined with a gradual change in color, from yellow grey (2.5Y 4/1 MSCC) to a dark grey-red color (10YR 3/2 MSCC). The transition is observed over a 8.5 cm interval, from 17.5 cm to 9 cm. As the sediments darkens, a slight decrease in mean particle size occurs, falling from ~16 to ~12  $\mu\text{m}$ , alongside an increase in magnetic susceptibility from 200 – 400  $10^{-5}\text{SI}$ .

With a decrease in grainsize, the Fe-, Pb- and Zn-content increase significantly. Throughout the unit, the iron-content increases from ~9 – 13 % (correlates well with % hematite and magnetite), Ca from ~2.8 - ~4 %), Pb from ~150 - ~350 ppm and Zn from ~350 - ~550 ppm. The silica-content on the other hand, decreases about 2 %. The element-ratios show the same trends, except Ca, which remains somewhat constant throughout the unit. The heavy metal ratios decreases slightly towards the top of the unit, showing the same offset as seen in core P1502-013. Furthermore, magnetite is present in the upper 2 cm of the unit, increasing to 0.3% at the top of unit B.

#### **4.1.3.3 Unit P1502-0015C (9-0cm)**

Unit C show significant color changes within the first 5cm of the unit. The sediment changes from a darkish red (10YR 4/2 MSCC), towards a brighter red (7.5YR 3/2 MSCC). Apart from color-change, the unit is considered massive, with no structures, and a relatively constant grainsize, medium silt (~12 $\mu\text{m}$ ). In unit C, the increase in magnetic susceptibility from unit B continues, peaking between 5 – 2.5 cm (800  $10^{-5}\text{SI}$ ), followed by decrease towards the top.

As of element-ratio, Si and Ca increases, while Pb and Zn decrease significantly and Fe has a slight decline. Quantitative XRF measurements reveal that  $\text{Fe}_2\text{O}_3$  increases and remains stable at 16 %,  $\text{SiO}_2$ -content is reduced to about 48%, CaO increase to 4.5 %, Pb declines with about 200 ppm (3 – 100 ppm) and Zn is reduced with ~300 ppm (550-250 ppm). Furthermore, the mineral-assemblage changes, as more iron-oxide-bearing minerals are present. The hematite content continues to increase up the unit towards the upper 2 cm, reaching 7 %. Magnetite increases to 1% at 2 cm.

#### **4.1.3.4 Interpretation**

Core P1502-015 contains a change in sediment color from similar to those observed in core P1502-001, towards a red sediment, with similarities to the red color observed in core P1502-013. Ultimately, unit A and C represent two different depositional environments. Unit A is

what seems to be of natural origin (as described in 4.1.1.4), while unit C mostly derives from Rana Gruber (as described in 4.1.2.4).

Unit B represents a combination of the two environments. The sudden introduction of hematite as well as magnetite correlates well with both grain size and magnetic susceptibility, thus indicating a contact between natural sediments and tailings. At first, the heavy metals correlate with changes in Fe-content, but at the top of unit B this relationship changes, whereas Fe-increases Pb and Zn declines significantly. This implies that the source of heavy metal is not directly connected to the tailings disposal, but more likely from polluted natural sources (pollution from local industries, as described in 4.1.2.4.)

All in all, the core show a gradual transition from a relatively unaffected fjord-depositional environment, into a more tailings dominated depositional environment. Ultimately, the high rate of mine waste deposition exceeds natural input, resulting in a homogenous, Fe-bearing (hematite), red, fine-grained silty sediment.

#### **4.1.4 Core P1502-004**

Core P1502-004 is located in inner Ranfjorden and is 24 cm long (figure 20). The core is divided into three units, unit P1502-004A, P1502-004B and P1502-004C (figure 30).

##### **4.1.4.1 Unit P1502-004A (24-15 cm)**

At 24-23.5 cm the sediments are yellow-grey, but throughout the unit a gradual darkening of the grey sediment occurs (MSCC 2.5YR 3/2). No visible structures occur in the lowermost 5 cm of the core (24 – 19 cm), and based on the XRI, there are no indications on internal structures. On the sediment surface, on the other hand, black lenses are observed, accompanied with red lenses (18.5 cm, 17 cm and 15 cm). Unit A is dominated by distinct fluctuations in grain size. The mean grain size is coarse silt, varying between 18 and 28  $\mu\text{m}$ . From the depth where the red lenses occur, a drop in mean particle size and an increase in magnetic susceptibility is observed. The susceptibility increases from  $\sim 200$  -  $\sim 600$   $10^{-5}\text{SI}$  in the interval 17.5 – 15 cm. The boundary towards unit B, is characterized with a gradual reddening of the sediment.

The XRF data show a high fraction of Fe/Sum relative to the other element-ratios, which goes as high as  $\sim 0.65$  versus  $\sim 0.16$  for Si. Fe, Pb and Zn have an inverse relationship to Si and Ca.

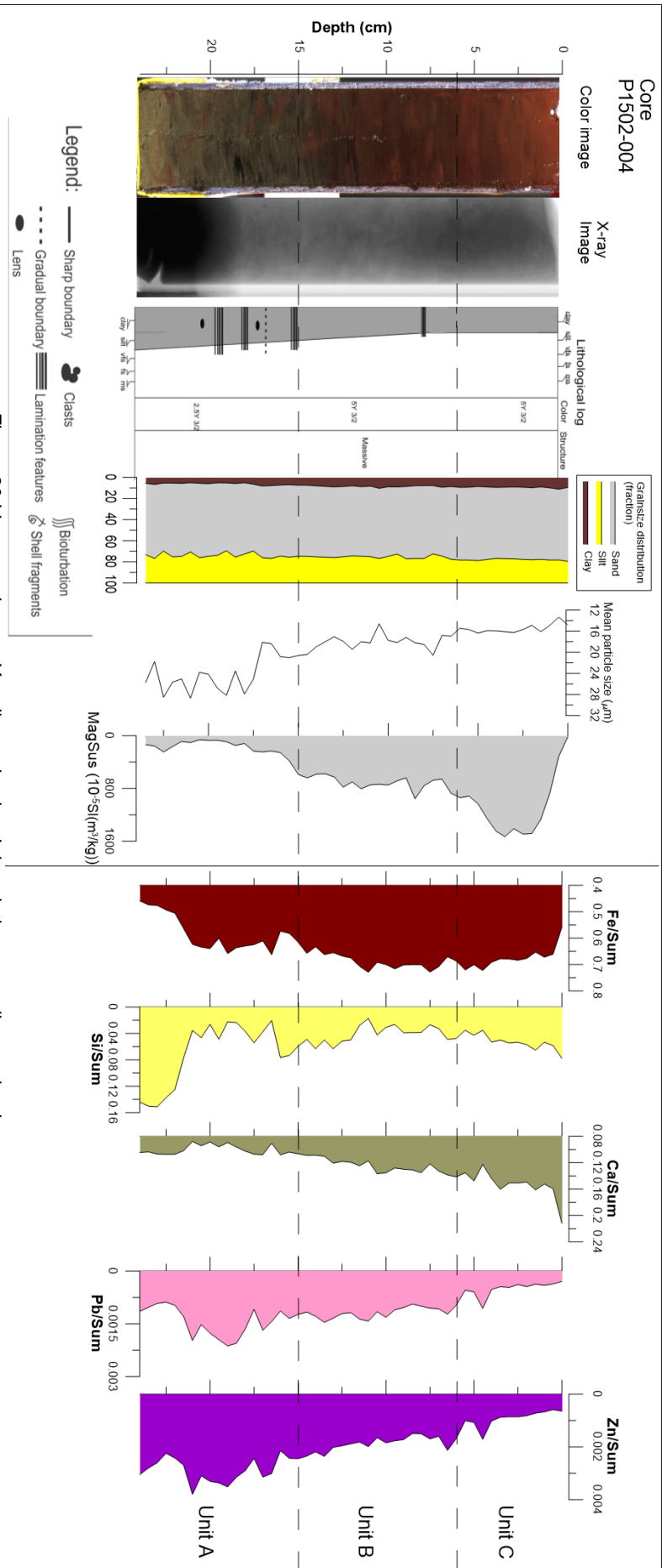


Figure 30 Line-scan image, X-radiograph, visual description, as well as grain-size distribution, physical properties and element geochemistry of core P1502-004.

The first 3 cm, the Fe-, Pb- and Zn-ratios increase (Zn and Pb peaks) significantly, with respect to a slight decrease in the Ca-ratio, and a significant decrease in the Si-ratio. From 21-15 cm, the Fe- and Si-ratio stabilizes, the Ca-ratio increases, while Pb and Zn remains relatively high, followed by a slight decrease towards the top of unit A (18-15 cm).

#### **4.1.4.2 Unit P1502-004B (15-6 cm)**

Unit B is defined by a gradual reddening of the sediment (2.5YR 3/2 MSCC to 5YR 3/2 MSCC). The unit is massive, except lamina features occurring at 7.5 – 6 cm and 15- 12.5 cm, alternating between red and dark grey lamina. Unit B is dominated by coarse silt, with fluctuations ultimately decreasing the mean grainsize from 20 – 16  $\mu\text{m}$ . The magnetic susceptibility increases gradually throughout unit B from 600 – 850  $10^{-5}\text{SI}$ , from bottom to top, respectively. In Unit B, Fe increases and stabilizes to a ratio about 0.7. The same goes for the Ca-ratio, which increases continuously up-core, from 0.10 towards 0.14 at the top. Both Pb and Zn have an opposite trend, with a continuous decrease towards the top of the unit, while the Si-ratio varies repeatedly.

#### **4.1.4.3 Unit P1502-004C (6-0 cm)**

The uppermost 6cm of core P1502-004 are dominated by a distinct reddening of the sediment (5YR 4/8 MSCC). There are no visible structures, and the lithology is dominated by coarse silt the lower 3 cm of the unit and medium silt the upper 3 cm. A major increase in magnetic susceptibility occurs at ~5cm, reaching a peak between 4 and 2 cm (~1600  $10^{-5}\text{SI}$ ). Despite significant changes in magnetic susceptibility, little change in the Fe-ratio is seen. Both the Pb- and Zn-ratio continue to decrease from the top of unit B and throughout unit C. The Si-ratio almost doubles throughout unit C, and Ca peaks towards the top of the unit, towards a value about 0.22.

#### **4.1.4.4 Interpretation**

The decrease in grainsize and increase in magnetic susceptibility correlates, showing a gradual transition from natural sediments to tailings-dominated sediments. As described in 4.1.3.4, the core show three stages of depositional environments. The bottom unit, unit A, represents sedimentation of natural sediments (as described in 4.1.1.4), whereas unit B represents the transitional zone, as the sediments gradually becomes darker in color and more magnetic susceptible, towards unit C, hence more tailings dominated.

## 4.2 Bøkfjorden

See figure 21 for core location map.

### 4.2.1 P1505-011

Core P1505-011 is a 31 cm long core, located in outer Bøkfjorden (figure 21). The core is divided into two units: P1505-011A and P1505-011B (figure 31).

#### 4.2.1.1 Unit P1505-011A (31 – 5 cm)

Unit A is mostly massive throughout the unit, with a yellow-grayish color (2.5Y 4/2 MSCC). Black structures sporadically occur on the sediment surface, but are not visible in the XRI. Bioturbation marks are observed in the interval 17.5 – 13 cm. Furthermore, a lens of bright colored sediment (2.5Y 4/1 MSCC) is observed at 12 – 10 cm. Above this lens, less structures are observed. Based on the XRI, multiple internal clasts are located at 13-8 cm. The boundary to the overlaying unit is defined by a gradual density change at 5 cm. The grain size is generally coarse silt (26  $\mu\text{m}$ ) throughout the core, which in certain sections decrease to fine silt (12  $\mu\text{m}$ ). The bright lens at 12 – 10 cm was defined in the lab as coarser sediment relative to the surrounding sediment. The grain size distribution show the opposite, as it is defined as medium silt. The unit is mostly not susceptible, with only a value of  $\sim 50 \cdot 10^{-5}\text{SI}$ , until 12.5 cm, where an increase in susceptibility occurs. Finally, the susceptibility peaks at the boundary (5 cm) to  $450 \cdot 10^{-5}\text{SI}$ .

The unit reflects little changes in geochemistry, whereas the heavy metals Pb and Zn show the most significant changes, although the values are very low. The Fe- and Ca-ratios correlate, with no distinct changes the lowermost 13 cm of the unit. From 13 – 5 cm, the ratios gradually increases. Si decreases gradually the upper 8 cm of the unit. The mineral assemblage consists mostly of quartz (26 %), plagioclase (26 %) and amphibole (11 %) and biotite (8 – 9 %). At 13 cm and further up-unit, the quartz-, amphibole- and calcite increases- content increase, whereas plagioclase and biotite are reduced 10 % and 3 %, respectively.

#### 4.2.1.2 Unit P1505-011B (5 – 0 cm)

Unit B consists of massive sediment, with the same color as described in unit A (2.5Y 4/2 MSCC). What differs from unit A, is a less dense sediment, which the XRI implies. Furthermore, mean grain size decreases slightly relative to the top part of unit A ( $\sim 19 - 16 \mu\text{m}$ ). From the bottom to the top of unit B, the magnetic susceptibility declines from  $450 - 0 \cdot 10^{-5}\text{SI}$ . All element-ratios increase from 5 – 2.5 cm, followed by a distinct drop, whereas Si/Sum gradually declines toward the top.

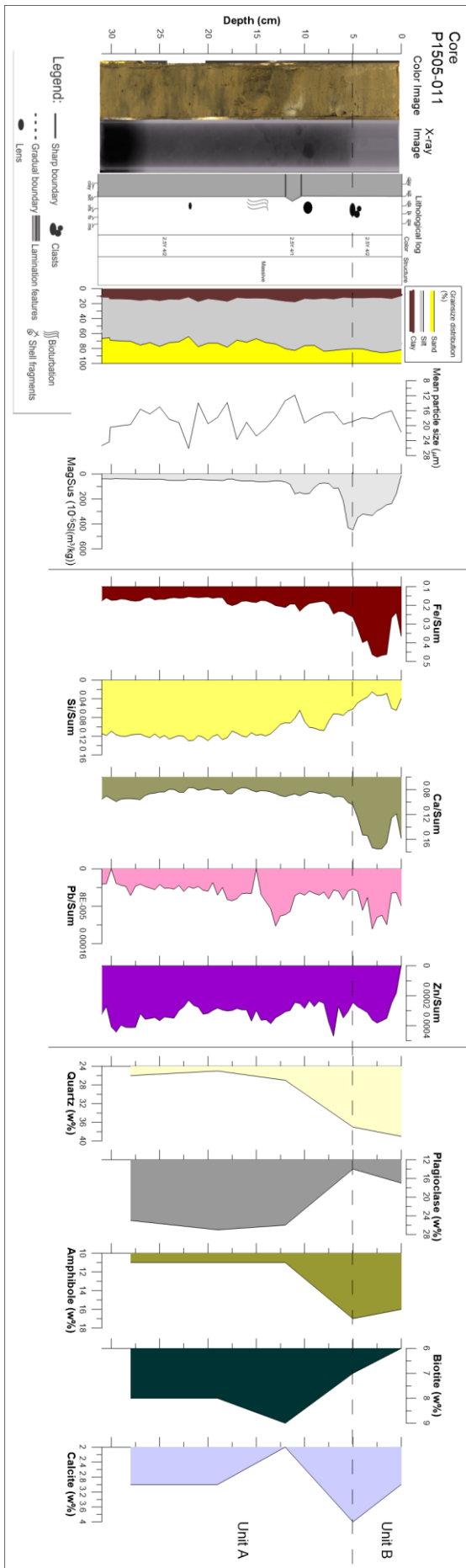


Figure 31 Line-scan image, X-radiograph, visual description, as well as grain-size distribution, physical properties and element geochemistry of core P1505-011

Based on the element ratios, the Si-ratio has an inverse relation to the other ratios. Despite a decrease in Si-ratio, the quartz content gradually increases by ~2 %, accompanied by a ~2 % increase in plagioclase. All other minerals decline about 1 %.

#### **4.2.1.3 Interpretation:**

Based on geochemical data, the core is relatively stable up to 12 cm. The XRD-data shows distinct changes in the mineralogical composition, with a distinct increase in quartz, amphibole and calcite, whereas the other elements decline. The element-ratios show that the distinct change occurs at 7 cm, which is most likely the case, due to a higher data-resolution in XRF data relative to the XRD. The geochemical change indicates a change in sediment input, which based on magnetic susceptibility and Fe/Sum indicate an iron-bearing sediment. The stabilization of grainsize towards the top 10 cm of the core supports the geochemical data, indicating a change in depositional environment.

The occurring change is most likely due to an increased influence of tailings, as the tailings contain amphibole, quartz and magnetite, therefore changing the mineralogy and increasing the magnetic susceptibility. The sediments below 7 cm represent a natural depositional environment without influence of tailings. The stable element ratios imply that the area received sediments from one source, whereas the fluctuation in grainsize indicates that the sediments are deposited in pulses. The stabilization of grainsize in the upper 7 cm of the core shows that the area has been exposed to a more continuous depositional input.

Black spots indicate decay of organic matter (Neira & Rackemann, 1996). Alongside the bioturbation marks, the sediment is influenced by biological activity, which keeps the sediment oxidized.

#### **4.2.2 IG16-1811GC**

Core IG16-1811GC is 75 cm long, situated mid-fjord (figure 21). The core is divided into two units: IG16-1811A and IG16-1811B (figure 32).

##### **4.2.2.1 Unit IG16-1811A (75 – 29 cm)**

Unit A is massive, yellow-grayish colored sediment similar to the color described in chapter 4.2.1.1, only darker (2.5 Y 4/4 MSCC). Towards the top of the unit, an abrupt boundary to the overlaying unit is defined due to a distinct color change. Black spots and bioturbation, as seen in unit P1505-011A, are observed throughout the whole unit. From 75 – 48 cm, the mean particle size increases from medium silt to very coarse silt (12.5 – 45 µm). From 48 – 29 cm, the mean particle size fluctuates up and down, ultimately resulting in a decline to ~15 µm.



Despite fluctuations in grain size, the magnetic susceptibility is very low throughout the unit. The upper 2 cm of the unit shows a slight decrease in magnetic susceptibility. XRF-data shows little change the first 25 cm of the unit, except a gradual increase in Ca-content. From 40 – 35 cm, the Fe-ratio increases significantly, which leads to a decline in Si- and Ca-ratio, and an increase in Pb- and Zn-ratio (as observed in other cores). Towards the top of the unit, Fe-, Si-, Ca- and Pb-content increase while Zn declines.

#### **4.2.2.2 Unit IG16-1811B (29 – 0 cm)**

As mentioned, the defined boundary to unit B is mainly based on color, which has become bright grayish (10YR 7/1 MSCC). Furthermore, stratification of the unit is present throughout the core, which is alterations between bright-greyish and dark/black (2.5 Y 3/1 MSCC) layers. Unlike unit A, the mean particle size varies from bottom to top, whereas bright layers correlate with coarser sediment (very coarse silt (45  $\mu\text{m}$ )), and darker layers with finer sediment (medium silt (10  $\mu\text{m}$ )). From 9 cm and towards the top of the unit, the high rate of fluctuations in grain size sizes, and gradually increases from medium ( $\sim 7 \mu\text{m}$ ) to coarse silt (30  $\mu\text{m}$ ). Unit B shows a significantly more magnetic susceptible sediment, where the susceptibility increases the bottom 8 cm to  $\sim 1500 \cdot 10^{-5} \text{SI}$ . Between 21 and 9 cm, the susceptibility drops to a value about 400, followed by an increase to a value of 2100. Changes in susceptibility correlate with changes in the stratification and grain size.

Based on XRF-data, the unit is characterized by more prominent changes. The Fe-, Si- and Ca-content continues to increase from the underlying unit A. The  $\text{SiO}_2$ -content increases from 60 – 71 % over a 16 cm sequence up-core, with only small changes further up-unit. The CaO-content increases about 0.6 % from 29-28 cm, followed by a stabilization further up-unit. The  $\text{Fe}_2\text{O}_3$ -content increases to a peak at 14.5 % at 23 cm, followed by a 4.5 % decline the following 6 cm. Finally, the Pb- and Zn-concentration drop above the unit boundary and stabilizes at 8 and 40 PPM, respectively.

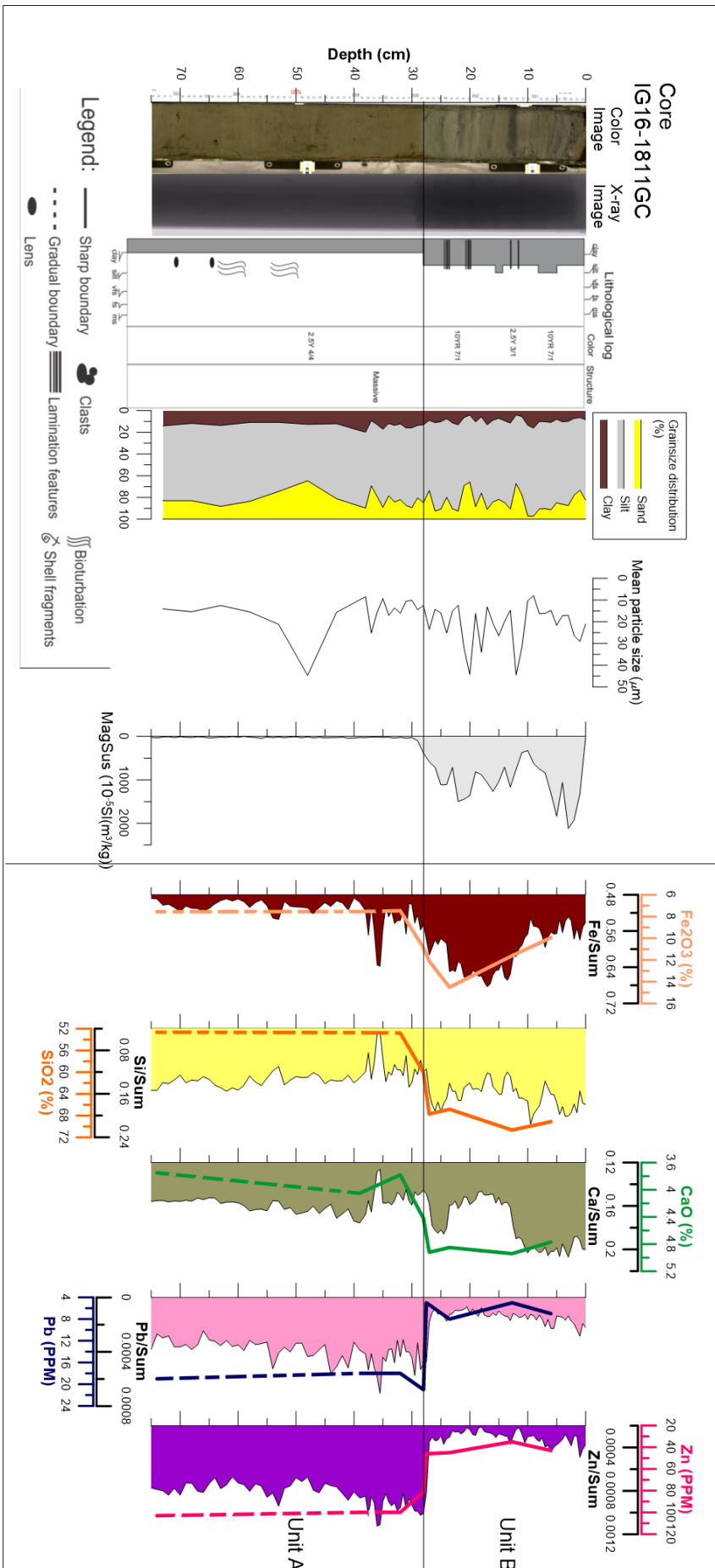


Figure 32 Line-scan image, X-radiograph, visual description, as well as grain-size distribution, physical properties and element geochemistry of core IG16-1811GC.

#### **4.2.2.3 Interpretation**

Based on sediment color, traces of organic activity, uniform magnetic susceptibility and element-ratios, unit A represents a natural depositional environment. Unit B shows what is interpreted to be influenced by tailings, due to the marked increase of Fe<sub>2</sub>O<sub>3</sub> and the magnetic susceptibility. The input of tailings seems to have been deposited in pulses, as the lamination-features may indicate. The tailings correlate with fine-grained sequences in unit B, for instance, the peak in Fe<sub>2</sub>O<sub>3</sub>-content correlates with a drop in mean particle size and sand-content (23 cm), whereas the element-ratio for iron also correlates with a decline in mean particle size. The reason for this may be seasonal changes in the fjord, ultimately effecting whether or not tailings are transported further out-fjord by suspension. Another explanation for episodically occurring tailings is submarine mass movement, which originate from areas further in-fjord, most likely connected to the submarine meandering channels located outside the output source. Furthermore, the marked drop in heavy metal concentration indicates that the natural sedimentation has been reduced, due to an excess input of sediments, diluting the natural input of heavy metal through natural sedimentation.

The boundary between the two units are abrupt and is a good implication on physical and geochemical isolation between the natural sediments and the sediments influenced by tailings influenced.

#### **4.2.3 IG16-1798GC**

Core IG16-1798GC is 135 cm long, situated in the inner part of Bøkfjorden (figure 21). The core is divided into two main units, IG16-1798A and IG16-1798B (figure 33).

##### **4.2.3.1 Unit IG16-1798A (150 – 135 cm)**

Unit A is more or less the same as unit IG16-1811A, as the color (2.5Y 4/4 MSCC) and lack of structures are the most prominent physical characteristics of the unit. The mean particle size of unit IG16-1798A fluctuates, varying between medium (10 µm) to coarse silt (30 µm). The magnetic susceptibility is low from 150 – 144 cm, followed by an increase to 400 10<sup>-5</sup>SI from 144 – 141 cm. The increased susceptibility correlates with a fining of the sediment.

Throughout the unit, the element ratios show no major changes, except for Ca/Sum, which increases towards the top of the unit. The quantitative data show that Fe<sub>2</sub>O<sub>3</sub>-, SiO<sub>2</sub>- and CaO increase towards the boundary, while Pb and Zn decreases significantly (about 50 %).

#### **4.2.3.2 Unit IG16-1798B (135 – 0 cm)**

Unit IG16-1798B is defined as a unit with greyish, stratified sediment. A significant drop in mean particle size is observed at the unit boundary. Despite color difference, the unit have similar characteristics to unit IG16-1811B.

Throughout the 135 cm up-core, the sediment color changes multiple times, mainly alternating between a dark grey-greyish (2.5Y 5/2 MSCC) and a slightly brighter grey (2.5Y 6/2). Between 53 and 26 cm, a purple-brown-greyish colored sediment-sequence is observed (2.5Y 3/2). The mean particle size declines at the lower boundary towards unit A, becoming medium silt (~11  $\mu\text{m}$ ) and remains stable up-core to 15 cm. From 15 cm and to the top of the core, the mean particle size increases to coarse silt (30  $\mu\text{m}$ ). The magnetic susceptibility changes throughout the unit, but correlates with changes in sediment color. From the boundary to the middle of a layered sequence, the susceptibility increases, followed by a decline towards the upper layer boundary. The element-ratios show high values for the Fe- and Si-ratio, while Ca, Pb and Zn show low values. Above the unit boundary, the Si-, Pb- and Zn-ratio is continuously low. The Ca-ratio decreases from the peak at the boundary, towards 100 cm, then stabilizes (except three peaks at 95, 32 and 5 cm). The Fe-ratio correlates with magnetic susceptibility and has an inverse relationship to both Si and Ca. Quantitative data supports the element-ratio, as  $\text{Fe}_2\text{O}_3$ ,  $\text{SiO}_2$  and CaO increases and stabilize above the boundary, and Pb and Zn drop and stabilize.

#### **4.2.3.3 Interpretation**

Core IG16-1798GC shows an abrupt transition from natural to tailings derived sediments, as indicated by the distinct change in both physical and geochemical properties. The stable grainsize indicates a continuous settling of suspended and relatively fine-grained sediments, which over time has resulted in the thick tailings-influenced sediment package. It is worth noting that fluctuations in magnetic susceptibility implies that the influence of tailings has varied throughout history. Furthermore, the distinct geochemical differences between the two units indicate little physical mixing of the sediments.

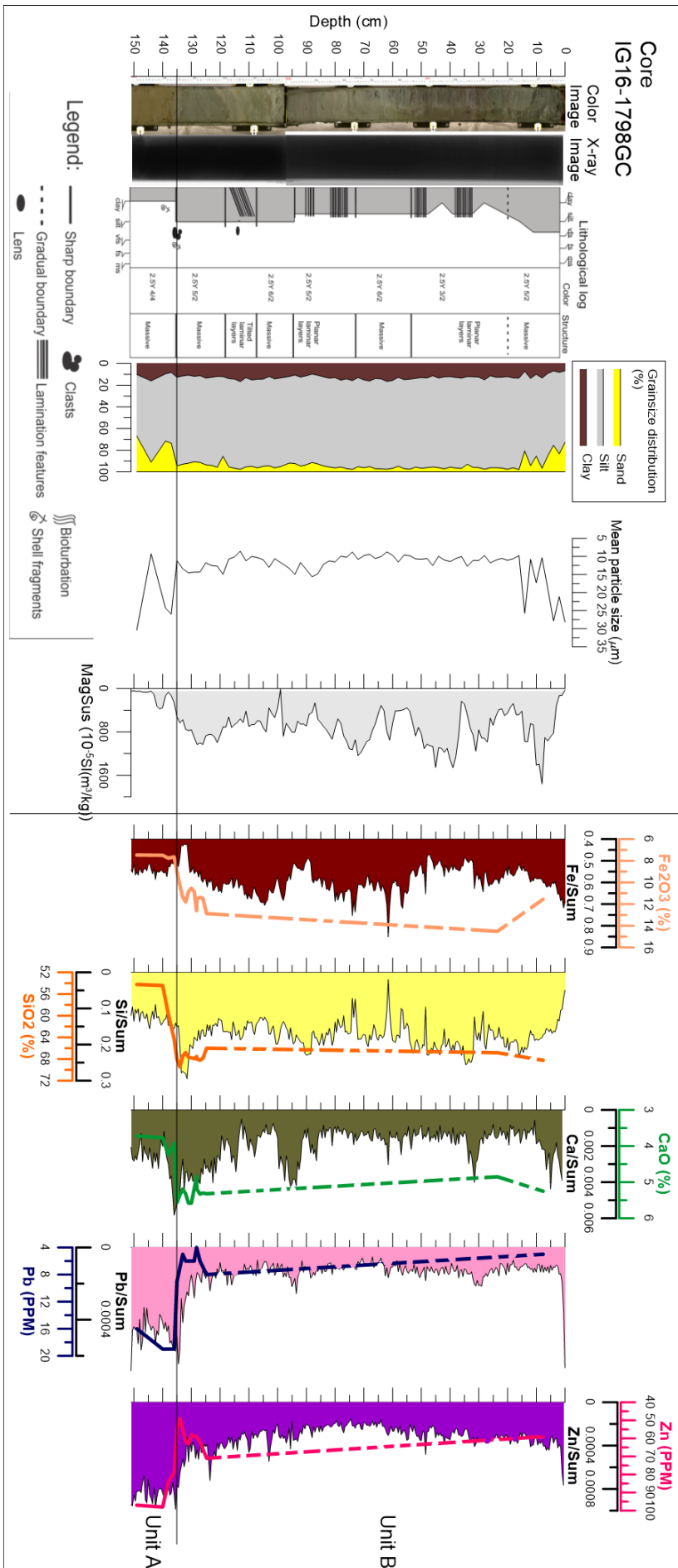


Figure 33 Line-scan image, X-radiograph, visual description, as well as grain-size distribution, physical properties and element geochemistry of core IG16-1798GC.

## 4.3 Stjærnsundet

See figure 22 for core location map of Stjærnsundet.

### 4.3.1 Core P1707-005

Core P1707-005 is located mid-sound, south-east of Lillebukta (figure 22). The core consists of one unit (figure 34).

Core P1707-005, is a 28 cm long, massive, homogenous, brown colored (10YR 4/2 MSCC) sediment core. Presence of bioturbation marks and shell fragments are observed. The sediment is predominantly a medium silt, whereas a coarsening of the sediment appears at 14 cm and up-core. The magnetic susceptibility is relatively low, with a value of 140-120  $10^{-5}$  SI, which gradually increases to 240 from 17 cm to the top of the core.

Element-ratios show that the sediment constitutes mainly Si (0.24 – 0.37), followed by Ca(0.19 – 28) and Fe (0.16 – 0.25). Al fluctuates mainly between 0.08 and 0.06 and K increases from 0.06 – 1.13 from bottom to top. The Pb- and Zn-ratio show a discontinuous data record, which stabilizes in the upper 12 cm of the core. The Pb/Sum-values are very low throughout the core, hence making the data less reliable. The Fe- and Ca-ratio correlate, as they both increase from 28 – 12 cm, peaking at 12 cm. In relation to an increase in Fe and Ca, both Si and Al decrease gradually, followed by a drop at 12 cm. Fe and Ca have an inverse relation to both Al and Si. After the drop at 12 cm, both Si and Al recover back to the same levels as observed prior to the drop, as Fe and Ca gradually decrease towards the top. K, as mentioned, gradually increases in the upper 10 cm of the core (from 0.07 to 0.13).

### 4.3.2 Interpretation

Due to the homogenous characteristics of the cores, the sediments are likely to derive from one source, with the surrounding bedrock as the main sediment source. The bedrock is mainly gabbro (figure 19), which consists of plagioclase, pyroxene, hornblende and apatite, and are associated with quartz rich gneisses (Heier, 1964). Based on geochemical data from Heier (1961), the main elements of the gabbro are  $\text{SiO}_2$  (~43 %),  $\text{Al}_2\text{O}_3$ (15-26 %), CaO (~3-20 %), FeO (~7-9%) and  $\text{Fe}_2\text{O}_3$  (4-12 %). Regarding the composition of the nepheline syenite from Stjernøya, the main elements are Si (~25 %), Al (~12 %), K (~7 %), Na (~6 %), Ca (~2 %) and Fe (~2 %) (Heier, 1964).

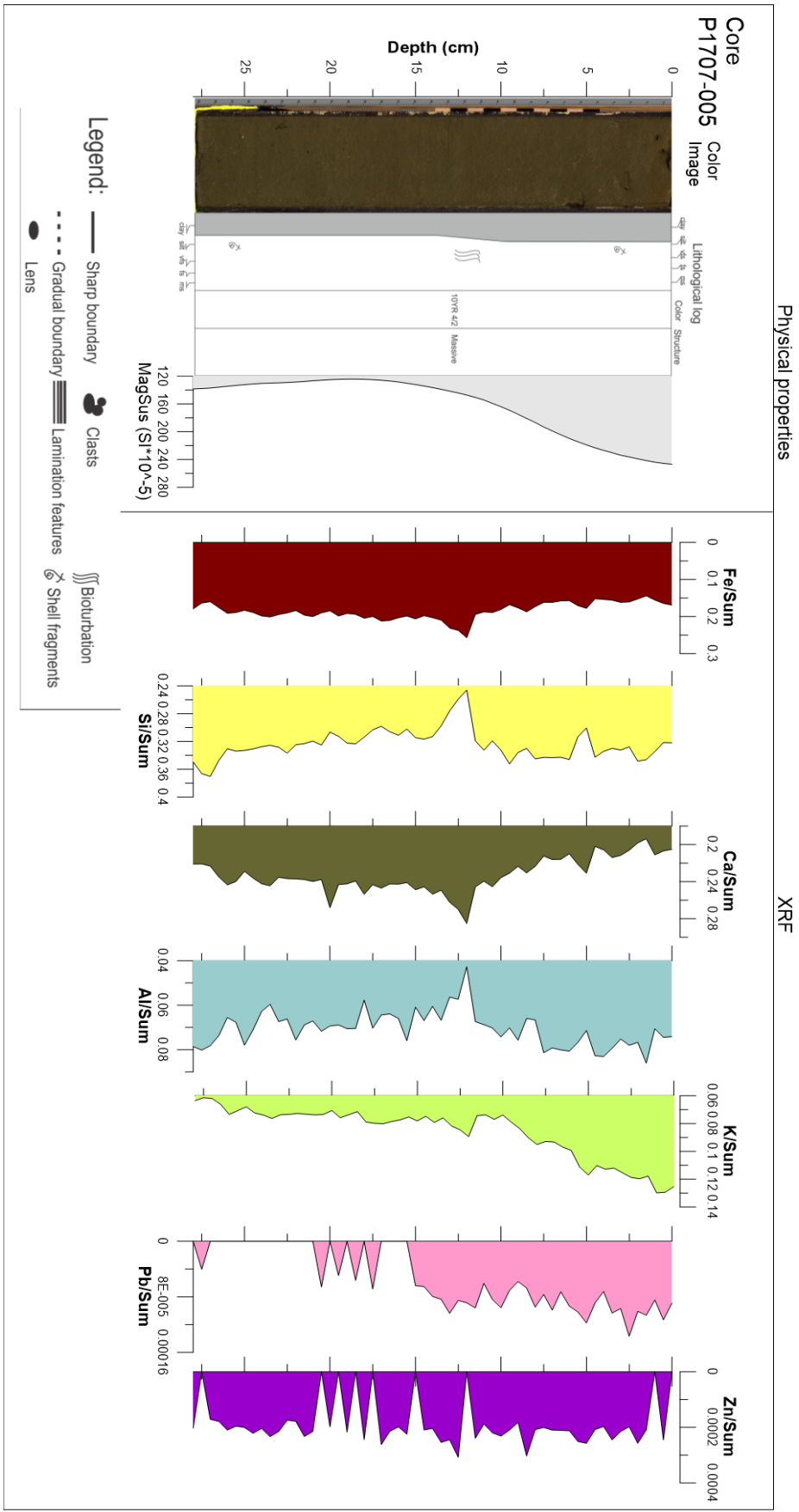


Figure 34 Line-scan image, X-radiograph, visual description, as well as grain-size distribution, physical properties and element geochemistry of core P1707-005.

The most abundant elements in core P1707-005 are Si, Ca and Fe, which seems to match the findings of Heier (1961). If there were influence of tailings in the sediment, one would expect a lowered Si- and Ca-ratio, as the nepheline syenite from Stjernøy has a Si- and Ca-deficiency relative to the gabbroic rocks (43 % SiO<sub>2</sub> in the gabbro vs 25 % Si in nepheline syenite and 3-20 % CaO vs ~2 % Ca in nepheline syenite).

Additionally, from the coarsening of grainsize and increase in magnetic susceptibility, one would expect a direct correlation with the iron-content. In fact, the Fe-ratio shows an inverse relation to grainsize and magnetic susceptibility. The explanation for this relationship may be the two different Fe-oxide types, as more Fe<sub>2</sub>O<sub>3</sub>-input may increase the magnetic susceptibility slightly (Powell et al., 2002).

The most prominent correlation with magnetic susceptibility is the significant increase in the Pb-ratio, occurring at ~15 cm and the about 100% increase in K-ratio in the upper 10 cm. As the magnetic susceptibility starts to increase prior to the K-ratio increasing, it seems likely that Pb and the susceptibility is connected.

### **4.3.3 Core P1707-018**

Core P1707-018 is 31 cm long, situated mid-sound, south of Lillebukta (figure 22). The core is divided into three units. P1707-018A, P1707-018B and P1707-018C (figure 35).

#### **4.3.3.1 Unit P1707-018A (31 – 15 cm)**

Unit P1707-018A is a homogenous, massive dark-brown colored sediment (10YR 3/2 MSCC). Shell fragments occur sporadically. The grainsize is considered fine-grained silt in the lower 13.5 cm. From 17.5 to 15 cm, the grainsize gradually coarsen to fined sand. The boundary to the overlaying unit is gradual, and defined by the mentioned coarsening of the sediment. Increasing grainsize correlates with increasing magnetic susceptibility. The bottom 13 cm of the core shows a gradual increase in susceptibility (200 – 400 10<sup>-5</sup>SI), followed by a significant increase towards the top of the core (400 to 1000 10<sup>-5</sup>SI).

The element-ratios show that Fe, Si and Ca are the most prominent elements. The Fe- and Ca-ratio have an inverse relation to the Si- and Al-ratio, which is evident at 22.5 cm, where Fe and Al peak and Si and Al drop. Towards the top of unit A, Si declines slightly. Pb and Zn fluctuate between low values, and the Zn-ratio is discontinuous throughout the unit.



#### **4.3.3.2 Unit P1707-018B (15 – 12 cm)**

Unit B is similar to unit A, with the same color (10YR 3/2) and lack of structures within the sediment in the lower cm of the unit. At 14 cm, an erosive boundary marks the abrupt transition to a 2 cm thick coarse-grained layer with dark sediment and white shell fragments. Both grain size and magnetic susceptibility form a peak within the dark layer, as medium sand is the dominating sediment. The magnetic susceptibility reaches a value of  $1400 \cdot 10^{-5} \text{SI}$ . The layer ends abruptly to the overlaying unit C.

The Fe- and Ca-ratio increase throughout unit B, whereas Si, Al and K decline. The Si- and Al-ratio remain low, while K rises back to “normal” levels, prior to dropping. Fe remains high towards the boundary, and Ca drops to about 0.2.

#### **4.3.3.3 Unit P1707-018C (12 – 0 cm)**

The uppermost unit has similar characteristics to unit A, except an elevated presence of shell fragments and a slightly less brown color (10YR 3/1). Furthermore, the unit is dominated by fine sand. The magnetic susceptibility gradually decreases, but remains relatively high, compared with unit A ( $1400 - 1100 \cdot 10^{-5} \text{SI}$ ).

Si, Ca and Al remain low from the unit boundary to 5 cm. Fe and Pb increase within the same interval. The upper 5 cm, the Fe-, Si and Al-ratios changes significantly, showing a significant decrease in Fe (0.4 – 0.15) and a marked increase in Si (0.1 – 0.38) and Al (0.02 – 0.11). Ca show a slight decrease. The K-ratio gradually increases throughout the core.

#### **4.3.3.4 Interpretation**

Unit A is derived from natural sediments. The erosive black layer that occurs in unit B is most likely a sediment gravity flow, which the abrupt boundary and input of coarse grained material show. Furthermore, the sediments are most likely to derive from Lillebukta as the magnetic susceptibility increases alongside the observed change in geochemical signals, which shows a Si-deficient sediment, meaning the sediments are likely tailings. The sediments above the erosive layer are defined as a mix between both natural sediments and tailings as the magnetic susceptibility remains high. The main input may be of the fine tailings-fraction ( $<20 \mu\text{m}$ ).

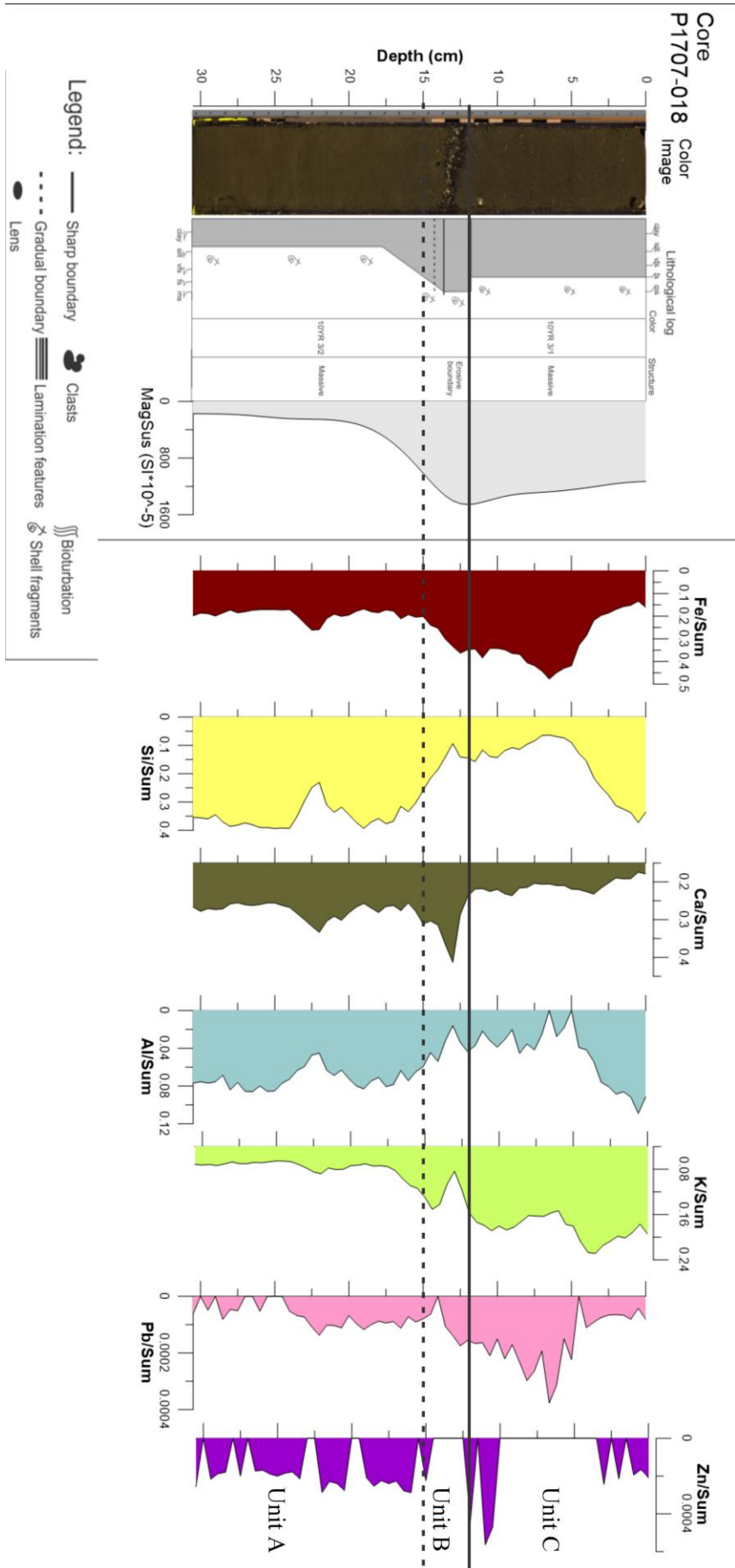


Figure 35 Line-scan image, X-radiograph, visual description, as well as grain-size distribution, physical properties and element geochemistry of core P1707-005.

#### **4.3.4 Core P1707-010**

Core P1707-010 is 22 cm long and is situated in Lillebukta (figure 22). The core is divided into two units: unit P1707-010A and P1707-010B (figure 36).

##### **4.3.4.1 Unit P1707-010A (22 – 4.5 cm)**

Unit A is a massive, brown-greyish colored (10YR 4/1 MSCC) clay. The only structures observed within the unit are two black spots at 17.5 and 8 cm, respectively. Between 7 – 5 cm, the sediment color changes slightly, to a lighter grey. The boundary to the overlaying unit is characterized as an abrupt erosive boundary. The lower 12 cm of the unit is characterized as low magnetic susceptible, but from 10 cm and up-core towards the top of the unit, the susceptibility increases gradually to a value above 2000  $10^{-5}$ SI.

The element-ratios are relatively stable throughout the unit, with an elevated Si- and Al-ratio compared to the two previously described cores. Pb and Zn values are low and discontinuous.

##### **4.3.4.2 Unit P1707-010B (4.5 – 0 cm)**

Unit B consists mainly of a black colored, coarse and massive sediment. The lower boundary of the unit is defined by a tilted, erosive contact, superimposed by a 1 cm laminated sequence, alternating between dark and brown sediment of fine sand. Above the laminated layer, the massive, dark, medium sand dominated sediment is prominent. The magnetic susceptibility increases significantly throughout the core, from ~2000 at 4.5 cm to 6000  $10^{-5}$ SI.

Most of the element-ratios change in the core, whereas the most distinct change is observed in Si/Sum, which declines from ~0.58 – ~0.36. In correlation with the Si-decline, all other elements increase, with a peaking of the Al- and Ca-ratio and drop in Fe at 3 cm.

##### **4.3.4.3 Interpretation**

The two units observed in Core P1707-010 represent two environments. Unit A belongs to a natural environment, which due to its physical properties (grainsize and color) and geochemical data (elevated Si-content) is part of a low-energy depositional environment with one sediment source. Unit B on the other hand, represents a tailings influenced environment, which is dominated by silica deficient, coarse-grained sediments. The grainsize, geochemistry and erosive boundary indicate a sudden deposition, implying that a submarine mass movement event has occurred. The coarse dark layer reduces the silica-content alongside a major increase in magnetic susceptibility, hence implying major influence by tailings from nepheline syenite. Additionally, the magnetic susceptibility shows that there is a transition from natural to tailings-dominated sediments, as the sediment becomes gradually more susceptible from ~10 cm and further up-core. As previously mentioned, the tailings are

deposited in different grainsizes, (45 % <63 μm and 15% <20 μm). Therefore, it is likely that the finer fraction of the tailings has been deposited alongside natural sediments, which has led to a slight color-change observed at ~7 – 4.5 cm.

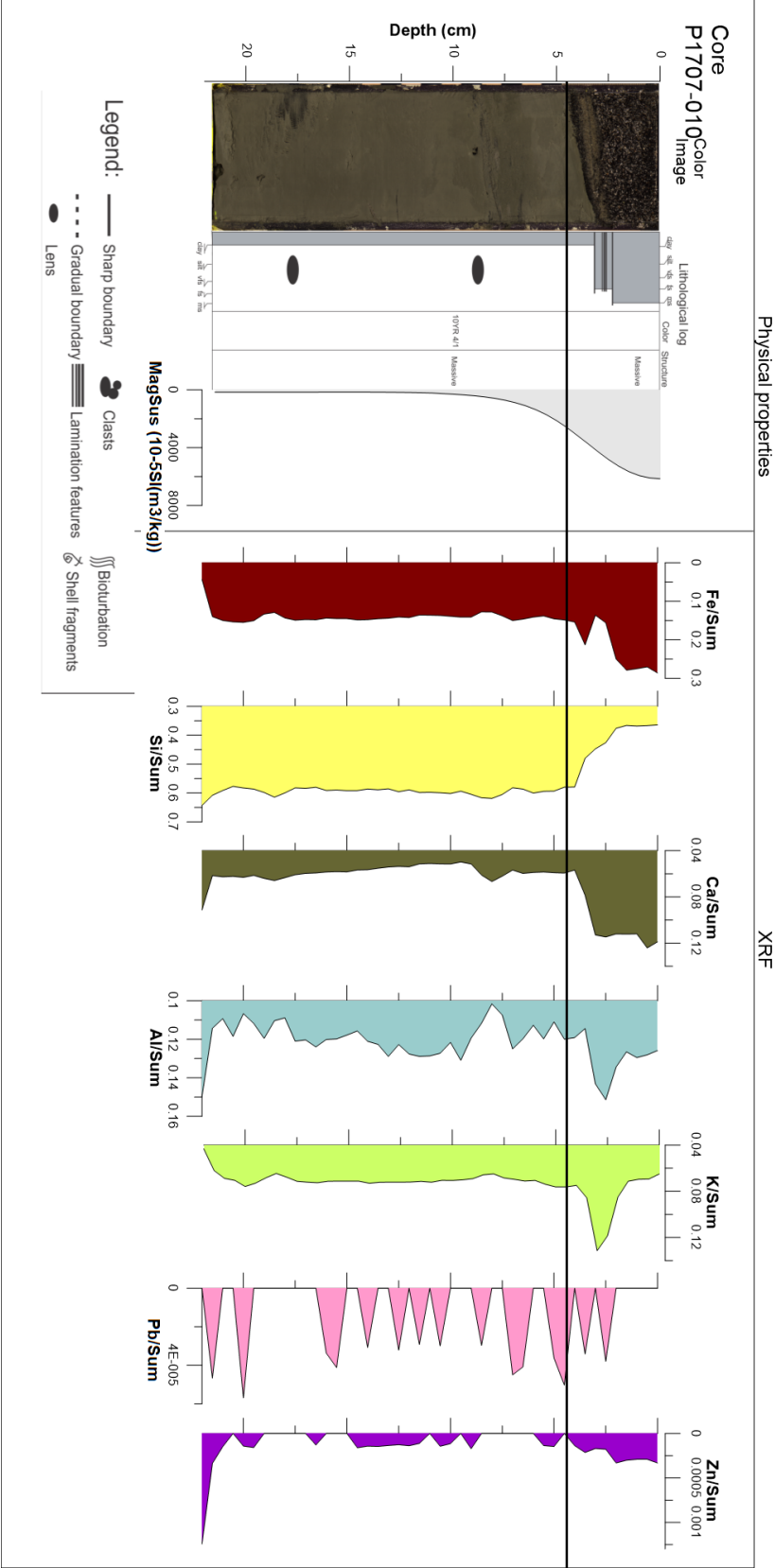


Figure 36 Line-scan image, X-radiograph, visual description, as well as grain-size distribution, physical properties and element geochemistry of core P1707.010

## 5 Discussion

### 5.1 Sedimentary processes in Ranfjorden, Bøkfjorden and Stjærnsundet

#### 5.1.1 Ranfjorden

Based on the findings as described in chapter 4.1, the fjord shows two depositional endmembers.

##### 5.1.1.1 Endmember 1 (naturally derived sediments)

The first endmember is part of the natural depositional environment in the fjord, with the following characteristics:

1. Yellow and bright grey colored, massive sediments
2. Increasing up-core or fluctuating mean grainsize (10 – 50  $\mu\text{m}$ )
3. Low, stable magnetic susceptibility ( $<50 \cdot 10^{-5}$  SI)
4. Generally low, fluctuating element ratios
5. High Pb/sum and Zn/sum ratios
6. High  $\text{SiO}_2$ -content ( $\sim 52\%$ )
7. Low  $\text{Fe}_2\text{O}_3$ -content ( $\sim 8\%$ )
8. Dominated by quartz and clay minerals

Cores containing endmember 1: **P1502-001**, **P1502-004** and **P1502-015**.

Similar to all cores containing endmember 1 is that the core locations are situated in relatively shallow waters within the innermost basin of Ranfjorden. Core P1502-001, which contains the longest sediment sequence record of endmember 1 (figure 27), is situated in a relatively isolated area 17 km out-fjord from the tailings output source. Core P1502-004 and P1502-015 are located further in-fjord, along the western fjord-slope in the innermost basin of Ranfjorden, proximal to the tailings output source (figure 20).

The uniform characteristics of the natural sediments found in the cores (figure 27, 28 and 30), indicate a continuous and one-sided depositional environment, which according to Syvitski and others (1987) derives from Ranaelva, feeding Ranfjorden with a sediment input of about 27 000 tons/year. Transportation and settling of suspended river-sediments occur within the fjord surface layer, which flows out-fjord due to the estuarine circulation (Johansen et al., 2004). The observed fluctuations in grainsize in endmember 1 are result of variations in river runoff, leading to a relative coarsening of sediments when the runoff is high.

### 5.1.1.2 Endmember 2 (tailings-derived sediments)

Endmember 2 is part of the tailings-dominated depositional environment in the fjord, with the following characteristics:

1. Red colored, massive sediments
2. Fine-grained sediments ( <20  $\mu\text{m}$ )
3. High, increasing (up-core) and fluctuating magnetic susceptibility (400 – 1400  $10^{-5}$  SI)
4. High, fluctuating element ratios
  - a. Relatively high Fe/sum- and Ca/sum- ratios
  - b. Relatively low Si/sum-ratio
5. Low Pb/sum and Zn/sum ratios
6. Low SiO<sub>2</sub>-content (~47 %)
7. High Fe<sub>2</sub>O<sub>3</sub>-content (~16 %)
8. Dominance of quartz, clay and iron-oxide minerals (hematite and magnetite)

Cores containing endmember 2: **P1502-013**, **P1502-004** and **P1502-015**.

Endmember 2 is present in cores located in shallow and deep waters. Core P1502-004 and P1502-015, situated in the fjord-slope west of Ranaelva, have about 10 cm long sequences containing tailings-influenced sediments, whereas P1502-013, situated at the submarine channel at the fjord-bed, has a 38 cm thick sequence long record of tailings-influenced sediments (see figure 20). The varying sediment-thickness of endmember 2 implies that depth is a key factor in tailings influence, implying that the sedimentation is higher towards the fjord-bed compared to the slopes. Furthermore, the submarine channels are another indication that both erosion, transportation and deposition occurs along the fjord bed (see figure 10).

According to the study conducted by Rygg et al. (1994), transmission and sediment trap measurements from the inner part of Ranfjorden showed an elevated particle presence in the water column at 25 m, 60-65 m and towards the fjord-bed. This indicates that the input of tailings controlled by two sedimentary processes: 1) suspension plumes, which occur at 25 m water depth and 2) bed-load transport (gravity flow) occurring at 60 m and deeper, along the fjord bed. The fine-fraction of tailings are likely to occur within the suspension plume at 25 m, whereas the coarse-fraction would dominate the bed-load transported sediments (Rygg et al., 1994).

The presence of tailings in cores P1502-004 (figure 28) and P1502-015 (figure 30) is connected to the suspension plume at 25 m, which due to flocculation ultimately leads to deposition of tailings. The suspension plume is according to Rygg and others (1994), likely to be transported across the fjord, underneath the brackish surface-layer that moves from the fjord-head and out-fjord.

The tailings in core P1502-013 are mainly massive (figure 29), indicating a continuous input of suspended fine-grained tailings. These sediments are likely to be connected to what Tesaker (1978) identified in his study in Ranfjorden as a sinking suspension current of tailings, moving out-fjord from the tailings output source, with a velocity of 25 cm/s, 1 m above the fjord-bed (as cited in Syvitski et al., 1987). In opposition to unit A and C, unit P1502-013B's characteristic stratification of sediments show similarities to cores described by Hay and others (1983), a study conducted on tailings deposits in Rupert Inlet, British Columbia. Hay and others (1983) defined the stratification within their tailings-influenced cores as fining-upward turbidities, which are similar to the stratification seen in unit B at two occasions (27.5 – 25 cm and 23 – 17.5 cm) (see figure . It is likely that the stratification within the core is a result of episodic slope failures due to rapid deposition of tailings at the fjord-head slope (Tesaker, 1978 (as cited in Syvitski et al., 1987), which ultimately leads to erosive turbidite currents, hence eroding the sediment bed, which has formed the submarine canyon and channels (Syvitski et al., 1987).

Furthermore, Tesaker (1978) concludes that the submarine landforms (canyons and channel) outside Rana harbor, are a direct result of erosive mass movements, whereas the 50 m deep canyon situated outside the tailings disposal site is eroded until bare rock was exposed (as cited in Syvitski et al., 1987). Calculations conducted by Tesaker (1978) estimated that ~18% of the discharge is transported by suspension plumes, whereas 82% is transported by bed load (as cited in Syvitski et al., 1987).

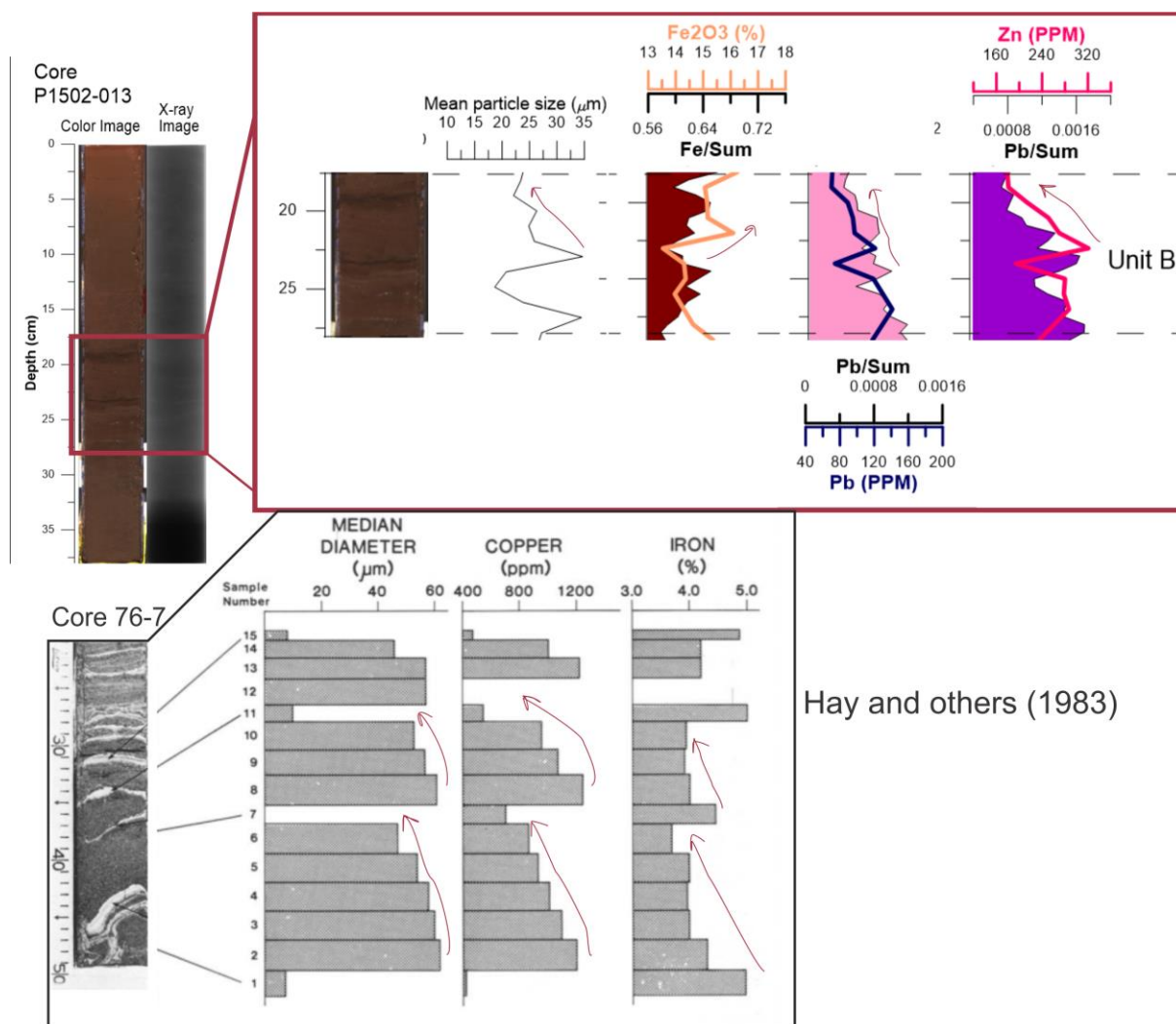


Figure 37 Comparison between vertical sediment profiles of tailings from core P1502-013 from Ranfjorden (above) and core 76-7 from Rupert Inlet, British Columbia (below). Due to low resolution of quantitative XRF, the most proper correlation in of the tailings in Bøkfjorden is magnetic susceptibility with respect to mean particle size.

### 5.1.1.3 Transition (mix of endmembers 1 & 2)

Transition zones are part of a depositional environment in the fjord with a mixed input of tailings and natural sediments, with the following characteristics:

1. Dark grey to dark red colored, massive sediments
2. Gradually decreasing mean grainsize
3. Gradually increasing magnetic susceptibility
4. Gradually increasing and decreasing element ratios
  - a. Increasing Fe/sum, Ca/sum, Pb/sum and Zn/sum ratios
  - b. Decreasing Si/sum-ratio
5. Significantly increasing Pb-content and Zn-content
6. Gradually decreasing SiO<sub>2</sub>-content (~52 – 49 %)



7. Gradually increasing Fe<sub>2</sub>O<sub>3</sub>-content (~9 – 13 %)
8. Changing mineralogy
  - a. Significant increase in iron-oxides (predominantly hematite)
  - b. Decrease in clay mineral content
  - c. Little change in quartz content

Cores containing transition zones: **P1502-004** and **P1502-015**.

Transition zones are visible in cores from the fjord slope in the inner part of Ranfjorden, which indicate that the slope is not exposed to erosive processes, hence preserving the transition from endmember 1 to endmember 2, representing a gradual change in depositional environment, as the environment becomes more tailings-influenced further up-core. The characteristics of the transition zones and location of the cores points toward a continuous input of sediments, related to settling of suspension plumes from river- and tailings discharge. At first, a dominating supply of sediments derived from the adjacent river, which seems to have been dominating from the bases of the cores and up to about 20 - 25 cm core depth, where magnetic susceptibility and hematite-content start to rise (core P1502-015). Further up-core, the natural sedimentation and tailings co-exist in the water column, whereas the natural sediments are exceeded by the high rate of tailings deposition from Rana Gruber, ultimately coloring the sediment due to oxidization of the hematite-particles (Lynn & Pearson, 2000). Furthermore, the transition in core P1502-015 shows a distinct increase in the heavy metals Pb and Zn (figure 30 and 38).

A study conducted by Skei and Paus (1979) identified and dated heavy metal pollution within a sediment core retrieved mid-fjord, 15 km out-fjord from the tailings output source. The conclusion was that the high metal levels within the fjord are connected to the various industrial activities. The high Fe<sub>2</sub>O<sub>3</sub>-content is related to Fe-bearing tailings from Rana Gruber, whereas the Pb and Zn pollution originates from a local zink-lead floatation plant (the local ironworks) that was established at the turn of the century (Syvitski et al., 1987), which <sup>210</sup>Pb-dating conducted by Skei & Paus (1979) supports.

By comparing the results from Skei & Paus (1979) and the results from chapter 4.3.1 (figure 38), it is likely that the transition from a natural- to a tailings-dominated depositional environment occurred in 1891 ±10 years AD. During the following years, tailings have gradually exceeded the natural deposition. Furthermore, the distinct drop in Pb and Zn observed in core P1502-015 marks the end of the transitional zone and the beginning of

endmember 2. The drop in heavy metals is mostly likely due to the closure of the local iron works in 1989 (Helland et al., 1994), which results in a Fe-bearing tailings dominated deposition in the fjord (endmember 2).

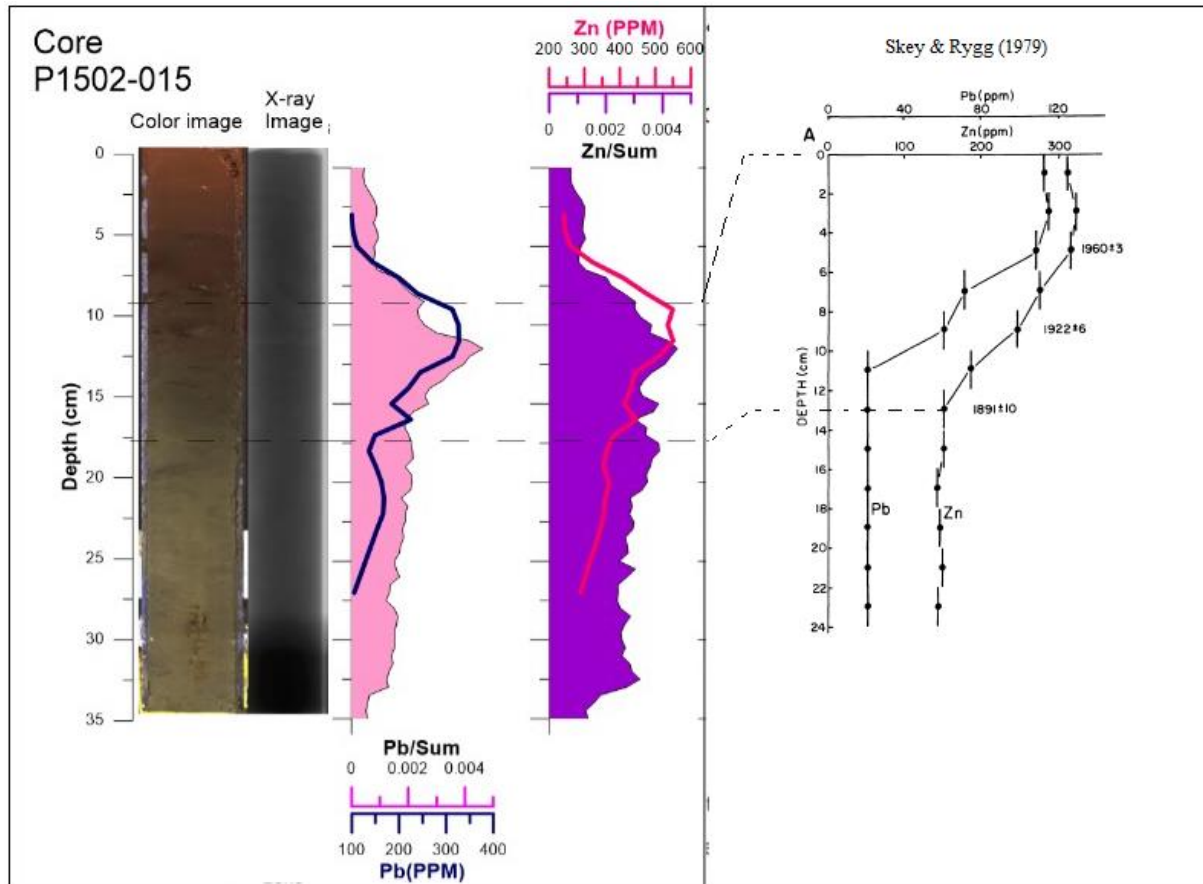


Figure 38 Vertical Pb and Zn profile from chapter 4.3.1 and Skei & Paus (1978), the dashed lines mark the start and end of the transition zones.

#### 5.1.1.4 Interplay between tailings and natural sediments

There are two sedimentary processes identified within Ranfjorden: settling from suspension plumes deriving from the local river and tailings discharge. Both lead to deposition of tailings and natural sediments, hence making tailings and natural sediments coexist within the sediments. During the past 100 years or so, settling of tailings has gradually exceeded settling of natural sediments, hence smothering fjord-bed fauna and limiting interplay with natural sediments in relatively shallow waters (Kirkerud et al., 1986). The transition in sediment-content is observed in core P1502-015 where changes in mineralogy occurring as hematite are introduced to suspension plumes. Additional, post closure of the ironworks, the heavy metal pollution in the core decreased, which may be a combination of a limited input of Pb and Zn

from local industry alongside dilution from the continued discharge of Fe-bearing tailings from Rana Gruber. The combination has led to about 10 cm burial of the polluted sediments relative to Skei & Paus' core (1979). Based on geochemistry-data from core P1502-015, the tailings from Rana Gruber have led to a physical and chemical isolation of the polluted sediments. Ultimately, the sedimentation of Fe-bearing tailings from Rana Gruber leads to a capping effect of previously polluted sediment, which can be characterized as an *in situ* capping (Azcue et al., 1998). Sediments deposited in the deeper parts of the fjord show no presence of natural sediments. Based on observations from Tesaker (1978), the main sedimentary process in the inner parts of Ranfjorden are gravity flows (bed load of tailings). Periodically, slope failures lead to erosive subaqueous mass movements, which forms submarine canyons and channels, hence remobilizing previously deposited sediments. The stratification within core P1502-013 is a good indication of physical mixing between polluted (ironworks) and non-polluted (Rana Gruber) tailings, as an alternation between high and low Pb and Zn concentrated sediments occurs. Therefore, it is likely that physical mixing between natural sediments and tailings occurs as turbidity currents move down slope, mixing already deposited natural sediments with tailings, moving further out-fjord. Figure 39 summarizes the mentioned sedimentary processes within Ranfjorden.

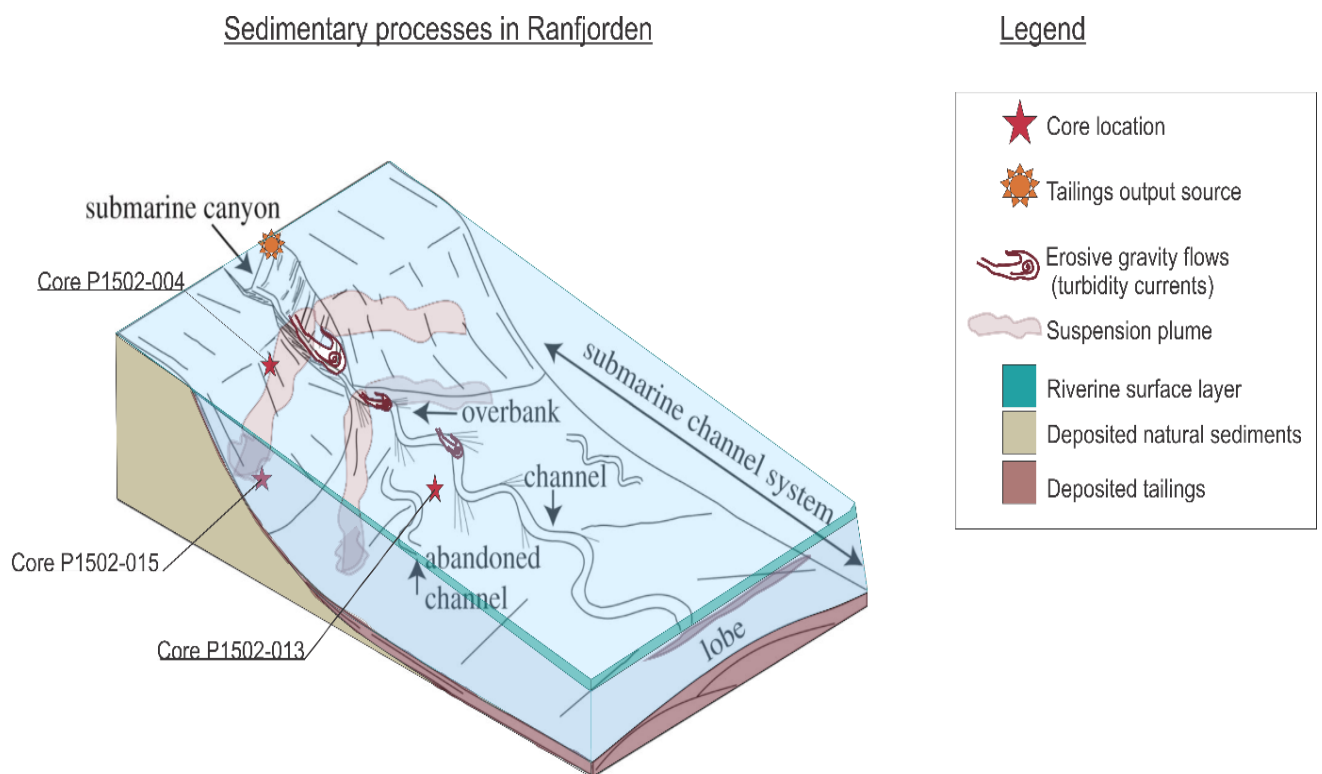


Figure 39 Summary of the sedimentary processes occurring in Ranfjorden.

## 5.1.2 Bøkfjorden

Based on the findings as described in chapter 4.2, the fjord shows two depositional endmembers.

### 5.1.2.1 Endmember 1 (naturally derived sediments)

Endmember 1 is part of the natural depositional environment in the fjord, with the following characteristics:

1. Yellow-greyish, massive sediments
2. High presence of bioturbation and organic content
3. Fluctuating grainsize (~10 – 50  $\mu\text{m}$ )
4. Low magnetic susceptibility (~50  $10^{-5}$  SI)
5. Stable element-ratios
  - a. Low Fe/sum ratio
  - b. High Si/sum, Ca/sum, Pb/sum and Zn/sum ratios
6. Low  $\text{Fe}_2\text{O}_3$ -content (~7.5 %)
7. Relatively low  $\text{SiO}_2$ -content (~53 %)
8. Low heavy metal concentrations
9. Relatively stable mineralogy dominated by quartz and plagioclase

Cores containing endmember 1: **Core P1505-011, IG16-1811GC and IG16-1798GC.**

All cores from Bøkfjorden contain endmember 1, whereas the degree of burial varies throughout the fjord. The naturally derived sediments are the most prominent in core P1505-011 (figure 31), situated in the outer part of Bøkfjorden (figure 21). The core is not buried by overlying tailings, but contains a 7 cm long tailings influenced sediment-sequence towards the top, whereas endmember core IG16-1811GC and IG16-1798GC are buried by relative thick tailings-cover (endmember 2) (figure 32 and 33, respectively). Based on these observations, it is clear that the burial of natural sediments decreases with increasing distance from tailings output source, making natural sedimentation more dominant further out-fjord.

The characteristics of endmember 1 indicate a stable and continuous input of sediments, due to input of erosional products from the surrounding bedrock from rivers or organic material from biological activity in the water column (Skei & Rygg, 1989). Hypopycnal sedimentation is likely the main contributing process for sedimentation of natural sediments within the fjord, which in the neighboring fjord, Korsfjorden, is estimated to be 4 mm/year (Syvitski et al., 1987).

### 5.1.2.2 Endmember 2 (tailings-derived sediments)

Endmember 2 is part of the tailings-dominated depositional environment in the fjord, with the following characteristics:

1. Alternating gray and dark, stratified/laminated sediment
2. Fine-grained mean particle size ( $\sim 10 \mu\text{m}$ )
3. High, fluctuating magnetic susceptibility ( $1000 - 2000 \cdot 10^{-5} \text{ SI}$ )
4. Varied fluctuating element ratios
  - a. High fluctuations in the Fe/sum, Si/sum and Ca/sum ratios
  - b. Low fluctuations in the Pb/sum and Zn/sum ratios
5. Very high  $\text{SiO}_2$ -content ( $\sim 66 - 70 \%$ )
6. High  $\text{Fe}_2\text{O}_3$ -content ( $\sim 12 - 14 \%$ )
7. Very low heavy metal concentration
8. Changing mineralogy
  - a. High abundance of quartz
  - b. Lower abundance of plagioclase
  - c. Increased input of amphibole

Cores containing endmember 2: Core **IG16-1811GC** and **IG16-1798GC**.

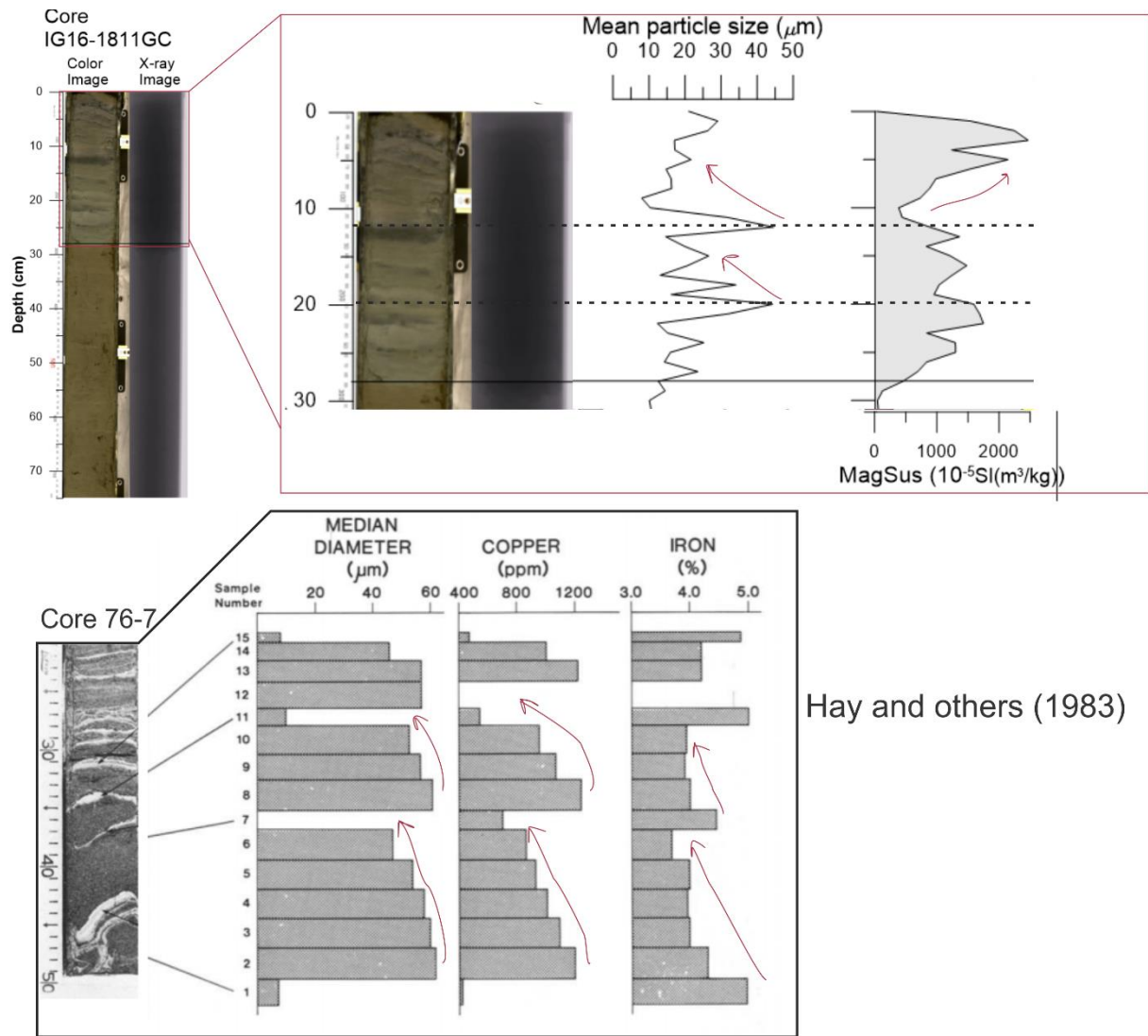
The two cores containing endmember 2 are found in the middle and inner part of the fjord. In core IG16-1811GC, retrieved from 234 m water depth in the central fjord (figure 21), the defined sequence of endmember 2 is 34 cm thick (figure 32). Core IG16-1798GC, retrieved from 105 m water depth in the inner part of Bøkfjorden, contains a 135 cm long sediment sequence of tailings (figure 33). Based on the observed presence of endmember 2 in the two cores, tailings influence is controlled by distance from output source, decreasing further out-fjord.

Based on turbidity measurements from the western side of Bøkfjorden conducted by Berge and others (2011 and 2012), the main processes of transport and sedimentation of tailings are 1) hypopycnal suspension plumes and 2) bed load (figure 17A and 17B). The highest concentration of tailings are situated along the fjord bed, proximal to the tailings discharge source. As tailings are transported further out-fjord, the particles within the sinking bed load current are most likely deposited along the way, hence weakening the measured turbidity. The bed load is relatively concentrated up to 6 km out-fjord ( $>1 \text{ FTU}$ ). Beyond 6 km, smaller concentrations of particle transport are observed ( $<1 \text{ FTU}$ ), most likely due to transport of

very fine-grained particles. These particles reach as far as 14 km out-fjord. Furthermore, as most of the tailings sink as bed load, some particles are released up into the water column, likely as a result local tide-driven currents (Berge et al., 2012). Also, the suspended particles show the same sinking trend as the bed load current.

A mapping of the fjord-bed around the tailings discharge pipe conducted by Arctic Dive in 2012 (Øie, 2013), identified local submarine channels, stating that the subaqueous structures are of tailings origin (figure 14). This implies that episodic events of slope failures have occurred, leading to erosive mass movements, resulting in sedimentation of tailings further out-fjord (Tesaker (1978), as cited in Syvitski et al., 1987). The stratified deposits in core IG16-1811GC, located about 4 km further out-fjord from the channel mouth, north-west of Reinøy, are likely deposited by this process, which contain evident stratification within the endmember 2 sequence. Compared to the study conducted by Hay and others (1983), there are similarities within core IG16-1811 and 76-6, as both cores show fining-upwards sequences (figure 40), which are interpreted to be turbidites deposits. In core IG16-1811GC, tailings influenced sediments are identified as relatively fine-grained sediments, with an elevated magnetic susceptibility (fine-grained magnetite-particles), whereas the coarse-grained sediments are less susceptible, implying that the coarser layers are dominated by natural sediments or quartz dominated tailings.

Cores IG16-1798GC and 76-7 show poor correlation, as the mean particle size in the Bøkfjorden-core is relatively stable, with no indication of fining-upwards sequences (figure 41). Furthermore, there are little evidence of erosive features within the core. Due to the lack of fining-upwards sequences and erosive features, it is less likely that these deposits are directly deposited by turbidite currents (although turbidites do not always deposit fully preserved fining-upwards sequences (Bouma (1962), as cited in Forwick, 2001).

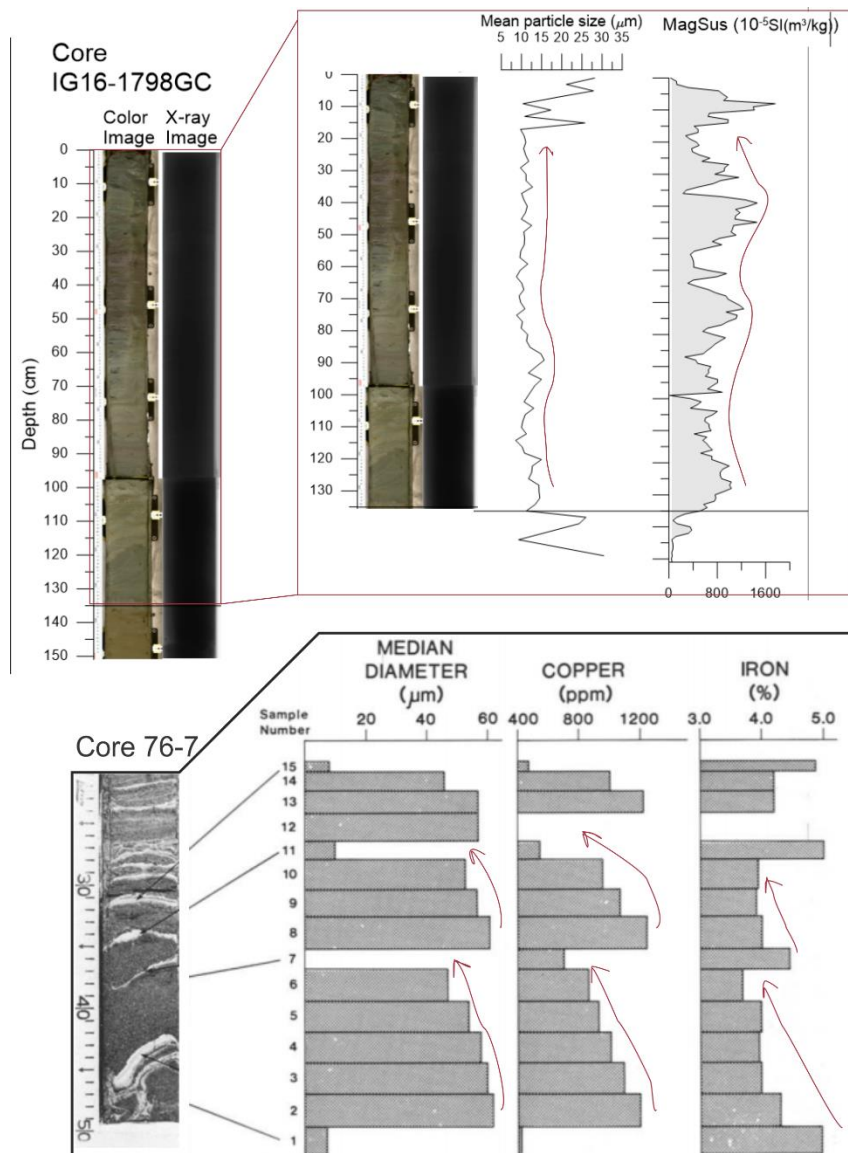


Hay and others (1983)

Figure 40 Comparison between vertical sediment profiles of tailings from core IG16-1811GC from Bøkfjorden (above) and core 76-7 from Rupert Inlet, British Columbia (below). Due to low resolution of quantitative XRF, the most proper correlation in of the tailings in Bøkfjorden is magnetic susceptibility with respect to mean particle size. Red arrows mark observed trends.

The most likely sedimentary process is settling of suspended tailings, due to high turbidity from the tailings output source (Berge et al., 2011 & 2012). Moreover, deposited tailings are also likely a result of overspilling turbidity currents. According to a study of a subaqueous canyon outside Andøya in Troms, Norway, conducted by Amundsen and others (2015), fine-grained spill over occurred due to a high and continuous sediment supply from an adjacent ice-stream. In Bøkfjorden the submarine channel is fed with a high sediment supply from the tailings discharge site, resulting in turbidity currents, hence leading to over spills. When over spill occurs, coarse sediments are contained within the channel or proximal to the levee,

whereas fine-grained particles are dispersed to more distal areas, with a large lateral extent (Amundsen et al., 2015).



Hay and others (1983)

Figure 41 Comparison between vertical sediment profiles of tailings from core IG16-1798GC from Bøkfjorden (above) and core 76-6 from Rupert Inlet, British Columbia (below). Due to low resolution of quantitative XRF, the most proper correlation in of the tailings in Bøkfjorden is magnetic susceptibility with respect to mean particle size. Red arrows mark observed trends

### 5.1.2.3 Interplay between tailings and natural sediments

In Bøkfjorden, the interplay between tailings and natural sediments are limited in the innermost part of the fjord. Since the fjord was used as recipient of tailings in 1971, the transition from natural to anthropogenic derived sedimentation has been quick, indicated by the sharp contact between tailings and natural sediments. The contact between endmember 1 and 2 in the inner part of the fjord is not erosive and therefore likely due to elevated settling rate of tailings in suspension. Based on the 135 cm thick tailings-sequence deposited at the



core site of IG16-1798GC over 45 years, a rough estimation of sedimentation show a yearly deposition of 3 cm (equation 1), which is 15 times higher than the estimated natural sedimentation (2 mm/year) (Skaare, Oug & Nilsson, 2007).

Eq. 1:

$$\text{Sedimentation rate} = \frac{\text{accumulated thickness}}{\text{years of disposal}} = \frac{135 \text{ cm}}{45 \text{ years}} = \frac{3 \text{ cm}}{\text{year}}$$

This elevated sedimentation rate is likely the cause of the non-erosive contact. The sudden elevation in sediment discharge to the fjord has led to a rapid transition from natural dominated deposition to tailings dominated deposition. Ultimately, the rapid transition has resulted in burial and isolation of the underlying natural sediments, limiting physical and geochemical mixing. The capping effect of natural sediments is clearly based on heavy metal XRF-data, showing a distinct drop in Pb and Zn concentrations at the contact in core IG16-1798GC (figure 33) and IG16-1811GC. Moreover, the sharp boundary in core IG16-1811 between endmember 1 & 2 is most likely due to turbidite currents. If so, it is likely that physical mixing between natural sediments and tailings occurs (erosion and remobilization), hence, leading to a mixed deposition, which the stratification implies. Furthermore, the out-fjord transportation of tailings by mass movements likely results in suspension of very fine-grained tailings that are dispersed to the outer part of Bøkfjorden. It is likely that small amounts of Fe-bearing particles are settling alongside natural sediments, leading to the observed increase or “transition” in magnetic susceptibility in P1505-011, situated 13 km out-fjord. According to Berge and others (2012), the tailings are unlikely to reach areas outside the sill, 17 km out-fjord. Figure 42 summarizes the sedimentary processes in Bøkfjorden.

## Sedimentary processes in Bøkfjorden

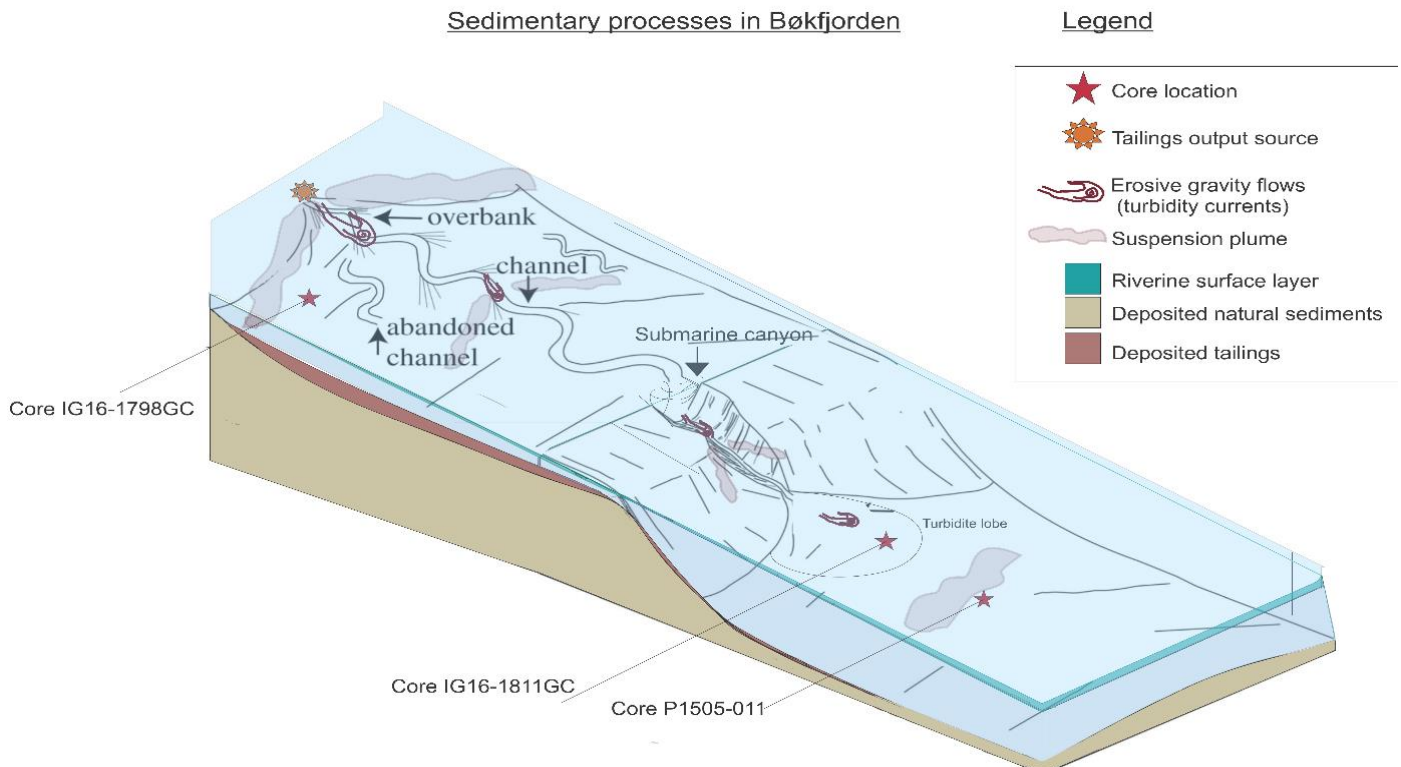


Figure 42 Summary of sedimentary processes in Bøkfjorden.

### 5.1.3 Stjernesundet

Based on the findings as described in chapter 4.3, the fjord shows two depositional endmembers.

#### 5.1.3.1 Endmember 1 (naturally derived sediments)

Endmember 1 is part of the natural depositional environment in the sound, with the following characteristics:

1. Brown colored, massive, homogenous sediment
2. Silty and clayey sediment
3. Low magnetic susceptibility
4. Stable element ratios
  - a. Consist mainly of Si/sum, Ca/sum and Fe/sum ratios

Cores containing endmember 1: **Core P1707-005, P1707-018 and P1707-010.**

The cores containing endmember 1 are situated in both deep and shallow water. The sediment sequences containing endmember 1 are becoming longer by moving further away from the discharge source. Core P1707-005 (figure 34), located mid-sound, about 5 km south-east of

Lillebukta contains exclusively natural sediments (figure 22). Core P1707-018 (figure 35), located mid-sound about 2 km south of Lillebukta, reveals a 14 cm endmember 1-sequence, whereas core P1707-010 (figure 36), retrieved from Lillebukta, on the slope-margin, contains 12 cm.

The grain-size distribution analyses reveal two different types of natural sediments. Core P1707-005 and P1707-018, both located in the deep mid-sound, are composed of generally coarser natural sediment, relative to core P1707-010, which is located in shallow water outside Lillebukta. Based on the available geochemical data from the cores, the natural sedimentation is likely to derive from input of erosional products from the surrounding bedrock. Due to high and steep mountainsides, the coarser material settles within the deep part of Stjernesundet, whereas the fine-grained particles are able to deposit in the shallower parts. Little literature regarding sedimentary processes in Stjernesundet have been published, but according to Freiwald et al. (1997), the water exchange within the fjord is driven by the estuarine circulation, so one would expect settling of suspended sediments from surrounding bedrock, alongside more distally transported sediments from Altafjorden.

#### **5.1.3.2 Endmember 2 (tailings-derived sediments)**

Endmember 1 is part of the tailings-dominated depositional environment in the sound, with the following characteristics:

1. Dark grey colored, massive sediment
2. Relatively coarse-grained (fine to medium sand)
3. High magnetic susceptible (4000 – 8000  $10^{-5}$  SI)
4. Changing element-ratios
  - a. Elevated Fe/sum, Ca/sum and K/sum ratios
  - b. Reduced Si/sum

Cores containing endmember 2: **Core P1707-010** and **P1707-018**.

Endmember 2 is most prominent in core P1707-010, which is situated about 300 m south of the discharge site at 50 m depth. Tailings are clearly visible the upper 4 cm of the core, which is defined as a relatively coarse-grained layer (figure . The erosive contact towards the underlying sediments indicate a rapid deposition, possibly an erosive submarine mass movement. Both the coarse- and fine-grained tailings are deposited within the tidal zone of Lillebukta, which heavily influences the shallow marine environment within the bay (highest particulate concentration at 20 m depth, lowest at 90 m depth), whereas the tailings show little

evidence of large scale dispersion to the deeper parts of Stjernesundet (Larsen et al., 1993 & 2004). The containment of tailings within Lillebukta is controlled by tidal currents and wind, as suspension plumes are transported to either west or east by the tide (Larsen et al., 2004).

The tailings found in core P1707-018, situated mid-sound about 450 m deep, appear within a 2 cm layer with erosive contact to overlying sediments and a sharp contact to the underlying sediments. This layer indicates that tailings have been transported by an erosive gravity flow towards the deep basin of Stjernesundet, followed by burial with natural sediments. Larsen et al. (1993 and 2004) state that episodically occurring mass movements have occurred, and are likely to occur in the future. Available data support that at least one mass movement event have occurred prior to the retrieval of the sediment cores.

#### **5.1.3.3 Transition (mix of endmembers 1 & 2)**

Transition zones are part of a depositional environment in the sound with a mixed input of tailings and natural sediments, with the following characteristics:

1. Brown colored, massive, homogenous sediment
2. Relatively coarse-grained (fine sand)
3. Elevated magnetic susceptibility, gradually decreasing or increasing (800 – 2000  $10^{-5}$  SI)
4. Fluctuating element-ratios – no clear trend (qualitative data)

Cores containing transition zones: **Core P1707-018 and P1707-010.**

The two cores containing endmember 2 also contain transitional zones, indicating a gradual change from natural to tailings dominated deposition or vice versa. Proximal to the tailings disposal site, core P1707-010 contains a 2 – 4 cm thick transition zone, which gradually changes physical properties, in particular an increase in magnetic susceptibility. This transition is likely connected to dispersion of the fine-grained fraction of tailings, as pointed out in the paper by Larsen et al. (2004).

Influence of fine-grained tailings is also evident in core P1707-018. Below the erosive layer, a gradual transition from natural sediments to tailings occurs, followed by an abrupt end in transition by the erosive coarse-grained tailings. Further up-core, above the coarse-grained tailings, the geochemical and magnetic properties of the sediment imply that sedimentation is still dominated by tailings, despite being similar to endmember 1 in terms of color.

Furthermore, the magnetic susceptibility gradually decreases, implying a re-establishment of a

natural depositional environment. The influence of tailings within the apparent natural sediments (by color and grainsize) are most likely due to mixed deposition of natural sediments and fine-grained tailings, as the fine-grained tailings are mobilized by the tide in Lillebukta (Larsen et al., 1993). Moreover, the “re-establishment” of natural deposition in core P1707-018 indicates that the natural sedimentation is relatively high at the basin of Stjærnsundet, indicating that the natural deposition is able to exceed deposition of tailings.

#### **5.1.3.4 Interplay between tailings and natural sediments**

The overall interplay between tailings and natural sediments is mostly limited within Lillebukta, as tailings are dominant, hence smothering natural sediments (Larsen et al., 1993 & 2004; Trannum & Vogele, 2000). The key factor controlling the dispersion of tailings is grainsize, whereas 64 % of the tailings are in the range of 45 – 212 µm, 15 % of the tailings are <45 µm. Therefore, it is likely that the observed transition zones in core P1707-010 and P1707-018 are mainly caused by settling of suspended fine-grained tailings, as they are easily mobilized. Further out-fjord/down-slope, the physical mixing of tailings and natural sediments are more prominent, as settling of suspended tailings coexist with deposition of natural sediments, resulting in a mixed sediment with an elevated susceptibility and changed geochemistry. Despite the geochemical changes, the influence of tailings show little to no significant influence on sound-bed sediments as the total organic carbon-content (TOC) is considered as normal (Larsen et al., 2004).

The re-establishment of a natural depositional environment after the mass-movement deposition indicates a decreased input of tailings. Fine-grained tailings and natural sediments have combined resulted in to a ~12 cm burial of the coarse-grained tailings since the local mine was established in 1961, which means that the average sedimentation rate is about 2 mm/year (eq.1). A sedimentation rate of 2 mm/year is according to Syvitsky et al. (1987) considered normal for Norwegian fjords (1 – 7 mm/year).

$$\text{Sedimentation rate} = \frac{\text{accumulated thickness}}{\text{years of disposal}} = \frac{12 \text{ cm}}{57 \text{ years}} = 0.21 \frac{\text{cm}}{\text{year}}$$

### **5.1.4 Comparisons between the fjords: similarities and differences**

#### **5.1.4.1 Natural sediments (Endmember 1)**

The natural deposition within all study areas are more or less the same. Due to similarities in physical properties and grainsize, the main supply of naturally derived sediments occurs from

hypopycnal sedimentation of local erosional products, as all fjords are strongly influenced by estuarine circulation. In opposition to Stjernsundet and Bøkfjorden, geochemical data from Ranfjorden shows that the natural sediments contain elevated Pb and Zn concentrations.

#### **5.1.4.2 Tailings (Endmember 2)**

Similar for both Bøkfjorden and Ranfjorden is the dominance of fine-grained tailings in shallow water and coarse-grained tailings in the deeper parts (figure 30 and 33). The sediment composition in Stjernsundet is, on the other hand, mostly coarse-grained within Lillebukta. In the deeper parts of Stjernsundet, the influence of tailings is predominantly by fine-grained tailings. In other words, grain size plays a key factor for tailings-dispersion. Within the fjords, the tailings are dispersed as both suspension plumes and gravity flows. The coarse-fractioned tailings are transported towards the deep basins as bed load (both erosive and non-erosive), likely contained within the submarine channels (figure 10 and 14). The fine-grained tailings are released into suspension as the tailings move down-slope (suspension plumes and gravity flow spill over), allowing both lateral and vertical spreading (figure 39 and 42). In Stjernsundet, the tailings-influenced bay Lillebukta is mainly controlled by tidal currents and, therefore, only finer particles are mobilized and transported by suspension plumes, whereas the coarse-grained tailings accumulate over time, followed by slope failure and bed load transport into Stjernsundet (at least one mass movement event) (this study).

Based on data acquired in this study, Bøkfjorden and Ranfjorden show a high lateral extent of tailings. In Ranfjorden most of the inner-most part of the fjord is heavily influenced by tailings, especially along the deep part of fjord-bed, up to 50 cm/year (Helland et al., 1994). Cores from Ranfjorden, studied by Helland et al., (1994) show that excess metals from tailings have influenced fauna in sediments as far as 56 km out-fjord, with a magnitude of little to moderate influence. The physical dispersion of iron-particles from Rana Gruber is defined by observations of extremely fine-grained particles (pure spherical iron-oxide particles  $< 1 \mu\text{m}$ ), reaching as far as 12 km from the discharge site (Syvitski et al., 1987). In Bøkfjorden, most of the tailings are deposited within 6 km out-fjord from the discharge source (Berge et al., 2011 & 2012). The fine-grained tailings show a high lateral extent as they are dominating the innermost part of the fjord, as well as being observed in lower concentrations further out-fjord. Fine-grained sediments are likely spread over large areas due to the low-gradient channel in the inner part of the fjord and flat fjord-bed at the foot of the submarine canyon (figure 14). Flat slope related to submarine channels lead to spreading of fine-grained particles in all directions (vertical and lateral) (Teles et al., 2016). As observed in

Ranfjorden, it is likely that extremely fine-grained tailings in Bøkfjorden are transported far out-fjord, as core P1505-011 (located 13 km off the fjord head (figure 20) indicates elevated magnetic susceptibility (figure 31). It is unlikely that tailings are transported and deposited beyond the sill separating Bøkfjorden and Varangerfjorden, located 17 km from the tailings discharge source (figure 17 A and 17 B). In opposition to both Bøkfjorden and Ranfjorden, lateral spreading of tailings in Stjersundet is more local; the maximum spreading of the tailings is limited to 2 km outside Lillebukta. It is mainly fine-grained particles, whereas the episodic gravity flows transport the coarse-grained tailings down-slope. The apparent low rate of episodic mass movements in Stjersundet is probably related to the low discharge of particles (300,000 tons annually) relative to Bøkfjorden (~3,000,000 tons annually) and Ranfjorden (~2,000,000 tons annually), allowing the sediments in Stjersundet to deposit under more stable conditions. According to Larsen et al. (1993 & 2004) and Trannum & Vögele (2000), the deposited tailings in Lillebukta have resulted in a compact sediment-bed, whereas the fjord-beds in Ranfjorden and Bøkfjorden are considered unstable (Tesaker (1978), as cited in Syvitski, 1987; Øie, 2013).

Geochemically, the tailings in each study area vary with the associated mining activity. In Bøkfjorden, the targeted ore in Bjørnevatn is extracted from an amphibolite, containing quartz-magnetite alternating BIFs. Therefore, the tailings in Bøkfjorden contain elevated quartz and iron-oxide content, a relatively high magnetic susceptibility and low heavy metal concentration. In Ranfjorden, multiple sources have deposited tailings within the fjord. Local mining activity has extracted iron, lead, zink and copper from the surrounding bedrock, using Ranfjorden as the tailings recipient. The extraction and processing of lead, zink and copper explain the elevated heavy metal concentrations within the fjord. Furthermore, the overall magnetic susceptibility of tailings-influenced sediment in Ranfjorden is lower than the tailings in Bøkfjorden, which is due to a higher hematite content, relative to magnetite (less susceptible) (Hunt et al., 1995) The tailings in Stjersundet are characterized by silica-depleted element ratios and high magnetic susceptibility compared to the other two fjords (figure 35 and 36). Due to extraction and separation of nepheline syenite, the deposited tailings contain magnetic susceptible and silica depleted sediment.

#### **5.1.4.3 Transition**

The transitions from natural sedimentation to tailings deposition occurred gradually in cores from Ranfjorden and Stjersundet, whereas transitions in Bøkfjorden occurred abruptly. Grainsize, sedimentation rate, submarine channels and slope inclination seems to be the

controlling factors for how the transitions appear within the sediment cores. The transitional zones in Ranfjorden are preserved sediment sequences (figure 28 and 30), reflecting a gradual change from more naturally derived sediments, to a tailings dominated depositional environment.

The explanation for defined gradual transitions in Ranfjorden and the lack of gradual transitions in Bøkfjorden is likely due to the slope-surface/bathymetry. According to Teles et al. (2016), important factors for behaviour and deposition of gravity flows are controlled by topography and slope gradients. Gravity flows flowing over low-gradient slopes tend to spread in all directions, whereas high-gradient slopes tend to follow the topography, increasing in extent downslope. Furthermore, coarse-grained sediments tend to be concentrated within the channel, and fine-grained sediments are likely to spread throughout the water column and deposited on topographic highs when it spills over. Therefore, the sudden change in depositional environment in Bøkfjorden is likely caused by a higher spill over rate, which due to bathymetry and slope is extended laterally, depositing on the flat fjord-bed. The coarse-grained sediments are concentrated within the channel, and led further out-fjord (at least to core location IG16-1811GC (figure 21)). In Ranfjorden, the suspension of fine-grained tailings are propagating downslope, and released into the water column with no adjacent topographic highs, which ultimately transports the suspension plumes to the fjord-slope across fjord (figure 39). Here the suspended particles are able to deposit, but the extended time spent in suspension “delays” the deposition of tailings relative to the deposition in Bøkfjorden.

In Stjernesundet, the transitional zones similar to the ones observed in Ranfjorden, show a gradual introduction of a more tailings-dominated depositional environment, superimposed by coarse-grained tailings (figure 36)). Unlike Ranfjorden, the slope seems to be exposed to erosional processes due to mass movements, as the transition in core P1707-018 is abruptly ended by an overlying layer of endmember 2 (figure 35). Above the coarse-grained layer, the transition towards a natural depositional environment is evident as the magnetic susceptibility decreases gradually up-core. In other words, the tailings input to the deeper part of Stjernesundet is limited compared to the gradually evolving dominance of tailings in both Ranfjorden and Bøkfjorden.



## 6 Conclusion

This study assessed the interplay between submarine tailings placements and natural sediments in the northern Norwegian fjords Ranfjorden and Bøkfjorden, and the sound Stjernesundet. The study area of Ranfjorden is situated in a fjord containing steep fjord slopes, two submarine canyons and a meandering channel along the fjord-bed. The study area of Bøkfjorden is a fjord, containing relative low-gradient fjord slopes, a submarine canyon and meandering channels. The study area of Stjernesundet is in a sound, with a shallow embayment Lillebukta stretching down the steep slope into the deep basin of Stjernesundet.

Multi-proxy analyses of 10 sediment cores, including physical properties (e.g. magnetic susceptibility), geochemical properties (qualitative and quantitative element geochemistry), bulk mineral assemblages and lithological analyses reveal three depositional environments in the study areas:

1. Natural depositional environment (**endmember 1**) – no to little tailings influence.
  - a. Fluctuating grain size.
  - b. Low magnetic susceptibility.
  - c. Stable geochemistry.
2. Tailings depositional environment (**endmember 2**) – significant tailings influence.
  - a. Fine-grained sediments.
  - b. High magnetic susceptibility.
  - c. Stable geochemistry – elevated levels of mining associated minerals/metals.
    - i. Quartz, amphibole and iron-oxides (mainly magnetite) in Bøkfjorden.
    - ii. Iron-oxides (mainly hematite, some magnetite) in Ranfjorden.
    - iii. Silica-deficiency in Stjernesundet.
3. Transitional depositional environment (**mix of endmember 1 & 2**) – gradual increased or decreased tailings-influence.
  - a. Gradually decreasing grainsize.
  - b. Gradually increasing (Ranfjorden) or decreasing (Stjernesundet) magnetic susceptibility.
  - c. Unstable geochemistry - gradual increase or decrease in mining associated minerals and metals.
    - i. Increasing iron-oxide content and decreasing silica-content in Ranfjorden.

- ii. No clear geochemical trends in Stjernesundet (only qualitative data).

The end members 1 and 2 occur in all study areas, whereas the transition from natural to tailings-dominated deposition occurred gradually in Ranfjorden and Stjernesundet. In Bøkfjorden, endmember 2 is deposited on top of endmember 1, marked with a sharp contact. The presence of end members and transitions are strongly connected to the tailings output source, discharge rate, the sedimentary processes and fjord-bed structures.

In the fjords, a high discharge-rate of tailings through submarine pipelines have led to unstable depositional conditions. Due to a higher density to the surrounding water and episodic slope failures, the majority of discharged tailings are transported further out-fjord as bed load currents. The bed load currents follow the local submarine canyons and channels, which amplify the lateral spreading of tailings. As the bed-load currents move further out-fjord, erosive processes may occur, leading to physical mixing of already deposited sediments and suspended tailings. Additionally, lateral and vertical dispersion of tailings in suspension plumes occur due to over spill and release of fine-grained particles from bed-load currents.

In Stjernesundet, relatively coarse-grained tailings are disposed into the tidal zone through a pipeline at a relatively low discharge-rate. These three factors contribute to a more stable depositional environment than in the two fjords. Occasionally, erosive bed load currents have transported tailings into Stjernesundet, but their influence is marginal.

Capping effect of previously deposited sediments (natural and tailings) was evident in cores from the two fjords, resulting in a gradual and an abrupt isolation of natural sediments in Ranfjorden and Bøkfjorden, respectively.

## Works cited

- Amundsen et al. (2015). Late Weichselian–Holocene evolution of the high-latitude Andøya submarine Canyon, north-Norwegian continental margin. *Marine Geology*, 363, 1-14.
- Arrobas et al. (2017). *The Growing Role of Minerals and Metals for a Low Carbon Future*, International Bank for Reconstruction and Development/The World Bank, Washington, 2017.
- Avaatech, (2018), Avaatech XRF Core Scanner journal.
- Azcue, J., M., Zemann, A., J., Förstner, U. (1998). International review of application of subaqueous capping techniques for remediation of contaminated sediments. Volume: 2; Remediation of polluted land and abandoned landfills re-use or by-products risk analysis, quality assurance and regulations, pp. 537-542
- Berge et al. (2012). Overvåking av Bøkfjorden 2011 og giftighetstesting av gruvekjemikaliene Magnafloc LT 38 og Magnafloc 10, Technical report, NIVA
- Blake, P., K. & Olsen, L. (1999). Deglaciation of the Svartisen area, northern Norway, and isolation of a large ice mass in front of the Fennoscandian Ice Sheet, *Norsk Geografisk Tidsskrift*, 53:1, 1-16.
- Bugge, W., A., J. (1948) RANA GRUBER GEOLOGISK BESKRIVELSE AV JERNMALMFELTENE I DUNDERLANDSDALEN, NGU, Oslo, 1948.  
[http://www.ngu.no/filearchive/NGUPublikasjoner/NGUnr\\_171\\_Bugge.pdf](http://www.ngu.no/filearchive/NGUPublikasjoner/NGUnr_171_Bugge.pdf)
- Christopher P. Hunt, Bruce M. Moskowitz, Subir K. Banerjee (1995). *Magnetic Properties of Rocks and Minerals*. American Geophysical Union. P. 189 –
- Cornwall, N. (2013). *Submarine Tailings Disposal In Norway's Fjords – Is it the best option?* Master of Science in Environmental Management and Policy, Lund, Sweden, September 2013.
- Ellis, D. (2008). *The Role of Deep Submarine Tailings Placement (STP) in the Mitigation of Marine Pollution for Coastal and Island Mines*, *Marine Pollution: New Research*. P. 23-51
- Forwick, M. (2001). *Development of the sedimentary environment in Balsfjord (northern Norway)*. Cand. Scient. Thesis in geology. University of Tromsø.

- Forwick M. (2013). How to use XRF core scanner data acquired with the Avaatech XRF core scanner at the Department of Geology, University of Tromsø, a short manual compiled by Matthias Forwick.
- Franks et al. (2011). Sustainable development principles for the disposal of mining and mineral processing wastes. *Resour. Policy* 2011, 36, 114–122. Found: <https://www.sciencedirect.com/science/article/pii/S0301420710000747>
- France, D., E. & Oldfield, F. (2000). Identifying goethite and hematite from rock magnetic measurements of soils and sediments. *JOURNAL OF GEOPHYSICAL RESEARCH*, VOL. 105, NO. B2, P. 2781-2795
- Freiwald, A., Henrich R, Pätzold, J. (1997) Anatomy of a deep-water coral reef mound from Stjernsund, west Finnmark, north Norway. *SEPM Spec Publ* 56: 142–162
- Geotek Ltd. (2016). Multi-Sensor Core Logger. User manual.
- Golmen, L., G., Norli, M. (2013). Sporstoff-forsøk i Ranfjorden 2012-2013. Technical report, NIVA
- Haugen, A., E. (unpublished). Msc. thesis. UiT, The Arctic University of Norway.
- Hay, A., E., Murray, J., W., Burling, R., W. (1983). SUBMARINE CHANNELS IN RUPERT INLET, BRITISH COLUMBIA: II. SEDIMENTS AND SEDIMENTARY STRUCTURES. *Sediment. Geol.*, 36: 317-339.
- Heier, S., K. (1961). LAYERED GABBRO, HORNBLENDITE, CARBONATITE AND NEPHELINE SYENITE ON STJERNØY, NORTH NORWAY. *NORSK GEOLOGISK TIDSSKRIFT* 41.
- Heier, S., K. (1964). GEOCHEMISTRY OF THE NEPHELINE SYENITE ON STJERNØY, NORTH NORWAY. *NORSK GEOLOGISK TIDSSKRIFT* 44. P. 205 – 214.
- Helland, A., Rygg, B., Sørensen, K. (1994). Ranfjorden 1992/1993. Hydrografi, sedimenterende materiale, bunnsedimenter og bløtbunnsfauna. Technical report, NIVA
- Hicks, C., E., Bungum, H., Lindholm, D., C. (2000). Seismic activity, inferred crustal stresses and seismotectonics in the Rana region, Northern Norway. *Quaternary Scuebce Reviews*, 19 p, 1423 – 1436.

- Hunt, C., P., Moskowitz, B., M., Banerjee, S., K. (1995) Magnetic Properties of Rocks and Minerals. American Geophysical Union. P. 189 – 191.
- Johnsen et al. (2004). Miljøundersøkelser I Ranfjorden 1994-1996, Technical report, NIVA
- Joseph P., Teles V., Weill P. (2016). Modelling approaches in sedimentology: Introduction to the thematic issue Comptes Rendus - Geoscience, Volume 348
- Konica Minolta. (2018). CM-700D SPECTROPHOTOMETER. User manual. Retrieved from <http://sensing.konicaminolta.asia/products/cm-700d-spectrophotometer/>
- Kirkerud, L. (1977). Resipientundersøkelse i Ranfjorden. Rapport nr. 2. Innledende hydrografiske, geokjemiske og biologiske undersøkelser. Technical report, NIVA.
- Kirkerud et al. (1986). Basisundersøkelse i Ranfjorden – en marin industriresipient. Smalerapport (overvåkingsrapport 207/86). Technical report, NIVA
- Ladstein, K., A. (2018). Natural and anthropogenic deposition in Bøkfjorden. Msc. Thesis, UiT, The Arctic University of Norway.
- Larsen et al. (1993). Miljøundersøkelse i Stjernesundet, Finnmark I forbindelse med utslipp av gruveavgang fra North Cape Nefelin AS. Technical report, Akvaplan-niva.
- Larsen et al. (2004). Miljøundersøkelse i forbindelse med utslipp av gruveavgang fra North Cape Minerals, Stjernøya, Finnmark, 2004. Technical report, Akvaplan-niva
- Larsen, L-H., Mannvik, H-P., Dahl-Hansen, I., E. (2012). Undersøkelse av miljøtilstand i Lillebukta og Stjernesund, Finnmark 2012. Technical report, Akvaplan-niva
- Lynn, W., C., Pearson, M., J., (2000) Exploring the chemistry of soil. The Science Teacher, p. 20-23.
- Løkeland, M. (2011). Notat om gruvedrift og internasjonalt syn på sjødeponi. Naturvernforbundet,
- Marthinussen, M. (1974). Contributions to the Quarternary Geology of North-easternmost Norway and the Closely Adjoining Foreign Territories. Norges geologiske undersøkelse Nr. 315, Universitetsforlaget 1974. P. 94-95.

- Martin, T.E., Davies, M.E., 2010. Trends in the Stewardship of Tailings Dams. Retrieved from <http://www.infomine.com/library/publications/docs/Martin2000.pdf> .
- Neira, C., Rackemann, M. (1996). Black spots produced by buried macroalgae in intertidal sandy sediments of the Wadden Sea: Effects on the meiobenthos. *Journal of Sea Research*, 36, 3-4, p. 153.
- Norwegian Mining Industry, 2014. Norwegian experiences with sea disposal of mine tailings. Report 1, 34 pp.
- Nowaczyk et al. (2002). Magnetostratigraphic results from impact crater Lake El'gygytgyn, northeastern Siberia: a 300 kyr long high-resolution terrestrial palaeoclimatic record from the Arctic
- Plassen, L., Bøe, R., Lepland, A. (2009). Geologi og bunnforhold i Andfjorden og Stjernesundet/Sørøysundet. Technical Report. 2009.027
- Powell et al. (2002). AN ASSESSMENT OF THE MAGNETIC RESPONSE OF AN IRON-SMELTING SITE. *Archaeometry* 44, 4. P. 660.
- Ramberg, I. B., Bryhni, I., Nødtvedt, A. og Rangnes, K. (red),. (2013). Landet blir til - Norges geologi (2. ed.). Trondheim: Norsk Geologisk Forening.
- Ramirez-Llodra et al. (2015). Submarine and deep-sea mine tailing placements: A review of current practices, environmental issues, natural analogs and knowledge gaps in Norway and internationally, *Marine Pollution Bulletin* 97 (2015), p. 13–35.
- Reichl, C., Schatz, M., & Zsak, G. (2017). World Mining Data 2017. International Organizing Committee for World Mining Congresses.
- Richter et al. (2006). The Avaatech XRF Core Scanner: Technical Description and Applications to NE Atlantic Sediments. *Geological Society London Special Publications* 267(1):39-50
- Rygg, B., Helland, A., Sørensen, K. (1994). Ranfjorden 1992/1993. Hydrografi, sedimenterende materiale, bunnsedimenter og bløtbunnsfauna. Technical report, NIVA.
- Simón et al. (2001). Soil pollution by oxidation of tailings from toxic spill of a pyrite mine, *Science of The Total Environment*, Volume 279, Issues 1–3, 2001, Pages 63-74,
- Simonsen, A. M. T. (2017). Environmental impacts of submarine tailings disposal from an iron-ore mine, Norway - A study of metal dispersion, availability and bioaccumulation

- of metals in the sediments of Bøkfjorden. Master thesis, Department of Geosciences and Natural Resource Management, University of Copenhagen.
- Sitko, R. & Zawisza, B. (2012). Quantification in X-Ray Fluorescence Spectrometry. Department of Analytical Chemistry, Institute of Chemistry, University of Silesia, Poland
- Skaare, B. B., Oug, E. and Nilsson, H. C. (2007), Miljøundersøkelser i fjordsystemet utenfor Kirkenes i Finnmark 2007, Technical report, NIVA.
- Skei, J. & Paus, P., E. (1979). Surface metal enrichment and partitioning of metals in a dated sediment core from a Norwegian fjord. *Geochim. Cosmochim. Acta* 43: 239-246.
- Skei, J. (1990). Miljøundersøkelser i fjordsystemet utenfor Kirkenes i Finnmark. 2. Partikler i vannmassen sommeren 1989. Technical report, NIVA.
- Skei, J. & Rygg, B. (1989). Miljøundersøkelser i fjordsystemet utenfor Kirkenes i Finnmark. 1. Bløtbunnfauna og sedimenter. Technical report, NIVA.
- Skei, J., Rygg, B. (1989). Miljøundersøkelser I fjordsystemet utenfor Kirkenes i Finnmark. 1. Bløtbunnfauna og sedimenter. Technical report, NIVA
- Skei, J., Rygg, B. and Sørensen, K. (1995), Miljøundersøkelser i fjordsystemet utenfor Kirkenes i Finnmark, Technical report, NIVA.
- Suryanarayana, C., Norton, G., M. (1998) X-Ray Diffraction A Practical Approach. Plenum Publishing Corporation, New York. P. 238
- Syvitski, J., P., M., Burrell, D., C., Skei, J., M. (1987). *Fjords: Processes and Products*. Springer-Verlag, New York. P. 309 – 314.
- Teles et al. (2016). Modelling approaches in sedimentology: Introduction to the thematic issue *Comptes Rendus - Geoscience*, Volume 348
- Trannum, H., C., Vögele, B. (2000). Miljøundersøkelse i Stjernsundet, Finnmark, 2000, i forbindelse med utslipp av gruveavgang. Technical report, Akvaplan-niva.
- Vogt, C. (2013). International Assessment of Marine and Riverine Disposal of Mine Tailnigs – Final Report Adpoted by the International Maritime Organization, London Contention/Protocol
- Walday et al. (2004). Environmental assessment of Ranfjorden, northern Norway, 2003. Technical report, NIVA.

Weltje, J., G. & Tjallingii, R. (2008). Calibration of XRF core scanners for quantitative geochemical logging of sediment cores: Theory and application. *Earth and Planetary Science Letters*, Volume 274, Issue 3-4, p. 423-438.

Øyehaug, T., E. (2016). Grottekartlegging og strukturgeologisk påvirkning på grottedannelse sør for Reingardslivatnet, Rana. Msc. thesis, University of Bergen.